SOLUTES IN ANHYDROUS HF

A CONDUCTOMETRIC AND SPECTROSCOPIC INVESTIGATION OF SOME SOLUTES IN ANHYDROUS HF

By

SETH MORLEY BROWNSTEIN

A Thesis

Submitted to the School of Graduate Studies

in Partial Fulfilment of the Requirements

for the Degree

Doctor of Philosophy

McMaster University

February 1970

DOCTOR OF PHILOSOPHY (1970) McMASTER UNIVERSITY

(Chemistry) Hamilton, Ontario.

TITLE: A Conductometric and Spectroscopic Investigation of Some Solutes in Anhydrous HF

AUTHOR: Seth Morley Brownstein, B. A. (University of Saskatchewan)

SUPERVISOR: Professor R. J. Gillespie

NUMBER OF PAGES: xi, 205

SCOPE AND CONTENTS:

Conductivity measurements on liquid hydrogen fluoride solutions of some simple bases and fluoroanion salts were carried out, and a set of equivalent ionic conductivities have been determined. The conductivities of electrolytes in hydrogen fluoride have been compared to those of analogous electrolytes in water and strong acid solvents. A method for the investigation of more complex electrolytes was developed.

The mode of ionization of adducts of sulfur tetrafluoride, thionyl tetrafluoride and selenium tetrafluoride with fluoride acceptors in hydrogen fluoride has been investigated by conductivity and nmr spectroscopy. The structures of the solid adducts have also been investigated by Raman spectroscopy. The structure and stability of other sulfur-oxide-fluoride adducts have been investigated and found to differ from adducts of thionyl tetrafluoride.

ACKNOWLEDGEMENTS

The author wishes to express his gratitude to Dr. R. J. Gillespie who suggested this problem, and under whose direction the work was done.

Also, he would like to express his thanks to colleagues whose friendship and advice has been appreciated.

Thanks are due to Mrs. B. Spiers for assistance with the laser Raman spectrometer, and to Mr. J. I. A. Thompson for technical assistance with the nmr spectrometer. Thanks are also due to members of the glass blowing shop for construction of much of the glass apparatus, to members of the University machine shops for fabrication of metal and plastic equipment, and to Miss C. Kett for the drawings in this thesis.

Finally, the author would like to thank the National Research Council of Canada for financial support.

TABLE OF CONTENTS

LIST OF TABLES

LIST OF FIGURES

CHAPTER I

INTRODUCTION

Anhydrous hydrogen fluoride is a solvent of importance both in the laboratory and in industry. Though its corrosive nature to silicaceous materials, and indeed to human skin seems formidable, the favourable physical and chemical properties of hydrogen fluoride strongly recommend its utilization as a solvent. It is a highly acidic, very fluid medium of high dielectric constant suitable for dissolving electrophilic species unstable in more basic solvents. The classic example of such a cation is the nitronium ion, NO_2^+, originally shown to exist in sulfuric acid, [1] and more recently used directly as a nitrating agent in hydrogen fluoride as the BF_4^- salt. [2]

Hydrogen fluoride does not react with the majority of solutes to change their oxidation state. Only an extremely powerful oxidizer could be reduced by hydrogen fluoride, as the product of the reaction will be elemental fluorine. Conversely, hydrogen fluoride itself is not an oxidizing solvent, unlike the other strong acid solvents; sulfuric acid, fluorosulfuric acid and perchloric acid. It has a convenient liquid range, and its relatively low boiling point compared to the other common strong acids allows easy removal by evaporation.

Complicating solvent dissociations such as those in sulfuric and fluorosulfuric acids do not occur. Only the simple ionic self dissociation

reaction is present, and to a much lesser degree than in these other acids. This not only simplifies interpretation of physical measurements, for example, conductivity and cryoscopy, but also sulfonation of dissolved compounds does not occur.

Hydrogen fluoride is of considerable industrial importance. Fluorine is produced by the electrolysis of hydrogen fluoride in fused potassium hydrogen fluoride. (3) The fluorine is then used in the preparation of many other fluorine chemicals. Electrochemical fluorination of organic compounds in HF is an important method as it gives fully fluorinated compounds without removing the organic functional groups. (4) HF is also used in the production of chlorofluorocarbons. (5)

Uranium tetrafluoride, also prepared with hydrogen fluoride, can be either reduced to give uranium metal, or further fluorinated to give uranium hexafluoride. The hexafluoride is then separated by diffusion processes to give $^{235}UF_6$ and $^{238}UF_6$.

Perhaps of more general importance is the use of hydrogen fluoride as a catalyst and solvent in a large number of organic reactions; e.g. alkylations, rearrangements and nitration. (6)

Anhydrous hydrogen fluoride as a solvent has been the subject of several recent reviews. (7, 8) There are also several reviews covering its application in industrial processes. (3, 4, 6, 9, 10)

Pertinent physical properties of hydrogen fluoride are summarized in Table 1.1. It can be seen (Table 1.2) that hydrogen fluoride shows abnormal properties, as compared to the higher hydrogen

TABLE 1.1*

Some Physical Properties of HF

melting point [11]	-83.55°C
boiling point	19.51°C
cryoscopic constant [11]	1.55±0.05°C $mole^{-1}$ kg^{-1}
density	1.1231 g/ml at -50°C
	1.002 g/ml at 0°C
critical density	0.29±0.03 g/ml at 188°C
viscosity (η)	0.570 centipoise at -50°C
	0.256 centipoise at 0°C
dielectric constant (ε)	175 at -73°C
	134 at -42°C
	111 at -27°C
	84 at 0°C
conductivity [12]	8×10^{-7} at 25°C

* all data from reference 7 except those indicated

TABLE 1.2

Some Physical Properties

of the

Hydrogen Halides and Chalcogenides

		m.pt.	b.pt.	liquid range	ΔH_f	ΔH_{vap}
		°C	°C	°C	cal/mole	
HF	(7)	-83.55	19.5	102	939	1789
HCℓ	(13)	-114.6	-84.1	30.5	476	3860
HBr	(13)	-88.5	-67.0	21.5	600	4210
HI	(13)	-50.9	-35.0	15.9	686	4724
H_2O	(13)	0	100	100	1440	9720
H_2S	(14)	-85.5	-60.7	25	-	-
H_2Se	(14)	-60.4	-41.5	19	-	-
H_2Te	(14)	-49	-2	47	-	-

halides, similar to the behaviour of water and the higher hydrogen chalcogenides. As in the case of water, this abnormal behaviour can be attributed to hydrogen bonding. Indeed the bond with fluorine is the strongest hydrogen bond known, with a bond strength of about 6 Kcal/mole in neutral H—F---H—F. [8]

Hydrogen bonding is present even in the gas phase, with hydrogen fluoride being probably "the most imperfect gas known". [15] Vapour density measurements over a range of pressure and temperature have been interpreted in terms of a monomer - cyclic hexamer equilibrium, with the dimer and tetramer becoming more important species at low pressures. Others have interpreted results in terms of acyclic chains, but in any case, all measurements show HF is highly associated. These measurements show that gaseous HF has an apparent molecular weight up to 4.7 times that of the monomer at 0°C at a pressure in equilibrium with the liquid.

In the solid, X-ray diffraction on single crystal HF showed it to exist in zig-zag hydrogen-bonded chains with an H-F-H bond angle of 120°, [16] a fact additionally confirmed by the infra-red spectrum. [17]

The work on HF association in the liquid and solid states as well as for the gas has been well summarized by both Hyman [7] and Kilpatrick. [8]

Many properties of the liquid can be explained only by assuming a considerable degree of association. Among these are the high dielectric constant, lowering of the fundamental stretching frequency compared to the monomer and the appearance of polymer vibrations in the IR spectrum, and

a boiling point that is too high for the monomer molecular weight. The heat of vapourization is low for an associated liquid, but since the polymer is relatively strong, it has been concluded that not much change occurs in the average polymer size on going from the liquid to the gaseous state. The low viscosity, as Simons has commented [18] makes HF unusual among associated liquids. This is quite understandable however, when one remembers that the association in HF is only one-dimensional, as compared to three-dimensional hydrogen bonding in oxygen based solvents such as water and sulfuric acid.

Like many other solvents associated by hydrogen bonds, hydrogen fluoride undergoes self-ionization. A simplified description of the ionization is:

$$2HF \rightleftharpoons H_2F^+ + F^-$$

but both ions are certainly heavily solvated, and indeed must be part of the hydrogen-bonded molecular network, as shown by the abnormally high mobility of the fluoride ion [19] and the acidium ion. [20] This abnormal mobility can only be accounted for by chain conduction both by the fluoride ion

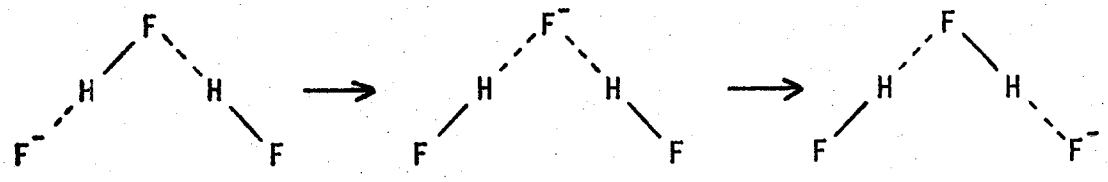

and the proton

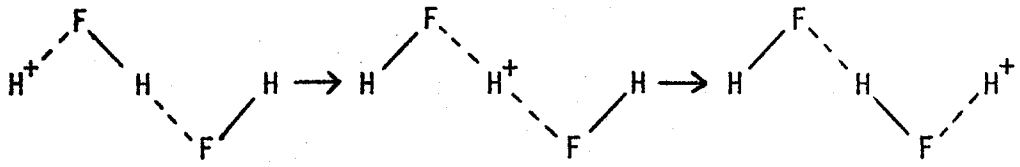

From the measurements of Kilpatrick and Lewis it can be seen that the difference in conductivity between the characteristic solvent ions and other ions is not nearly as great in hydrogen fluoride as it is in fluorosulfuric and sulfuric acids (Table 1.3). This is a result of the higher viscosities of these latter solvents.

Hydrogen Fluoride Solutions

A considerable number of solubility measurements were made by early workers in the field, and have been well summarized by Simons.[21] As can be expected from its high dielectric constant, hydrogen fluoride is a good solvent for ionic compounds. However, because of its high acidity, many compounds undergo reaction on solution, being converted to the corresponding fluoride which is generally soluble.

Oxides and hydroxides of course react to give water, which is then partly protonated. One of the few insoluble oxides is synthetic sapphire (alumina) which is used as a window material for spectroscopic studies in HF. The necessity of using physical rather than chemical methods to dry HF can be seen from its reaction with the powerful

TABLE 1.3

Equivalent Ionic Conductivities ($Ohms^{-1}$ cm^2 $equiv^{-1}$)

at Infinite Dilution

Hydrogen Fluoride [19, 20]*		η = 0.256 centipoise at 0°C
Na^+	117	
K^+	117	
BF_4^-	183	
SbF_6^-	196	
F^-	273	
H_2F^+	350	
Fluorosulfuric acid [22, 23]		η = 1.56 centipoise at 25°C
K^+	17	
NH_4^+	21	
SO_3F^-	135	
$H_2SO_3F^+$	185	
Sulfuric Acid [24]		η = 24.54 centipoise at 25°C
$H_3SO_4^+$	250	
HSO_4^-	166	
all other ions	<5	

* To be discussed in Chapter IV.

desiccant P_2O_5 to produce water instead of removing it:

$$P_2O_5 + 6HF \longrightarrow 2POF_3 + 3H_2O$$

The water is then further protonated.

In contrast to water with its similar dielectric constant, the other hydrogen halides; HCℓ, HBr and HI, are only slightly soluble in HF, and they behave as non-electrolytes. HCℓ has a solubility of only 0.17 M at 0°C. [25] They are formed on solution of the halides, which give the corresponding fluoride and evolve the hydrogen halide. [26] This has been used as a preparative method for some fluorides, starting with the generally easily obtainable chloride. Nitric acid and nitrates react in liquid HF to give the nitronium cation. [27]

$$HNO_3 + 2HF \longrightarrow NO_2^+ + H_3O^+ + 2F^-$$

Even sulfates are protonated to give sulfuric acid, which is ionized only slightly, if at all. On standing in HF, sulfuric acid is further solvolyzed to give fluorosulfuric acid, though the reaction can be considerably slowed by keeping the solution cold. [11]

Organic compounds are more soluble in HF than they are in water, even saturated aliphatic hydrocarbons having an appreciable solubility. [21] Oxygen, nitrogen and sulfur containing compounds are generally quite soluble giving conducting solutions, which indicates protonation is occurring. [26, 28, 29] Aromatic compounds are even more soluble than aliphatic ones, with some protonation on the ring occurring. The relative

basicity of the methylbenzenes in hydrogen fluoride has been investigated by several methods. [30, 31] Increasing the number of methyl groups substituted on the aromatic ring, increases the proton accepting ability of the ring. Studies of the rearrangement of the methylbenzenes through the protonated species have also been carried out. The xylenes isomerize to give m-xylene, [32] and the tetramethylbenzenes isomerize to give isodurene (1, 2, 3, 5 - tetramethylbenzene). [33] In both cases the most basic isomer is the product.

Quantitative solubility measurements were carried out by Jache and Cady on a large number of simple fluorides. [34] All univalent fluorides are quite soluble; the solubility increasing in the order Li < Na < K < Rb < Cs. Except for the alkali fluorides, the solubility of fluorides in HF is generally larger than the solubility of the corresponding hydroxides in water. Thus, the alkaline earth fluorides have an appreciable solubility in HF, decreasing in the order Sr > Ba > Ca > Mg > Be. Higher valent ionic fluorides have only limited solubility, probably due to their higher lattice energies. Simple covalent fluorides have an appreciable solubility in HF, particularly when there is a common liquid range. A considerable amount of work has been done on the UF_6 - HF system. [35, 36] Above 101°C the two are completely miscible. Based on conductivity and Raman spectrum studies, Frlec and Hyman found that there appears to be minimal interaction between solvent HF and UF_6, MoF_6, WF_6 or ReF_6. [37] Similar conclusions were reached for HF solutions of ReF_7 by Selig and Gasner. [38]

VF_5 is an exceptional compound. Conductivity measurements showed it to be completely unionized in HF, but Raman spectral studies give a spectrum different from that expected from non-interacting VF_5, and also different from that of KVF_6 in HF. (39)

Clifford et al. attributed the ability of several fluorides, e.g. SbF_5, AsF_5, BF_3 and SnF_4 to cause dissolution of insoluble fluorides and metals to their acting as acids in HF. (40) McCaulay et al. accounted for the ability of TiF_4, NbF_5, TaF_5 and PF_5 to increase the amount of m- and p-xylene extracted into HF from a solution in n-heptane to their acid behaviour.(41) These fluorides act as acids by accepting a fluoride ion from the solvent.

$$MF_n + 2HF \longrightarrow H_2F^+ + (MF_{n+1})^-$$

The strongest acid and one of the most extensively studied is SbF_5. (20, 42, 43) In dilute solution it is fully ionized to give the SbF_6^- anion. This solution of H_2F^+ SbF_6^- has been titrated with water to give H_3O^+ SbF_6^-, (43) with the conductivity going through a minimum and then again increasing in confirmation of the acid nature of the solution. Initially, chain conducting H_2F^+ ions are replaced by the less highly conducting H_3O^+ ions. After neutralization, the conductivity again increases as a greater number of conducting ions appear in solution. Polymerization occurs in more concentrated SbF_5 solutions, with formation of fluorine bridged antimony species. (20) The first

ion in this series is $Sb_2F_{11}^-$. With larger and larger proportions of SbF_5, the polymer grows until the cis-bridged chain of pure SbF_5 is present.

AsF_5 is similarly an acid in HF. [40, 43] Though the corresponding $As_2F_{11}^-$ anion has not been observed as a discrete entity in HF, it has been found in other systems. [44, 45] Evidence for the mixed $AsSbF_{11}^-$ ion has also been obtained. [44] The $As_2F_{11}^-$ ion was initially somewhat surprising, as AsF_5 does not polymerize in the liquid state, [46] as does SbF_5.

Boron trifluoride, which is only slightly soluble, is a rather weak acid in HF. [47] However, if any base is present, an equimolar quantity of BF_3 dissolves to form the BF_4^- salt. [48] BF_3 has been widely used, especially in studying protonation of organic systems. [33, 49, 50]

Complete miscibility with HF is shown by the halogen fluorides $C\ell F_3$, BrF_3, BrF_5 and IF_5. [51, 52, 53] The solutions are slightly conducting, with the halogen fluoride presumably acting as a weak base with the formation of a heterocation and a fluoride ion, for example:

$$C\ell F_3 + HF \longrightarrow C\ell F_2^+ + HF_2^-$$

Adducts of $C\ell F_3$ with fluoride acceptors, for example $C\ell F_3 \cdot AsF_5$ which has been recrystallized from HF without decomposition, were shown to have the ionic structure $C\ell F_2^+ MF_6^-$. [54, 55]

A great deal of interest has been shown recently in such heterocations, and a number of studies utilizing HF as a solvent have been carried out. All three possible nitrogen (V) based oxide-fluoride cations have been studied in HF. Nitronium tetrafluoroborate which is ionic in the solid state was shown to be completely ionized in HF solution. (56) The totally fluorinated analogue NF_4^+ has also been prepared and studied by nmr spectroscopy in HF. (57, 58) In this case it is not expected that the parent compound NF_5 will be found. Recently the mixed oxide-fluoride cation ONF_2^+ has been prepared, completing the series. (59)

Other nitrogen cations which have been studied are the N_2F^+ cation, derived from N_2F_2, (60) the $N_2F_3^+$ cation derived from N_2F_4, (61) and the NH_3OH^+ cation, prepared as the F^- salt by treatment of NH_3OH^+ $C\ell^-$ with anhydrous HF. (62)

Rare gas compounds also dissolve in HF. XeF_2 is quite soluble in HF, while XeF_4 is less so. (63) Neither solution conducts and cryoscopic studies show XeF_2 to give only one particle in solution. (11) In contrast, XeF_6 solutions are highly conducting. (63) The conducting species could be XeF_5^+, shown to exist by an x-ray structural determination of XeF_5^+ PtF_6^-, (64) and thought to be present in complexes of XeF_6 with other fluoride acceptors.

$$XeF_6 + HF \longrightarrow XeF_5^+ + HF_2^-$$

XeF_2 also forms complexes with fluoride acceptors, but the complex $XeF_2 \cdot AsF_5$ was recently shown to be nonconducting in HF, in contrast to solutions containing AsF_5 alone. (65)

Purpose of this Work

Although numerous studies have been reported of electrolytes in other strong acid solvents, for example, sulfuric and fluorosulfuric acids, at the time this investigation was commenced there had been very few studies in hydrogen fluoride of complex electrolytes, for example adducts of Lewis acids. The general purpose of this work was to investigate if similar studies of electrolytes in hydrogen fluoride could be carried out, in particular by conductometric and spectroscopic techniques, and to use these techniques to elucidate the ionization of certain complexes of interest to us. Because they had already received some attention in this laboratory and in others, the adducts of sulfur and selenium tetrafluorides were chosen for investigation.

Previously, some conductivity measurements on simple bases such as alkali metal fluorides had been reported, but the data was not adequate to enable a definite interpretation of conductivity data on solutions of more complex electrolytes. Therefore, an extensive program of conductivity measurements on univalent fluorides, divalent fluorides and salts such as potassium hexafluorophosphate was undertaken in order to provide a satisfactory basis for the

interpretation of the data obtained in the latter part of this work, and to compare the conductivities of electrolytes in hydrogen fluoride with those of analogous electrolytes in water and strong acid solvents.

The structures of adducts of sulfur tetrafluoride with various fluoride acceptor molecules such as boron trifluoride or antimony pentafluoride had been the object of considerable speculation and ionic structures based on the trifluorosulfur (IV) cation, e.g. $SF_3^+BF_4^-$, had been proposed. It was therefore decided to study the behaviour of these adducts as electrolytes in hydrogen fluoride solution by conductivity and nuclear magnetic resonance spectroscopy.

Adducts of thionyl tetrafluoride (sulfur oxytetrafluoride) with Lewis acids had also been reported and ionic structures proposed, but as there was no experimental evidence for these, it was decided to investigate these adducts as electrolytes in hydrogen fluoride solution also.

Similar adducts of selenium tetrafluoride had been prepared and studied, but they had not been investigated in hydrogen fluoride. Consequently, a similar conductivity and nuclear magnetic resonance study was carried out on the adduct, $SeF_4 \cdot BF_3$.

During the course of this work it was discovered that other sulfur compounds such as thionyl fluoride, methyl sulfuryl fluoride and sulfur dioxide form adducts with the Lewis acids used in this work. As their behaviour was found to be different from the other adducts

studied in that they decompose in hydrogen fluoride solution, they were studied in an inert solvent to obtain more general information on the structure and stability of Lewis acid adducts of sulfur compounds.

CHAPTER II

PREPARATION AND PURIFICATION OF MATERIALS

Anhydrous Hydrogen Fluoride

The toxic nature of hydrogen fluoride, and the difficulty in obtaining anhydrous hydrogen fluoride of sufficient purity for conductivity studies required handling by vacuum line techniques. However, the attack on glass by hydrogen fluoride necessitates using other construction materials. Initial transfer of hydrogen fluoride from the cylinder and preparative reactions were carried out in an all Monel vacuum line. Monel is a nickel copper alloy which forms a protective fluoride coating on initial exposure to HF and then resists any further attack.

High purity acid for conductivity and nmr studies was only allowed to come in contact with fluorocarbon plastics and platinum metals. Kel-F (polytrifluorochloroethylene) was the major construction material. It is transparent, completely inert to liquid hydrogen fluoride and its hardness makes it relatively easy to machine.

The more familiar fluorocarbon Teflon (polytetrafluoroethylene) was used to a much lesser extent. Though also completely resistant to the fluorides that were used in these experiments, it is white, translucent, and much softer than Kel-F. Thus, it was used primarily as a gasket material to achieve a vacuum tight seal when constructing the Kel-F equipment.

A glass vacuum line was also used in these experiments for preparation of compounds and drying of conductivity cells. Evacuated by a mercury diffusion pump, backed by a two stage mechanical pump, the line could be evacuated to 3×10^{-3} mm Hg. Kel-F 90 grease (3M Company) was used when working with reactive fluorides. In the section of the line not exposed to volatile fluorine compounds, Apiezon N and T greases were used.

Until the development of fluorocarbon plastics and the fabrication of vacuum lines from them, much greater experimental difficulties attended the use of HF. Construction materials used include platinum, silver, copper and nickel metals. However, visual observation of reactions and solubilities was of course impossible through these. As well, all these materials conduct a current and are unsuitable for conductivity cells. Conductivity cells were constructed out of wax by Hill and Sirkar [66] and gold and platinum with sulfur insulating the electrodes by Fredenhagen and Cadenbach. [67] Even fused quartz was used as a vessel in the qualitative observation of solubilities although it was slowly, but appreciably attacked. [68]

Early workers usually prepared anhydrous hydrogen fluoride by heating dried potassium hydrogen fluoride and further purified the HF by distillation. Hill and Sirkar dried the KHF_2 by heating and subsequently keeping it over sulfuric acid. It was then heated in an all platinum still, and the HF purified by repeated distillation. They obtained acid with a minimum conductivity of 2.7×10^{-2} mhos/cm, more than an order of magnitude greater than the present-day commercial product. [66]

Fredenhagen and Cadenbach dried their KHF_2 more rigorously. They found that almost all of the water remaining in the KHF_2 came over with the first 30% of the HF evolved. They discarded this first fraction and redistilled the rest of the HF collected. After repeated washing of their conductivity cell, acid was obtained with a conductivity of 1.4×10^{-5} mhos/cm. (67) Until comparatively recent times, this was the best acid produced. They used all silver equipment, except for the conductivity cell described on the preceding page.

Simons further dried the KHF_2 by electrolysis of the molten salt, continued until fluorine was evolved, indicating that all the oxygen had been evolved. (69) He then drove off the HF in copper equipment. As he points out, this should have been the best acid yet produced, but he reported no conductivity measurements on it.

Even as recently as 1953, acid of lower conductivity than that of Fredenhagen had not been obtained, Kilpatrick and co-workers using acid with a conductivity of 5×10^{-5} mhos/cm at -15°C. (30) However, Runner, Balog and Kilpatrick subsequently obtained acid with a conductivity of 1.6×10^{-6} mhos/cm at 0°C. (70) They used a Kel-F reflux distillation column which has been the design basis for most subsequent research groups, and Kel-F conductivity cells.

Shamir and Netzer have described a Kel-F distillation column in which the purified HF is taken off as the liquid condensate, rather than in the gas phase as done by all previous workers. (71) The design they describe allows somewhat larger amounts of consistently

low conductivity acid, in the order of 10^{-6} mhos/cm at 25°C, to be routinely obtainable. This is the lowest conductivity reported for liquid hydrogen fluoride.

Techniques for the manipulation of volatile fluorides have been reviewed in the series, "Techniques of Inorganic Chemistry." [72] Recent reviews on the hydrogen fluoride solvent system [7, 9] contained sections on equipment and on handling techniques.

Hydrogen fluoride was obtained as a liquid under pressure in steel cylinders from two sources, Matheson of Canada Ltd. and the Harshaw Chemical Co. Acid from both sources had to be purified before use. Impurities present were water, sulfur dioxide, fluorosulfuric acid, and silicon tetrafluoride, to a total of about 0.1%. The principal impurity present, water accounts for almost all the solvent conductivity. The 99.9% pure commercial acid has a conductivity of the order of 10^{-3} mhos/cm at 0°C. This compares with the lowest reported conductivity of 1×10^{-6} mhos/cm at 25°C. [71]

The vacuum line used in the purification is illustrated in Figures 2.1 and 2.2. The main manifold was 1/2" o.d. Monel tubing. Connections leading from it were 1/4" o.d. Monel tubing. The metal trap protecting the vacuum pump was also made of Monel. Originally, a copper trap was used, but the high thermal conductivity of copper caused the liquid nitrogen coolant to evaporate too quickly. However, if an automatic filling device were available copper would be a better material for construction of the trap. The vacuum manifold, the metal trap, the

Figure 2.1
HF Vacuum Line

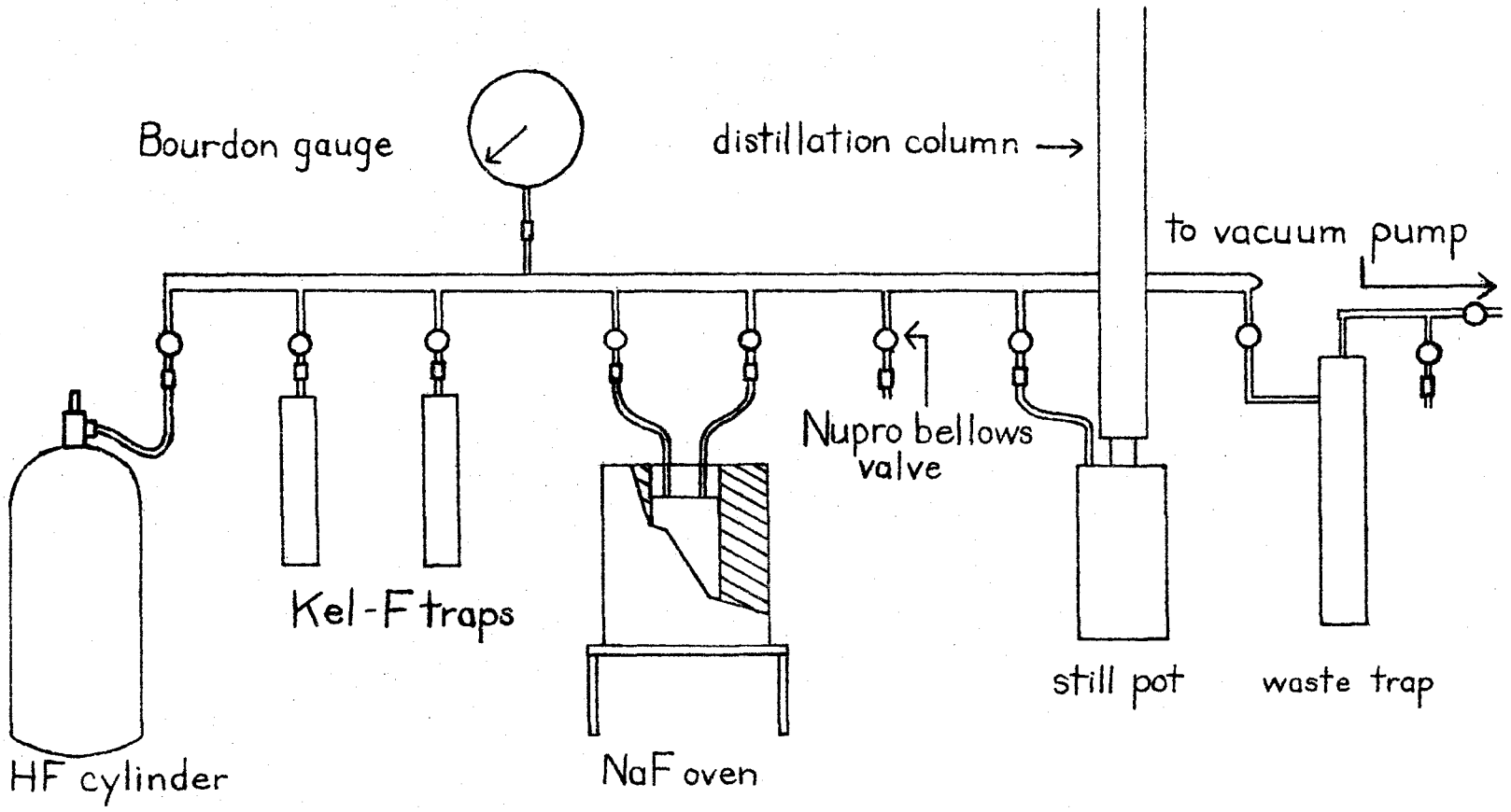

Figure 2.2
HF Line
High Purity Section

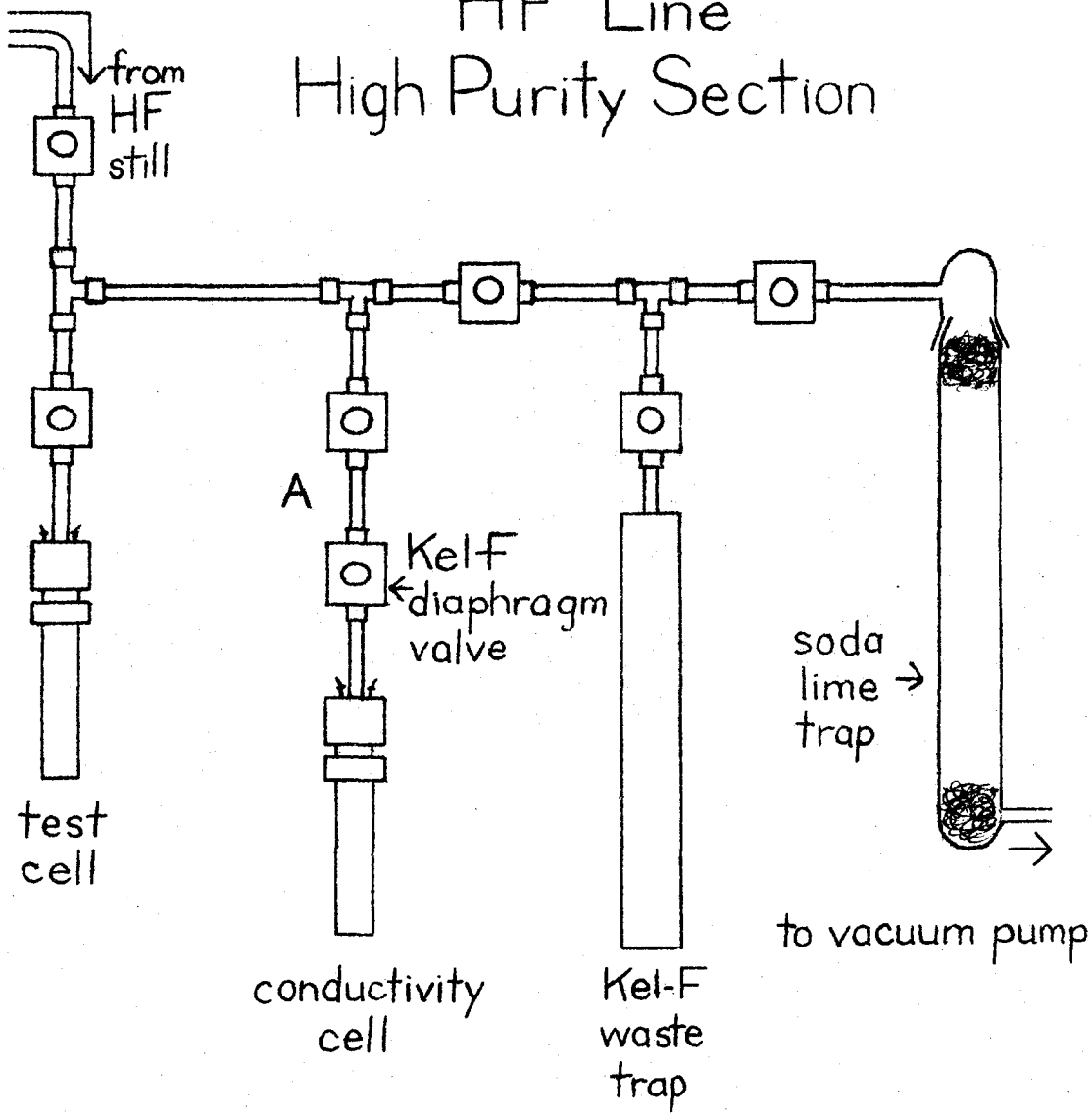

still pot and the sodium hydrogen fluoride ($NaHF_2$) oven were all constructed from Monel tube and plate which had been welded together under an argon atmosphere. After all leaks were initially eliminated, no further leaks developed at any joint.

The pressure in the vacuum manifold was measured using a Taylor Instrument Company model 62KF138 Monel Bourdon gauge adjusted to read 0 to 25 psia.*

Monel diaphragm valves (Nupro model M4B-K) were used throughout the metal part of the line. They were attached by 1/4" "Swagelock" couplings, which were one of the features of this type of valve. This type of coupling, in various materials, was used extensively throughout this work, even for joining together two pieces of glass tubing when a greaseless high vacuum joint was needed.

The manifold was wrapped with heating tape and kept at about 100°C. The heat was only turned off when HF was condensed into the still pot.

The large traps were drilled out of solid Kel-F rod. The end was threaded and a Kel-F top terminating in a 1/4" tube was screwed on. The trap was then attached to the line through the Swagelock coupling on the valve.

The distillation column was a 3 foot length of 1" o.d. heavy wall Kel-F tubing, packed with 5 mm Kel-F tubing chopped up so that the

---

* The units of pressure psia and psig stand for pounds/sq. in. absolute and pounds/sq. in. gauge measured relative to a vacuum and relative to atmospheric pressure respectively.

length was about the same as the diameter. At the top of the column was a rhodium plated Monel cold finger, cooled by tap water. (The water temperature measured after exit from the cold finger varied from 5°C in winter to 15°C in summer.) Details of construction of the vacuum seals at the ends of the column are shown in Figures 2.3 and 2.4.

After the distillation column only Kel-F or Teflon tubing was used. Special heavy-duty all Kel-F diaphragm valves were used (Fig. 2.5). They held a good vacuum and pressures of over 100 psig. Unlike the commercial Teflon valves, the Kel-F threads did not strip readily and they stood up well to use and abuse.

Hydrogen fluoride was condensed from the cylinder into a Kel-F trap with liquid nitrogen. The trap was evacuated to remove any permanent gases, and then allowed to warm to room temperature. The oven containing NaF pellets which had been previously vacuum dried was warmed to 200°C and the HF was absorbed by the sodium fluoride. The oven was then allowed to cool. It was then evacuated while being heated to 180°C over a period of 3 - 4 hours. The temperature was further increased and the first fraction of HF driven off was condensed in a trap and discarded. The remainder was collected in a second trap and subsequently condensed into the still pot with liquid nitrogen. In every step where HF was distilled from a trap, a small fraction was left behind at the end. Water impurity will concentrate in this fraction. The still pot was heated with an oil bath at about 35°C and the HF was refluxed for about an hour. It was then condensed into the test cell with an ice bath.

Detail of HF Still Pot Vacuum Seal

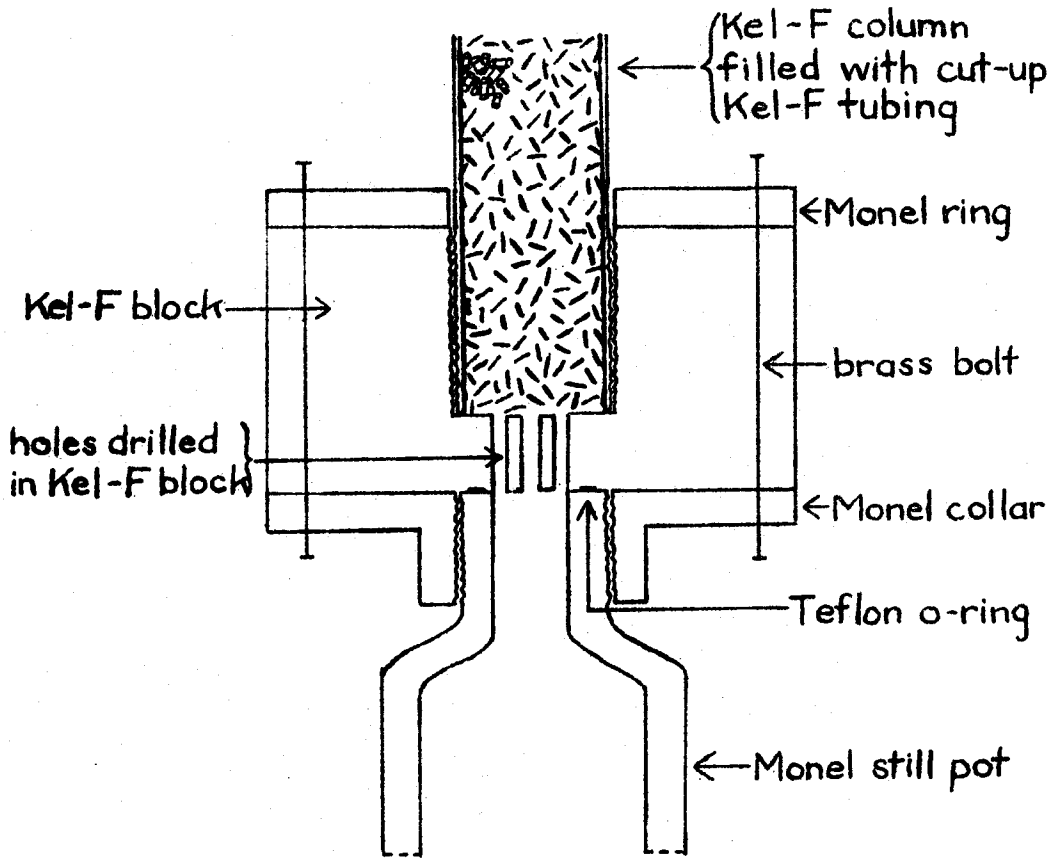

Figure 2.3

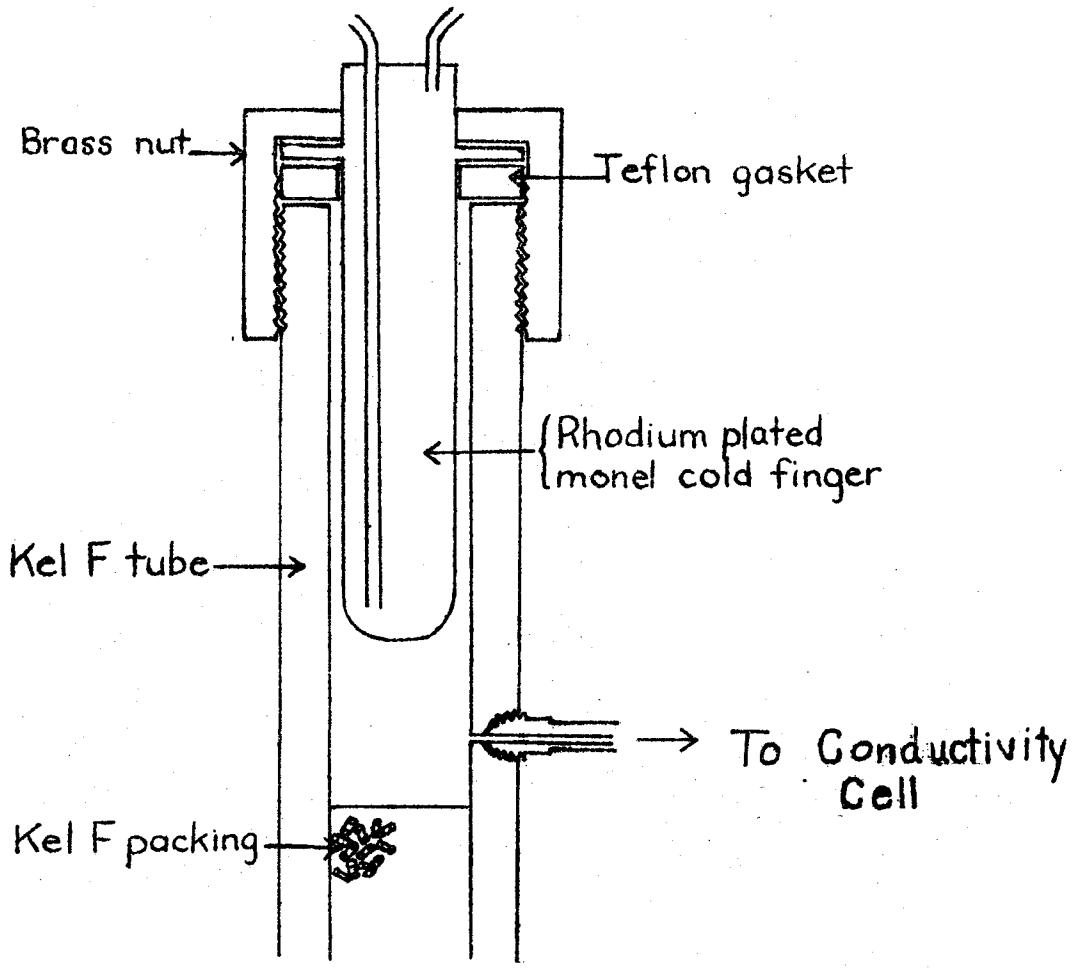

Detail of Cold Finger Vacuum Seal

Figure 2.4

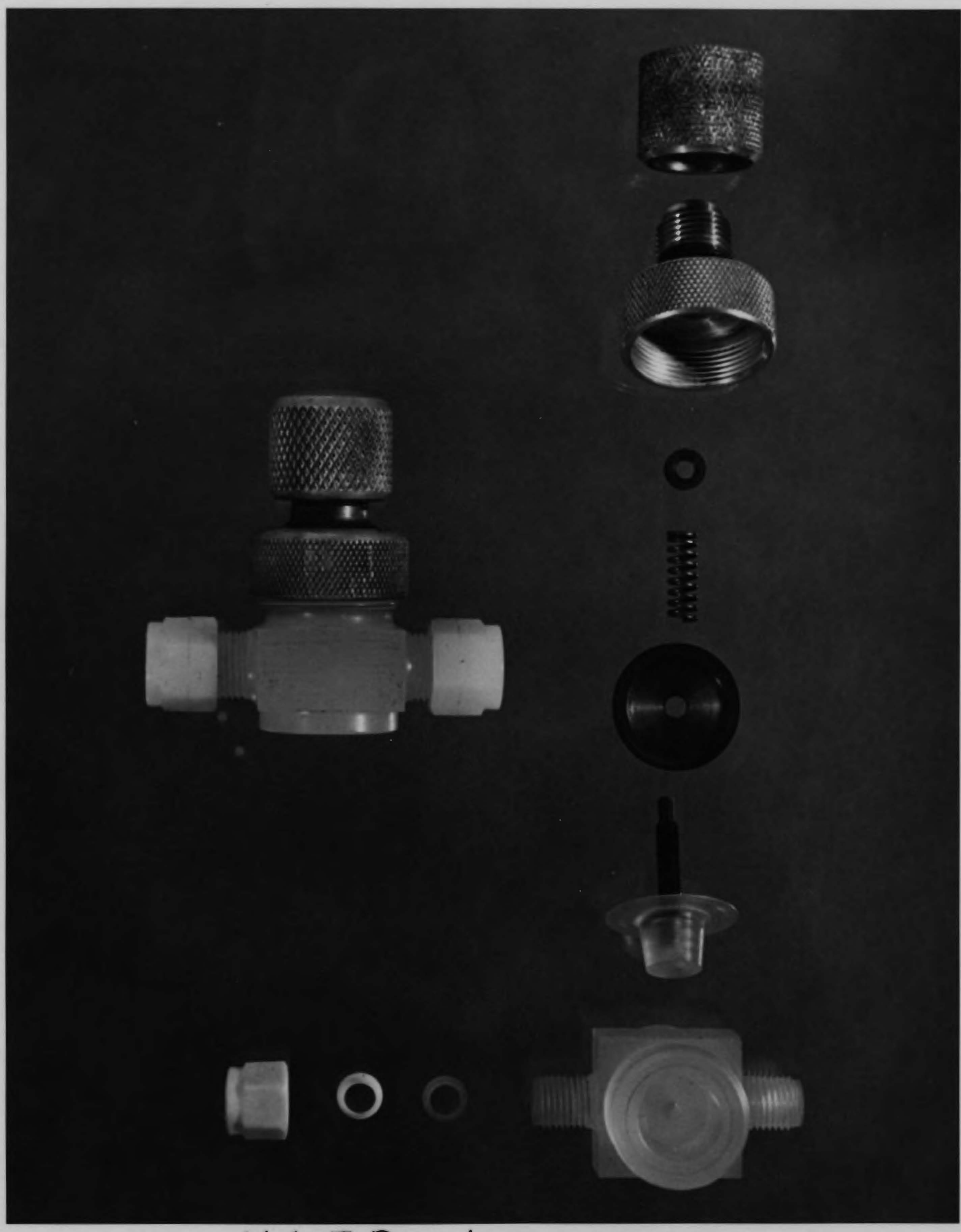

Kel-F Diaphragm Valve

Figure 2.5

The conductivity of the acid was checked using the resistance range of a Heathkit capacitor checker model IT-11 (accuracy ±5%). If the conductance was too high, the hydrogen fluoride was distilled into the waste HF trap. When useable acid was obtained, it was then distilled into the conductivity cell or nmr tube attached at A (Fig. 2.2). HF used in this work had a conductivity in the range 10^{-5} to 10^{-4} mhos/cm and only the lower part of this range was used as a solvent for study in dilute solutions. This corresponds to a water concentration of from 2.5×10^{-5} to 2.5×10^{-4} molal.

It was found that an appreciable improvement in conductivity was not obtained from pumping on the hot sodium bifluoride so this was discontinued in the latter stages of this work and the HF was condensed directly from a Kel-F trap into the still pot.

Aqueous Hydrogen Fluoride:

Baker and Adamson reagent grade 48% HF was used

Uni- and Di-valent Metal Fluorides:

The commercially obtained materials were dried before use. The fluoride was placed in a platinum crucible, which was placed in a glass vessel to be evacuated (Fig. 2.6). After being pumped on for a day, the fluoride was slowly heated to 220°C on a silicone oil bath while being pumped on, and then held at this temperature for a day before being allowed to cool. It was then stored in a desiccator over phosphorus pentoxide. Unless stated, no further purification was carried out.

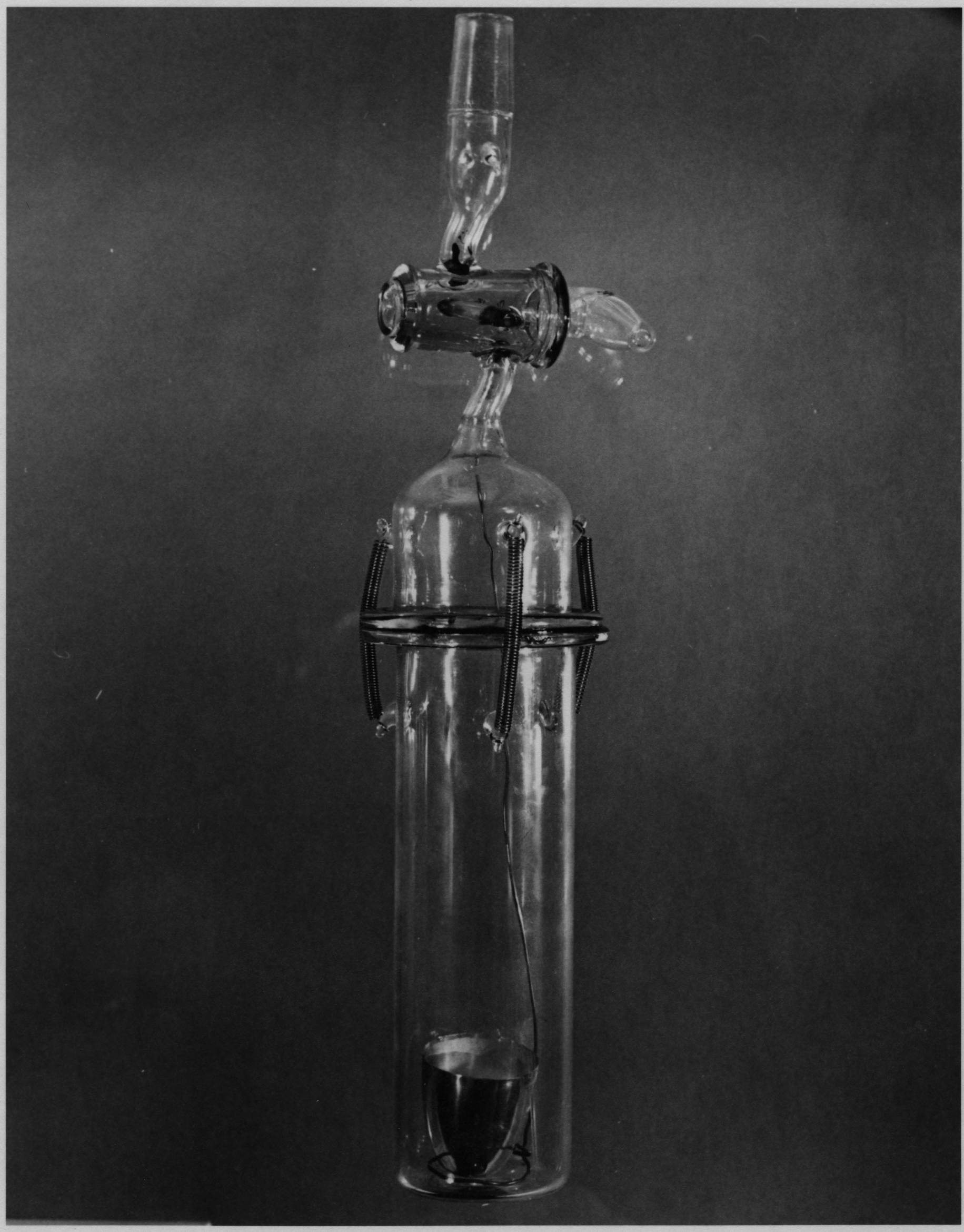

Apparatus for Drying Solids

Figure 2.6

Because of the very hygroscopic nature of a number of compounds used in this work, all operations involving their transfer, i.e. loading and unloading of the vacuum dryer, loading of conductivity cells, etc., were carried out in a drybox. Substances which were not hygroscopic were handled in the open air.

The lithium, sodium and calcium fluorides were Fisher Scientific Co. reagent grade chemicals. Baker and Adamson reagent grade, anhydrous potassium fluoride was used. Besides being dried as described above, a portion was fused in a platinum crucible. B.D.H. reagent grade potassium fluoride was used as well. All samples of potassium fluoride gave the same conductivity curves when dissolved in HF.

Rubidium fluoride (99.9%) and cesium fluoride (99.9%) were obtained from K & K Laboratories. They were dried as described above, being heated until constant weight was reached.

Thallium fluoride (99.9%) was obtained from K & K Laboratories. It was further purified by vacuum sublimation in a Vycor sublimation apparatus as described by Barrow et al. [73]

Strontium fluoride was prepared as described by Kwasnick. [74] Reagent grade strontium carbonate (J.T. Baker Chemical Co.) was reacted with excess 48% HF, in a Pt dish. It was evaporated to dryness, washed with 48% HF, and again evaporated to dryness. It was then dried as described above, until constant weight was reached. An X-ray powder photograph of the material showed no lines other than those

due to strontium fluoride.

Barium fluoride was prepared by the same method as strontium fluoride, using reagent grade barium carbonate (B.D.H.). An X-ray powder photograph of the material showed no lines other than those due to barium fluoride. Lead difluoride (B.D.H. extra pure) was vacuum dried before use.

Salts of Fluoride Acceptors:

Ozark-Mahoning Co. potassium hexafluorophosphate (98% minimum) was recrystallized twice from water, and dried at 200°C under vacuum.

Potassium hexafluoroarsenate was prepared from Matheson, Coleman and Bell reagent grade potassium arsenate according to the method of Dess. [75] The potassium arsenate was reacted with 48% HF to give $KAsF_5OH$. This was then treated with anhydrous HF several times to ensure complete conversion to $KAsF_6$. The $KAsF_6$ was recrystallized once from water, and then dried under vacuum at 200°C. It was analyzed for As by Dr. J. Passmore, (found 32.83%; calculated 32.85%).

Potassium hexafluoroantimonate from several sources was used. It was prepared by a modification of the method of Mazeika [76] starting from 48% HF and reagent grade potassium antimonate (B.D.H.). In addition, $KSbF_6$ was used as supplied from Ozark-Mahoning Co., after drying in vacuum. A second portion from this source was recrystallized from 48% HF. All samples gave the same conductivity curve when dissolved in anhydrous HF.

Sodium hexafluoroantimonate (Ozark-Mahoning Co.) was treated a number of times with anhydrous hydrogen fluoride in a Kel-F trap. Each time the supernatent liquid was poured off and the rest of the HF was pumped off. The $NaSbF_6$ was then pumped on overnight. Free flowing white crystals were obtained.

Initially, an attempt was made to prepare $NaSbF_6$ by the same method as for $KSbF_6$, i.e., from sodium antimonate and 48% HF. This material was recrystallized from 48% HF. Commercially obtained $NaSbF_6$ was also recrystallized from 48% HF. Both materials gave consistent conductivity curves, but the curves were about four times too high. Since the hexafluoroantimonate ion is known to be stable in 48% HF, the $NaSbF_6$ presumably crystallizes out with water of hydration. It appears that there are at least four molecules of water per $NaSbF_6$.

Potassium tetrafluoroborate was prepared according to Van der Muellen and Van Mater [77] by the reaction:

$$4HF + H_3BO_3 \longrightarrow HBF_4 + 3H_2O$$
$$KOH + HBF_4 \longrightarrow KBF_4 + H_2O$$

The stoichiometric amount of reagent grade boric acid was slowly added to 48% HF held at 0°C in a platinum dish. It was allowed to warm up and stand at room temperature for six hours. It was then recooled and neutralized with 5N reagent grade KOH solution to a methyl orange

end point. The crystals which came out of solution were filtered off and dried under vacuum as described earlier. When initially dissolved in water, the KBF_4 gave a negative test for fluoride with lead chloride solution.

Heterocation Salts:

Trifluorosulfur(IV) Tetrafluoroborate

The complex was prepared in a glass vacuum line. Sulfur tetrafluoride was condensed onto a slight excess of boron trifluoride in a trap. They were allowed to slowly warm until melting occurred followed by reaction. The trap was then cooled to dry ice temperature and evacuated to remove excess BF_3. The trap was warmed to room temperature and intermittently evacuated. This removes any SOF_2, which does not form a stable solid complex with BF_3 at these temperatures. The complex was then condensed into a trap with a break-seal tube and sealed off under vacuum.

The trap was then sealed on to an all glass and Teflon greaseless vacuum manifold. The break-seal was broken and the complex was condensed into a weighing trap sealed with a threaded glass Teflon valve (Fisher and Porter Co.) which was attached to the manifold with a Swagelock coupling. The first trap was drawn off. The weighing trap could be removed from the manifold and weighed on an analytical balance. Exactly known quantities of the complex could be condensed into the conductivity cell or nmr tube in this way.

Trifluorosulfur(IV) Hexafluorophosphate

Sulfur tetrafluoride was condensed onto excess phosphorus pentafluoride in the vacuum line. The mixture was allowed to warm up and react. The complex was then cooled to dry ice temperature and evacuated to remove excess PF_5 and any SOF_2 present as an impurity in the SF_4. SOF_2 does not form a complex with PF_5 and can be removed. The complex was warmed to room temperature, briefly evacuated to remove any POF_3, and the container was sealed under vacuum and stored in dry ice until used.

Trifluorosulfur(IV) Hexafluoroarsenate

This complex was preared in the Kel-F nmr sample tube or Raman capillary tube directly, since it is less volatile than the tetrafluoroborate or hexafluorophosphate. For nmr samples, the desired quantities of sulfur tetrafluoride and arsenic pentafluoride were measured by a mercury manometer. The AsF_5 was in contact with the mercury for too short a time for it to noticeably react. The SF_4 and AsF_5 were condensed into the nmr tube and then allowed to warm up and react. The complex was then pumped briefly at room temperature before connecting the tube to the HF line and adding the solvent. In the case of the sample containing excess AsF_5, the tube was not evacuated.

Trifluorosulfur(IV) Hexafluoroantimonate

Purified antimony pentafluoride was loaded into a B19 ground glass joint test tube (A) in the drybox. The tube was then placed on the

end of a manifold which had previously been flamed out under vacuum (Fig. 2.7). The vacuum was released and the top taken off the test tube only long enough to plug it into the manifold. The manifold was re-evacuated and the SbF_5 was degassed. The first small fraction of SbF_5 was pumped off and the remainder was condensed in C with a dry ice - trichloroethylene bath. A small amount was left behind in the test tube which was sealed off under vacuum at B. The SbF_5 was allowed to warm up and most of the SbF_5 was condensed by a dry ice - trichloroethylene bath at D. The previous trap was again sealed off and then the SbF_5 container and reaction vessel sealed off from the vacuum line at E.

The SbF_5 container and reaction vessel were then joined to a second manifold as shown in Figure 2.8. This was evacuated for a day before using. Sulfur tetrafluoride was purified and distilled into G. With the SbF_5 frozen in ice, the break-seal was broken by a stainless steel ball bearing. Some SF_4 was condensed into the reaction vessel. The SbF_5 was allowed to warm up and some of it was condensed onto the SF_4. The mixture was then allowed to warm up and react. This operation was repeated a number of times. A white solid formed in the reaction vessel. The SbF_5 in D reacted with SF_4 as well, so the SbF_5 no longer distilled over. The complex was then pumped on overnight to remove free SbF_5. To convert any $Sb_2F_{11}^-$ salt to the SbF_6^- salt, the complex with excess SF_4 pressure above it was then

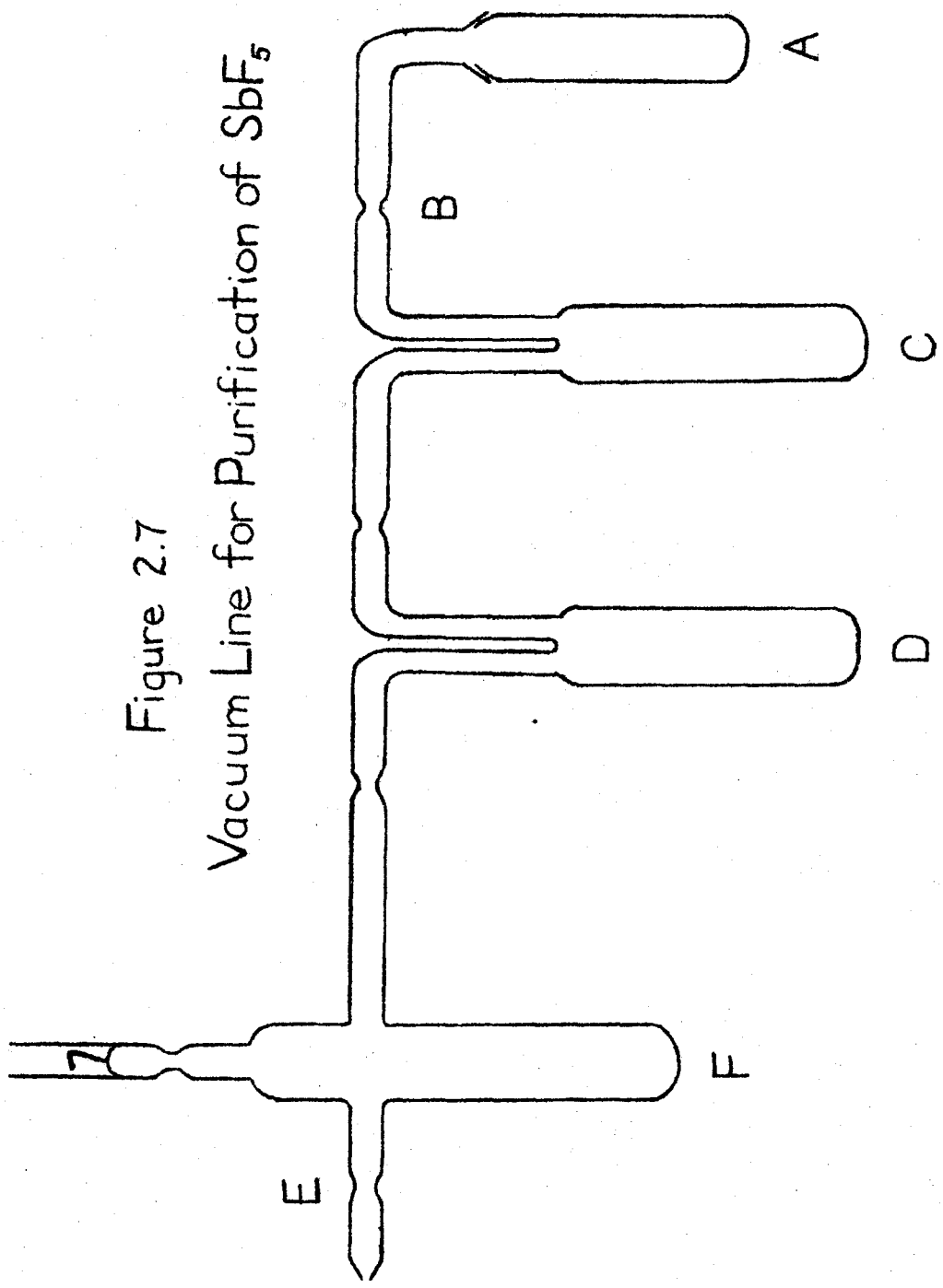

Figure 2.7
Vacuum Line for Purification of SbF_5

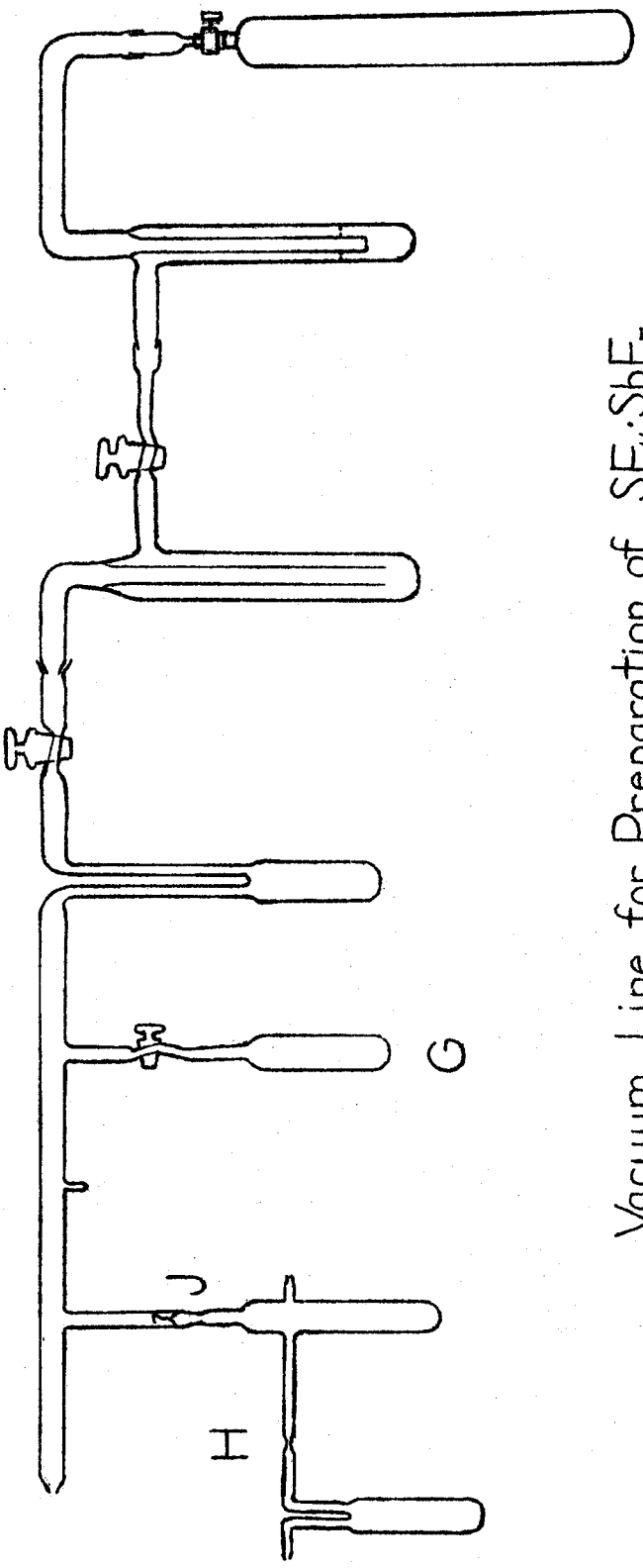

Figure 2.8

Vacuum Line for Preparation of $SF_4 \cdot SbF_5$

heated by an oil bath to 200°C for a period of several days. The complex was allowed to cool for a day with an atmosphere pressure of SF_4 above it, and then it was pumped on for a day before sealing off the reaction vessel under vacuum at H and J. The reaction vessel was opened in the drybox in which all transfers of the complex took place.

A powder X-ray photograph of the complex showed it to be the same material as that prepared by Bartlett. (78)

Trifluorosulfur(VI) Oxide Hexafluoroarsenate

Thionyl tetrafluoride and arsenic pentafluoride were condensed together directly into a weighing trap. They were allowed to warm up in dry ice - trichloroethylene slush bath and react. Any excess reactant was pumped off at dry ice temperature. The compound was then warmed to room temperature and pumped on to remove other sulfur oxyfluorides, which do not form stable complexes with AsF_5 under these conditions. The weighing trap was transferred to the greaseless vacuum line and the compound was distilled directly into the conductivity cell or nmr tube. Quantities were measured by weight difference.

Trifluoroselenium(IV) Tetrafluoroborate

$SOF_4 \cdot SbF_5$ was kindly supplied by Dr. P. A. W. Dean. It had been prepared in a glass vessel consisting of two arms separated by a glass sinter. One arm was sealed and the other terminated in a 1/4" o.d. glass tube. SbF_5 was introduced into the open arm in the drybox.

The vessel was then connected to a vacuum line by a Teflon valve so no contact with grease could occur. A slight excess of SOF_4 and the solvent $SO_2C\ell F$ were condensed onto the SbF_5 and the vessel was sealed off.

When the vessel was warmed to room temperature and shaken, a white solid formed. This was allowed to digest for about an hour. The solvent containing impurities such as $SOF_2 \cdot SbF_5$ and $SO_2 \cdot SbF_5$ was filtered into the other arm through the glass sinter, leaving behind $SOF_4 \cdot SbF_5$. It has been previously shown that these former types of adducts with SbF_5 are soluble in $SO_2C\ell F$. [79] The $SO_2C\ell F$ was then recondensed onto the $SOF_4 \cdot SbF_5$, leaving any impurities behind in the second arm. After a second digestion, the $SO_2C\ell F$ was again filtered into the second arm. This digestion and filtration was repeated a number of times. Finally, the second arm was cooled in liquid nitrogen to remove any last traces of $SO_2C\ell F$ from the $SOF_4 \cdot SbF_5$, which was then sealed off, resulting in an ampoule of the pure adduct. The ampoule was broken in the drybox, where all subsequent manipulations of the adduct were carried out.

Trifluoroselenium(IV) Tetrafluoroborate

Selenium tetrafluoride (3.9 grams) was distilled into a Kel-F trap. Hydrogen fluoride (14 grams) was distilled into the trap on the HF line to act as a solvent for the reaction. The trap was cooled in a dry ice slush bath and the line was then filled with boron trifluoride. The BF_3 pressure dropped and white crystals were precipitated. BF_3 was admitted to the line until no more was absorbed. The trap was held

for several hours at dry ice temperature with excess BF_3 pressure over it. The excess BF_3 was pumped off and the trap was allowed to slowly warm in order to pump off the HF. When all the HF appeared to be gone, the trap was transferred to the glass line and pumped on (yield 4.86 grams; 81% based on SeF_4). The product was purified in a Vycor sublimation apparatus at room temperature onto an ice cooled cold finger. The melting point of the purified compound was 53.5 - 55.3°C (lit. 54.0 - 55.3°C). (80)

Other Compounds:

Boron trifluoride (C.P. grade 99.5% minimum), sulfur dioxide (anhydrous grade 99.98% minimum), phosphorus pentafluoride (99% minimum), sulfuryl fluoride (99.5% minimum) and $CFC\ell_3$ (99.5% minimum) were obtained from Matheson of Canada Ltd. and used without further purification. The purity of the phosphorus pentafluoride was checked by observing its IR spectrum in a 10 cm Monel gas cell with silver chloride windows. Only bands attributable to phosphorus pentafluoride were observed. The purity of the sulfuryl fluoride was checked by its ^{19}F nmr spectrum, in which only one line was observed.

Sulfur tetrafluoride (Matheson of Canada Ltd.) was purified by bubbling through mercury to remove $SC\ell_2$ and then distilling on the vacuum line. Its purity was checked in the IR gas cell and it was found to contain 5% thionyl fluoride (SOF_2).

Thionyl fluoride (Peninsular Chemresearch Inc.) was used without further purification. It showed only one line in the ^{19}F nmr spectrum and no extraneous bands in its IR spectrum.

Thionyl tetrafluoride (SOF_4) was prepared by the method of Smith and Englehardt [81] by the reaction:

$$SF_4 + 1/2\ O_2 \xrightarrow{NO_2} SOF_4$$

Sulfur tetrafluoride (0.64 moles), oxygen (0.5 moles) and nitrogen dioxide (0.10 moles) were heated in a stainless steel bomb at 215°C for seven hours. The bomb was allowed to cool, and bled to the atmosphere through a dry ice - trichloroethylene cooled trap. The crude product which was trapped out was purified by condensing it on dimethylformamide in a metal can and allowing it to stand at room temperature for half an hour. It was then pumped off at room temperature. The purification was repeated with fresh dimethylformamide. This is supposed to remove most of the major impurities, other than sulfuryl fluoride. The product purity was checked by its ^{19}F nmr spectrum and found to be: SOF_4, 86%; SOF_2, 5%; SO_2F_2, 9%. No SF_4 was detected.

Arsenic pentafluoride (Ozark-Mahoning Co.) was used without further purification. Its purity was checked in the IR gas cell and no extraneous bands were found.

Antimony pentafluoride (Ozark-Mahoning Co.) was purified by double distillation in an atmosphere of dry air using an all glass

apparatus as has been previously described. [82] It was then distilled in vacuum before use.

Methyl sulfuryl fluoride (Eastman Organic Chemicals) was distilled and stored over molecular sieves.

Selenium tetrafluoride was prepared according to the procedure of Dodd and Robinson [83] by the reaction:

$$Se + 2F_2 \xrightarrow{0°C} SeF_4$$

Selenium metal was sublimed onto the walls of the glass reaction vessel to convert it to finely divided red seleium. A 1:1 fluorine - nitrogen mixture was passed over it. The fluorine was diluted and the reaction vessel kept at 0°C to prevent formation of selenium hexafluoide. The selenium tetrafluoride was distilled into a glass receiver with a break-seal and sealed off under vacuum. The selenium tetrafluoride was stored at dry ice temperature and purified by trap to trap distillation before use. ^{19}F nmr showed not more than 1% of fluorine containing impurities.

CHAPTER III

EXPERIMENTAL TECHNIQUES

Conductivity Measurements

The conductivity cell was constructed so that only fluorocarbon plastic and platinum came in contact with hydrogen fluoride (Fig. 3.1, 3.2). The cell compartment and cell top were both machined from Kel-F rod. The platinum leads passed through Teflon gaskets which were compressed to give a vacuum seal by hollow brass machine screws threaded into the Kel-F. A Teflon gasket was also used in a compression seal between the cell top and cell compartment. The 0.005" thick platinum foil electrodes were spot welded to the 0.025" diameter platinum lead wires so no other metal was present in the cell compartment.

In the type I conductivity cell, the platinum electrodes hung unattached to the cell compartment so the cell could be disassembled if desired. They were kept a fixed distance apart by a Kel-F spacer in which they were held against a ledge by Teflon washers of a diameter to give a very tight fit.

To prevent the cell constant from varying as a function of solution height, the lead wires were sheathed in Teflon "shrink fit tubing", (Pennsylvania Fluorocarbon Co.) which was then collapsed around the leads with hot air to give a tight seal. The effectiveness of the sheathing can be seen on platinization of the electrodes. Although the

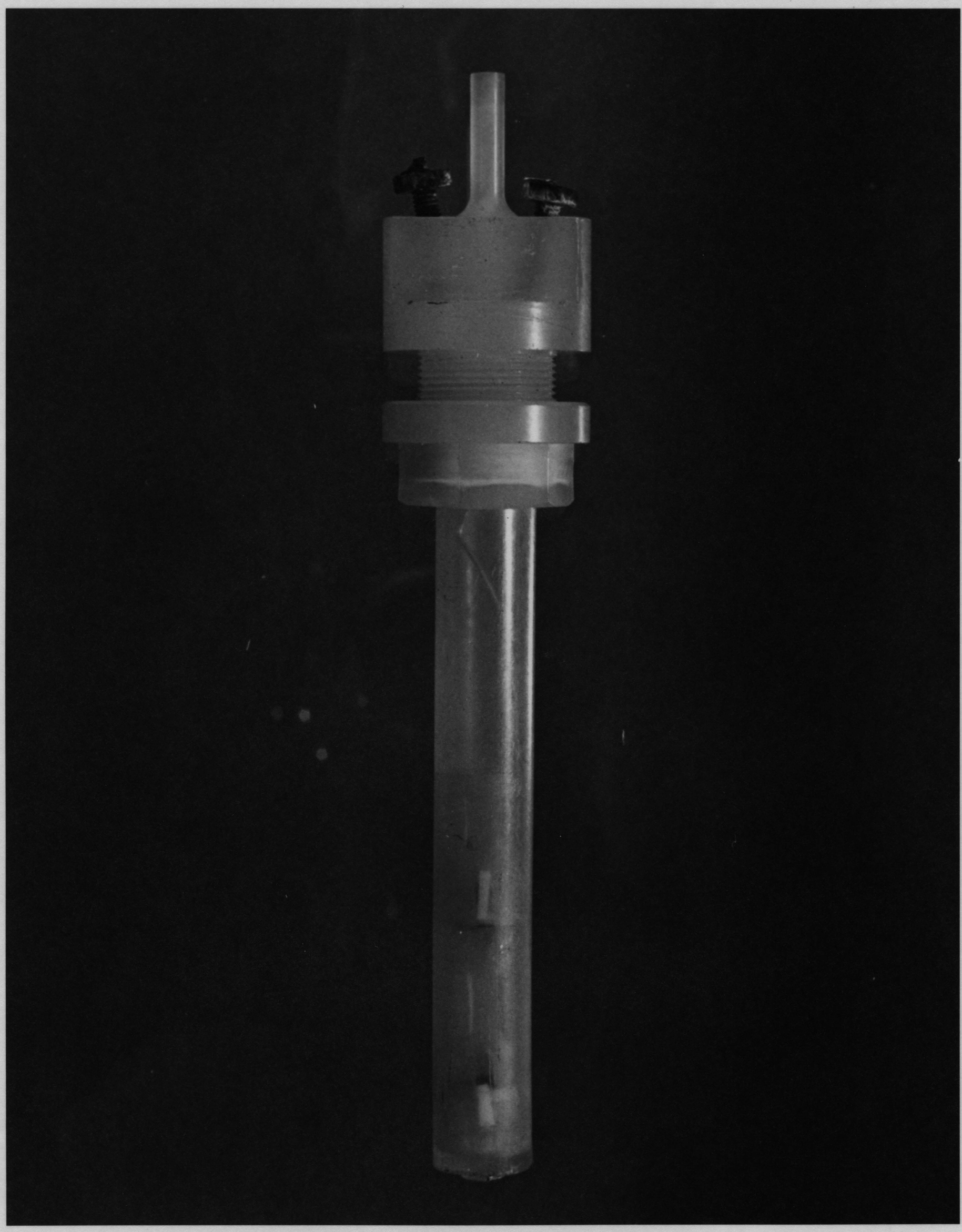

Type I Conductivity Cell
Figure 3.1

Type I Conductivity Cell

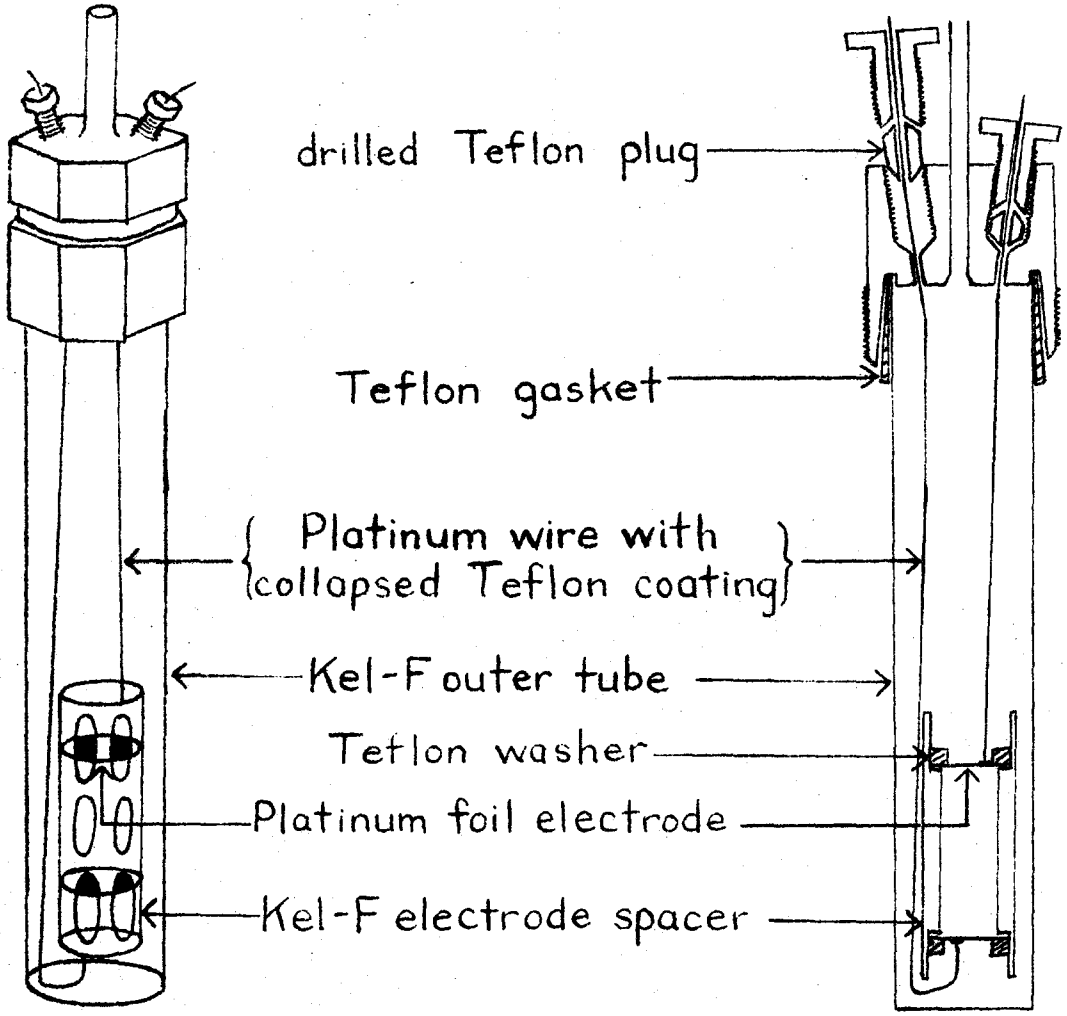

Figure 3.2

cell was filled with platinizing solution, no platinum black was deposited on any part of the sheathed lead wire, either in the initial platinization or on replatinizing after the cell had been in use for some time. This was not the case with earlier attempts in which Kel-F spaghetti tube was placed around the wires and the ends squeezed shut with hot pliers.

The type II cell had the same construction design as the type I cell for achieving a vacuum tight seal where the platinum lead wires were brought out of the cell, and between the cell compartment and top (Fig. 3.3, 3.4). However, there were two cell compartments with an electrode in the bottom of each, held against a ledge in the Kel-F compartment wall by a Teflon washer. The compartments were connected by two hollowed-out Kel-F bars, on which Swagelock fittings had been machined. The aluminum bars holding the two compartments were to increase structural rigidity. As the lead wires were so far apart, it was not necessary to put an insulating sheath on them. This eliminated all chance of anything being trapped inside the sheath.

Both the type I and II cells showed no leaks when checked under vacuum with a helium leak tester. They also showed no leaks when pressured up to 100 psig with Freon 12 ($CF_2C\ell_2$) and examined with a thermal conductivity leak detector (Bacharach Industrial Instrument Co., model SA63) which on its most sensitive range detects a leak rate of 1/2 oz. of Freon 12 per year.*

*This corresponds to a leak rate of 1.6 milligrams of Freon 12 per hour.

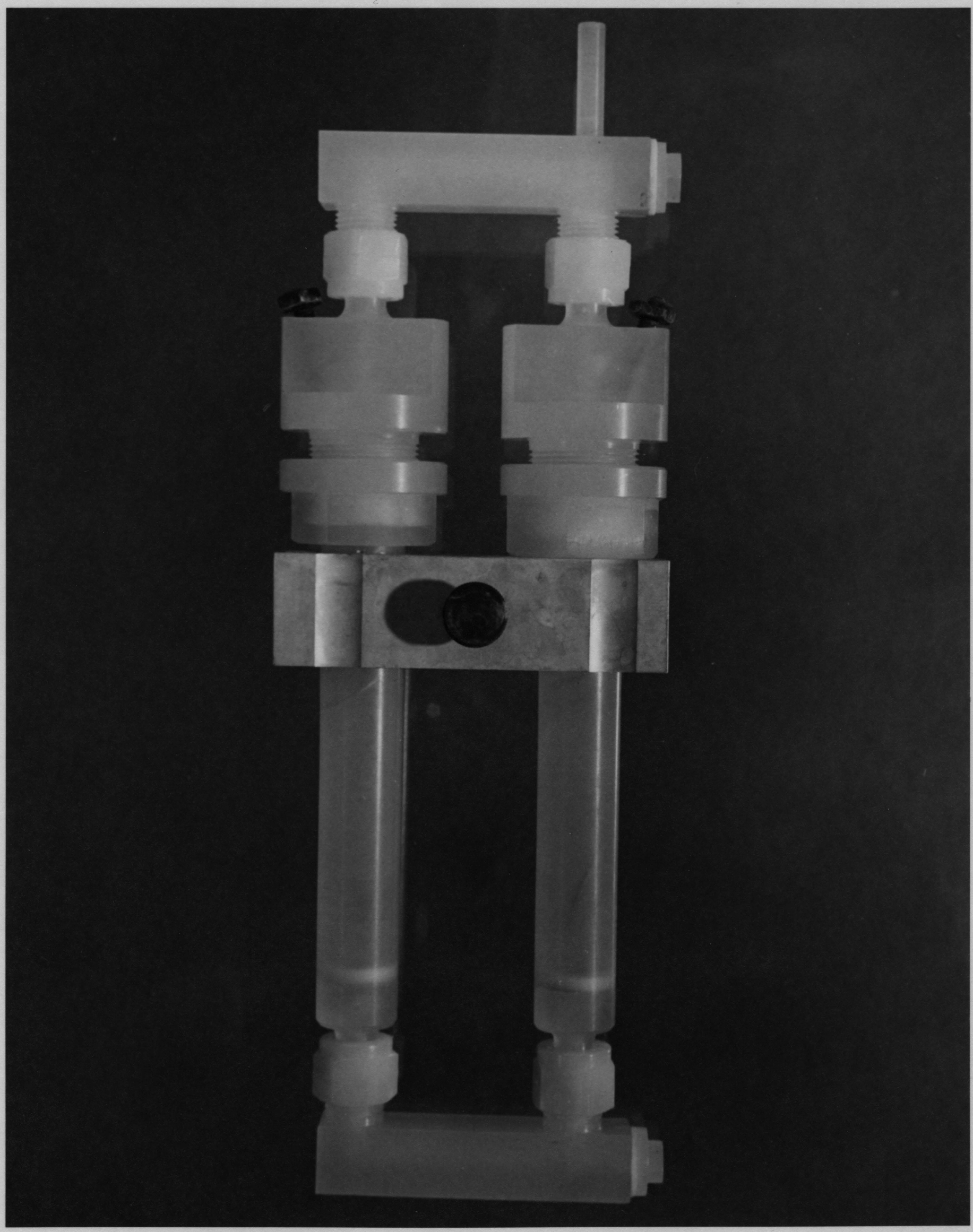

Type II Conductivity Cell
Figure 3.3

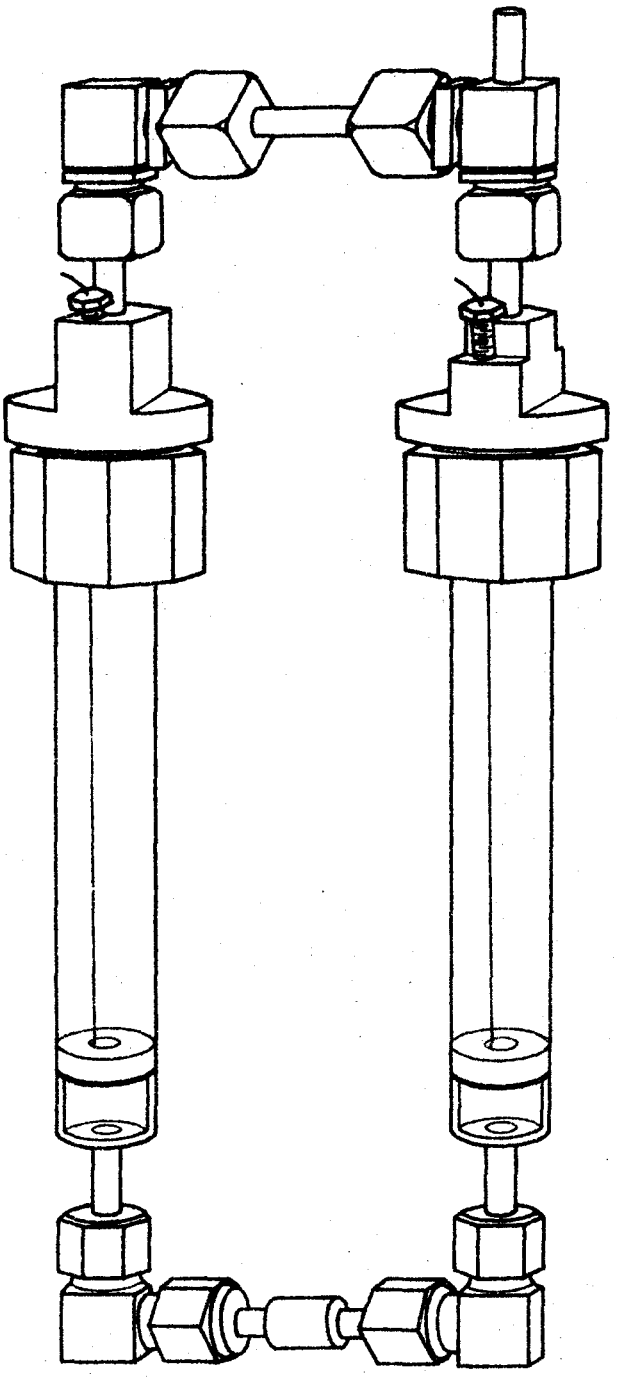

Type II Conductivity Cell

Figure 3.4

The platinum electrodes were platinized to reduce polarization errors. The cells were calibrated with a 0.1 Demal solution of potassium chloride [84] at 25.00±0.01°C in a regulated oil bath. It was found that some of the HF solutions attacked the platinum black coating. This difficulty was overcome by replacing the platinum electrodes, leads, and coating with the chemically more resistant rhodium. This completely eliminated any problems with attack on the electrodes.

Initially, a conductivity cell was washed with conductivity water until clean. It was dried under vacuum and washed and conditioned with hydrogen fluoride. Then, before each run, the cell was washed with conductance water and dried over night on the vacuum line. The valve was then attached and the entire cell and valve were evacuated for another half-day. Nonvolatile solids were added from a weight dropper. If the solid was hygroscopic, the addition was carried out in a dry box. The conductivity cell was then re-evacuated and weighed. HF was condensed into the cell with an ice bath from the test conductivity cell where its purity was checked. The quantity of HF added was determined by weight difference. The conductivities of the solutions were measured at 0.00±0.01°C. This temperature was obtained with a stirred bath containing ice and distilled water. The constancy of temperature of the bath was checked with a Pt resistance thermometer. When the conductivity reached a stable value after mixing several times, additional HF was added to give a more dilute concentration. Conductivities at three to five concentrations were measured in one run.

In the early part of this work, all conductivities were measured in type I cells. However, after their development, type II cells were used for nonvolatile solids.

Conductivities of all volatile substances were measured in type I cells. Reactive solid compounds were transferrred into the cell in a vacuum manifold (Fig. 3.5) constructed entirely of glass and Teflon, so the compound would not come in contact with grease. Quantities were measured by weight difference of the storage trap. Gases were condensed int the cell on the same vacuum manifold from light-weight Monel storage traps and measured by weight difference.

Non-reactive liquids were added to the predried cells with a syringe which was weighed before and after the addition. The cell was then frozen in liquid nitrogen and the air was pumped out without losing any sample.

For the first point of a run with a volatile sample, HF was condensed into the conductivity cell with liquid nitrogen to prevent losing any of the sample. Subsequent dilutions were carried out by condensing the HF in with a dry ice - trichloroethylene slush bath.

Conductivities of solutions were measured with an Industrial Instrument, RC-18 conductivity bridge, which has an accuracy of ±0.1%.

The type I conductivity cell was similar to that used by previous workers. [85] However, the type II cell was superior for several reasons:

It has a higher cell constant, in the region of 100 cm^{-1} compared

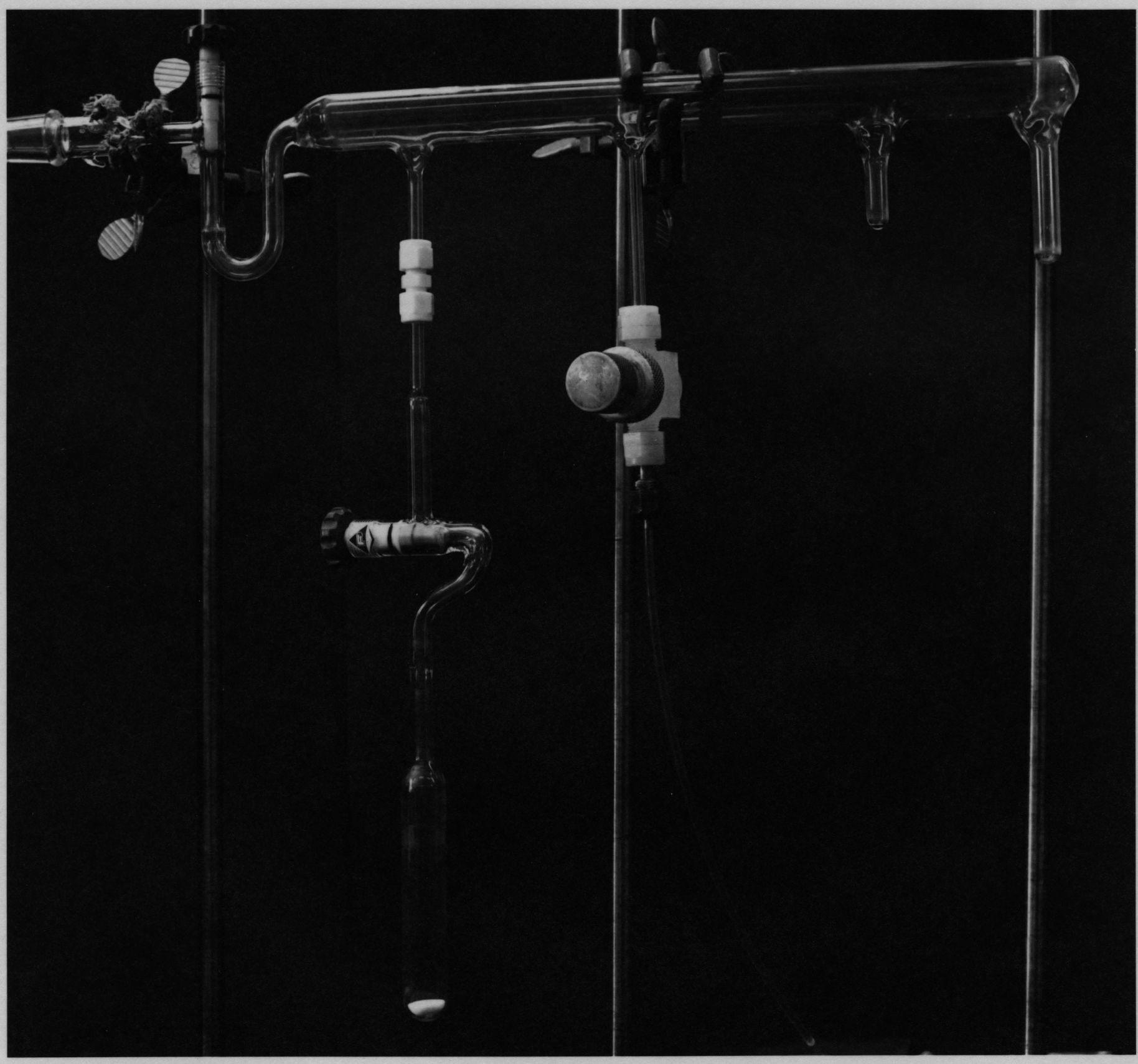

Grease Free Vacuum Line

Figure 3.5

to approximately 2 - 3 cm^{-1} for the type I cell. Thus, the measured resistance of the conducting solutions studied was in the centre of the available range of most commercial conductivity bridges, allowing greater accuracy of measurement. For checking the conductivity of the pure acid, the type I cell with its lower cell constant is preferable.

The type II cell has a larger volume, particularly in the compartments above the electrodes. This allows greater dilution of a solution so a greater concentration range can be studied in one run.

In addition, dilute solutions can be prepared more accurately, since the larger volume of solvent means a greater weight of solute for a given concentration.

In the type II cell, the electrode leads do not run up in close proximity through the same solution. The capacity between the two electrode leads is very small because of their much greater separation. As a result, the resistance measured is not a function of the current frequency of the conductivity bridge. Changing the frequency of measurement from 1KHz to 3KHz caused no measureable change in resistance within the precision of the bridge (0.01%) in its most accurate range of measurement.

Nuclear Magnetic Resonance Spectroscopy

^{19}F nuclear magnetic resonance (nmr) spectra were run on a Varian DA-60 IL nmr spectrometer operating at 56.4MHz. The 2500 Hz audio modulation sidebands forming part of the base line stabilization circuitry of the instrument usually overlapped part of the centerband

spectrum, and the "lock box" had therefore been modified to take an external manual oscillator frequency from a Muirhead D-890-A audio frequency oscillator. In this work the modulation frequency was varied up to 20,000 Hz. Spectra were then measured using the first upper sideband in the field sweep unlock mode. Some measurements were also made in the lock mode with frequency sweep using the external manual oscillator to supply a lock signal. Thus, signals which were beyond the range of normal lock mode operation (i.e. outside the limits -2000 Hz to + 1000 Hz from the lock signal) could be observed.

Low temperature spectra were obtained using a Varian V4540 temperature controller with the variable temperature probe. Proton nmr spectra were run on a Varian A-60 nmr spectrometer. A few of the proton and fluorine spectra were run on a Varian HA-100 nmr spectrometer operating at 100 MHz and 94.1 MHz respectively.

Nmr tubes for use with anhydrous HF were made from #8 AWG Kel-F tubing (0.128" o.d., 0.10" wall thickness). One end was sealed by pushing it into the end of a thin walled glass nmr tube heated in a metal block. The other end was flared for attachment to the vacuum line through a Monel adapter (Fig. 3.6). Hygroscopic solids were loaded into the nmr tubes in the dry box and they were attached to the HF line using the all Kel-F valve. Volatile compounds were condensed into the nmr tube using the vacuum manifold shown in Fig. 3.5. After filling with HF, the tube was frozen in liquid nitrogen, a section wrapped in aluminum foil and sealed by squeezing with hot pliers. During the

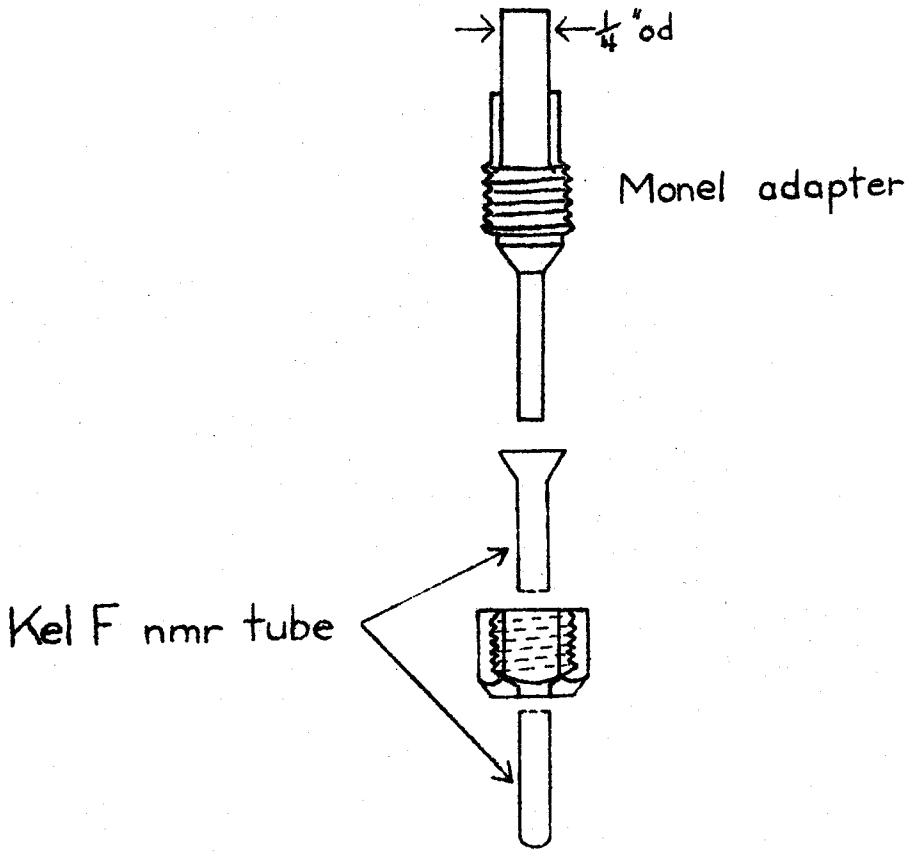

NMR Tube Adapter

Figure 3.6

course of this work, an improved sealing method was developed. An electric heating coil wound on a glass tube was used to soften the Kel-F tubing, which then collapsed under vacuum. The seal achieved by this method was more uniform and easier to make.

The Kel-F sample tube was placed inside a thin walled nmr tube, which was then placed in the nmr spectrometer probe. Generally, $CFCl_3$ was introduced in the annular space between the tubes as an external reference.

Samples not containing hydrogen fluoride were made up on the vacuum line in precision nmr tubes glassblown on to 1/4" o.d. glass tubing and attached to the line with Swagelock couplings. The amounts of gases condensed into the nmr tubes were measured by pressure difference from a calibrated vacuum line. If one of the components was a liquid at room temperature, it was added from a hypodermic syringe and measured by weight difference prior to placing the tube on the vacuum line. Some samples were prepared in tubes made from ordinary 5 mm glass tubing to enable the Raman spectrum to be run on the same sample. The precision nmr tubes available had frosted walls, and the special precision tubes with polished walls would not have been heavy enough to withstand the pressure that was often present in the tube at room temperature. When not being used, samples were stored in dry ice.

Raman Spectroscopy

Raman spectra were excited by laser illumination. A Spectra Physics model 125 He/Ne laser giving 50 mw at 6328.2Å and a Spectra

Physics model 140 argon ion laser giving up to 1 watt at 5145Å or 4880Å were used. The spectrometer was a Spex Industries model 1400 double monochromator with an I.T.T. FW 130 phototube detector, dc amplification and a strip chart recorder. The spectrometer had been calibrated with spectra of liquid indene excited by each laser line used. The Raman shift values of the lines were those of Hendra and Loader. (86) Most of these lines corresponded to standard lines approved by IUPAC for calibration of infra-red spectrometers.

Samples were loaded into 2 mm glass tubes. Volatile compounds were condensed into such tubes on the vacuum line. Samples of non-volatile hygroscopic solids were loaded into the tubes in the dry box. These latter tubes were then plugged with Kel-F grease and sealed with a flame outside the box. Some samples of low boiling liquids were condensed into 5 mm o.d. glass tubes and sealed off. The 5 mm tubes withstand a much greater pressure than the 2 mm tubes and they also enabled the nmr spectrum of the same sample to be obtained. When not being used, all reactive samples were stored in dry ice.

Sample tubes were mounted at right angles to the laser beam, and Raman scattered radiation was observed perpendicular to both these directions. This transverse excitation/transverse viewing configuration was developed at McMaster University by Dr. G. Pez. Its advantages for small samples have been well described by Freeman and Landon who showed that very good spectra could be obtained by this method on sample volumes as small as 0.008 ml. (87)

For low temperature spectra, sample tubes were mounted in a double walled quartz tube, with the space between the walls evacuated. It was silvered except for a centimeter band around the centre through which exciting radiation entered and scattered radiation was observed. Liquid nitrogen was boiled off from a dewar at a controlled rate by an electric heater and the cold gas was passed through the sample dewar. The temperature was measured with a thermocouple placed downstream of the sample.

CHAPTER IV

CONDUCTIVITY MEASUREMENTS IN HYDROGEN FLUORIDE

Introduction

It was seen in Chapter I that hydrogen fluoride is an excellent solvent for ionized solutes and the low viscosity of hydrogen fluoride results in their having a high conductivity. An obvious way of studying HF solutions therefore, is by their conductivity. The small degree of self-ionization of HF means that conductivity can also be used as a purity check, as the principal impurity is water, which is extensively protonated in dilute solution to give the conducting species H_3O^+ F^-. The improvement in purity of HF since its early use as a nonaqueous solvent as demonstrated by conductivity has been summarized in Chapter II.

Because of its high acidity, almost all ionized solutes studied in HF act as bases, either by ionizing to give a fluoride ion directly, or by accepting a proton from the solvent to leave a fluoride ion. The fluoride ion is the anion formed in the solvent self-dissociation, and is the strongest base which can exist in the HF solvent system. Stronger bases will accept a proton from the solvent. The majority of conductivity measurements that have been made have been on bases. Conversely, the strongest acid which can exist in HF is the H_2F^+ ion.

More recently, several salts have been studied as well as the acid SbF_5.

Hill and Sirkar first carried out conductivity measurements on the system HF - H_2O. [66] However, the lowest concentration of water they measured was 1 molal, and the conductivity of their solvent hydrogen fluoride indicates it was actually a 0.1 molal solution of H_2O in HF.

Much purer acid was obtained by Fredenhagen and Cadenbach and they carried out an extensive program of conductivity measurements, generally in the concentration range 0.5 to 0.01 molal. [68] All their measurements were at -15°C, and so cannot be directly compared to more recent observations, including those in this thesis. However, the relative conductivities of the various compounds studied do give information as to their behaviour in HF. Fredenhagen and Cadenbach were the first to study a strong base, KF, and they showed that it is completely dissociated in solution. They also studied AgF and found it to have the same conductivity as KF over the whole range studied. Assuming the mobility of the silver and potassium ions to be similar, it is concluded that AgF is also completely ionized in solution. This contradicts the findings of Clifford et al., [88] who found a dissociation constant for AgF in HF of 0.087 at 0°C. Clifford determined activity constants as a function of concentration from electrode potentials and assumed the deviation from ideality represented by the activity coefficients could be attributed entirely to incomplete dissociation. Humphreys also found AgF to be only partly dissociated and he obtained a value for the dissociation

constant of 0.15. [11] However, the small degree of dissociation is surprising in view of the high solubility of AgF in HF (6.6 molal at 12°C) found by Jache and Cady. [34] Fredenhagen also studied the conductivity of H_2O in HF and showed that it was less than KF at all concentrations, indicating it was only partially protonated.

Several compounds that are salts in aqueous solution were also studied by Fredenhagen. [68] In particular, potassium and silver nitrates gave a conductivity about two and a half times that of the corresponding fluoride, and it was concluded that nitric acid is protonated in HF to give the following mode of ionization.

$$KNO_3 + 2HF \longrightarrow K^+ + H_2NO_3^+ + 2F^-$$

However, it has since been shown by means of Raman spectroscopy that nitrates ionize in HF in the following manner: [27]

$$KNO_3 + 3HF \longrightarrow K^+ + NO_2^+ + H_3O^+ + 3F^-$$

At the time the initial work was carried out, the NO_2^+ cation was not known. When interpreting conductivity behaviour for this type of reaction, the weak basicity of water and its incomplete ionization must always be remembered.

A number of alcohols, organic acids, acetone, diethyl ether, glucose and phenol were also investigated and found to give solutions of varying conductivity. [68] It has been concluded that they all

act as bases in HF by accepting a proton from the solvent.

Kilpatrick and Luborsky determined the base strengths of the methylbenzenes in HF at 20°C by measurement of their conductivities. [30] They assumed that hexamethylbenzene was completely protonated in dilute solution to give the carbonium and fluoride ions, and that the mobilities of the various carbonium ions produced were the same as the mobility of protonated hexamethylbenzene. From the conductivities of the methylbenzenes, the degree of protonation was obtained, and from this the equilibrium constants for the protonation of the methylbenzenes were calculated. The results obtained agreed with the values determined by McCaulay and Lien [31] from distribution measurements of the methylbenzenes between liquid hydrogen fluoride and n-heptane. Kilpatrick and Luborsky also carried out conductivity titrations of the methylbenzenes in HF with BF_3. [30] Two types of behaviour were observed. The conductivity of the very weak bases which were only slightly protonated increased on addition of BF_3 until a 1:1 base:BF_3 ratio was reached, after which the conductivity remained steady on further addition of BF_3. The BF_3 reacts with the slight amount of fluoride produced on protonation and displaces the reaction to the left, yielding the carbonium ion and the BF_4^- ion. The conductivity of the stronger bases in HF decreased on addition of BF_3 until a 1:1 ratio was reached because the highly conducting fluoride ion from the fully ionized base was replaced with the less mobile BF_4^- ion.

Kilpatrick and Lewis measured the conductivity of NaF, KF, $KSbF_6$ and SbF_5 in HF at 0°C. [19] They concluded that within their experimental accuracy the conductance curves of NaF and KF were indistinguishable. However, they did not carry their measurements on KF above 0.025 molal. In addition, they state that a correction for solvent conductivity was made but do not give any values. Transport measurements were carried out on KF and NaF in a modified Hittorf type cell. The concentration of the solute in each compartment was measured by the conductance of the solution within that compartment. The precision of the transport numbers obtained was about ±15%. Several measurements were made on KF solutions at a concentration of about 0.23 molal. As no conductivities were reported for KF at this concentration, it must be assumed that they based their calculations on their conductivity data for NaF, which they determined to 0.6 molal. However, as will be seen later in this chapter, the conductivity of KF at 0.23 molal concentration is almost 10% greater than that of NaF. In any case, Kilpatrick and Lewis' conductivities for NaF do not agree with those found in this work. For these reasons, great reliance cannot be placed on their transport measurements and the equivalent ionic conductivities based on them in the literature and tabulated in Table 1.3 are of considerably lower accuracy than quoted. However, Kilpatrick and Lewis' results do show that the fluoride ion has an abnormal mobility when compared to the sodium and potassium ions. This is explained by a chain conduction

mechanism for the fluoride ion.

$NaSbF_6$ had a conductivity considerably lower than that of NaF, due to the lower conductance of the SbF_6^- ion compared to that of the chain conducting fluoride ion. Surprisingly, they found that SbF_5, which is completely ionized to H_2F^+ and SbF_6^- in the concentration range Kilpatrick and Lewis studied, had a conductivity even lower than that of $KSbF_6$. They concluded therefore, that the proton did not take part in a chain conduction process as it does in fluorosulfuric [22] and sulfuric acids. [89]

Hyman et al. investigated the conductivity of the HF - SbF_5 system over the whole range of composition, but they did not study any dilute solutions of SbF_5. [42] They also studied the infra-red and Raman spectra of SbF_5 in HF. In order to account for their data, they postulated an equilibrium involving SbF_5, and undissociated $H_2F^+SbF_6^-$ as well as the dissociated species. More recently, Hyman et al. measured the conductivities of a few dilute solutions of SbF_5 and showed that such solutions can be titrated conductometrically with water. [43] On addition of water, the conductivity decreases, passes through a minimum, and then increases again, presumably because of the neutralization reaction:

$$SbF_5 + 2HF \longrightarrow H_2F^+ + SbF_6^-$$
$$H_2F^+ + H_2O \longrightarrow H_3O^+ + HF$$

This demonstrates that SbF_5 is an acid, and that H_2F^+ has a higher

mobility than normally conducting ions such as H_3O^+.

Gillespie and Moss investigated the HF - SbF_5 system by conductivity and nmr. [20] Their conductivities agree with those found by Hyman et al. for high [42] and lower concentrations, [43] but are considerably higher than those of Kilpatrick and Lewis. They attribute the latters' low results to the presence of water which at least partially neutralized the H_2F^+. The higher conductivity values found by Gillespie and Moss confirmed the abnormal mobility of the H_2F^+ ion in HF. They explained their conductivity data by the formation of $Sb_2F_{11}^-$ and higher polymeric ions in more concentrated solution. They also showed from conductivity and nmr that SbF_4SO_3F is a weaker acid in HF than SbF_5, contrary to the findings in HSO_3F, [23] because complete solvolysis occurs:

$$SbF_4SO_3F + HF \longrightarrow SbF_5 + HSO_3F$$

and presumably the resulting HSO_3F acts as a weak base towards $HSbF_6$.

$$HSbF_6 + HSO_3F \longrightarrow SbF_6^- + H_2SO_3F^+$$

Kilpatrick et al. investigated the conductivity of nitronium fluoroborate, $NO_2^+BF_4^-$, in HF at 20°C and compared it to that found for KBF_4. [56] The conductivities of the two salts were almost identical, and it was concluded that NO_2BF_4 is completely dissociated in HF solution.

As such, it is an excellent nitrating agent for use in kinetic studies as the concentration of NO_2^+ in solution can be simply calculated. (2)

Simple Bases

The conductivities, κ, of solutions of lithium, sodium, potassium, rubidium, cesium and thallous fluorides in HF were determined at 0°C and are tabulated in table 4.1. The uncertainty in concentration is 1 or 2 units in the last figure except where that figure is dropped below the line, (e.g. 1.8_5) in which case the uncertainty is 3 - 5 units. A solvent conductivity correction of 0.2×10^{-3} mhos/cm has been applied to the conductivity measurements, and they have an uncertainty of 0.1×10^{-3} mhos/cm. The equivalent conductivities, Λ, were determined from the expression,

$$\Lambda = \frac{1000\kappa}{c}$$

where c is the concentration in equivalents per 1000 grams of HF.

The conductivities in HF at 0°C of calcium, strontium, barium and lead fluorides are tabulated in table 4.2. $\sqrt{I}$ where I is the ionic strength is tabulated here instead of $\sqrt{m}$ where I is defined by:

$$I = \frac{m}{2} \quad (\nu_1 z_1^2 \quad + \quad \nu_2 z_2^2)$$

TABLE 4.1

Conductivity of Univalent Fluorides in HF

molality $\times 10^2$	κ mhos/cm $\times 10^3$	$\sqrt{m}$ $\times 10^2$	Λ mhos cm^2/equiv.
		LiF	
1.8_5	5.4	13.6	292
2.6_9	7.6	16.4	282
4.1	11.3	20.3	275
6.9	18.0	26.3	259
11.2	28.2	33.4	252
17.0	39.9	41.3	234
17.5	41.1	41.9	234
25.8	56.1	50.8	217
$48._3$	89.6	69.5	185

Table 4.1 (Continued)

molality $\times 10^2$	κ mhos/cm$\times 10^3$	$\sqrt{m}$ $\times 10^2$	Λ mhos cm^2/equiv.
		NaF	
1.34	4.3	11.7	321
1.8_8	5.9	13.8	314
2.3_5	7.3	15.4	310
3.0_2	9.2	17.5	304
4.3_0	12.6	20.8	293
6.2	17.8	25.0	286
10.8	29.1	32.8	270
12.3	31.8	35.0	259
13.5	35.2	36.8	260
16.1	39.9	40.2	247
20.3	48.5	45.1	237
21.1	51.7	45.9	245
25.2	59.8	50.2	237
37.2	84.4	61.0	226
41.2	91.6	64.2	222
51.6	109.	71.8	211

Table 4.1 (Continued)

molality $\times 10^2$	κ mhos/cm$\times 10^3$	$\sqrt{m}$ $\times 10^2$	Λ mhos cm^2/equiv.
		KF	
7.3_1	21.5	27.0	294
10.3	29.1	32.1	281
10.5_6	29.5	32.5	279
10.6	29.6	32.5	279
11.7	32.0	34.3	272
13.2	36.1	36.3	273
13.8	37.7	37.2	272
14.3	39.4	37.8	275
15.5	41.7	39.4	268
17.8	46.8	42.1	263
18.0	47.9	42.5	265
23.0	59.5	47.9	259
36.9	86.2	60.7	233
$52._1$	112.9	72.1	216

Table 4.1 (Continued)

molality $\times 10^2$	κ mhos/cm$\times 10^3$	$\sqrt{m}$ $\times 10^2$	Λ mhos cm^2/equiv.
		RbF	
2.69	8.9	16.4	330
3.5_5	11.4	18.8	321
5.1_0	15.8	22.5	310
8.2	24.0	28.7	292
10.5_5	30.7	32.5	291
12.9	36.4	35.9	282
14.6	40.8	38.2	280
19.8	53.1	44.5	268
31.3	78.0	56.0	248
$42._3$	99.7	65.0	235

Table 4.1 (Continued)

molality $\times 10^2$	κ mhos/cm$\times 10^3$	$\sqrt{m} \times 10^2$	Λ mhos cm^2/equiv.
		CsF	
1.74	6.4	13.2	368
2.5_8	9.2	16.0	356
3.2_6	11.4	18.0	349
4.9_0	16.2	22.1	330
7.8_1	23.7	27.9	303
8.5	26.3	29.2	307
11.0	32.8	33.2	298
16.8	47.5	41.0	282
20.0	57.0	44.7	284
21.9	59.7	46.8	273
25.4	67.8	50.4	267
35.1	90.7	59.3	258
$63._2$	153.3	79.5	242
97.	222.	98.4	229

Table 4.1 (Continued)

molality $\times 10^2$	κ mhos/cm$\times 10^3$	$\sqrt{m} \times 10^2$	Λ mhos cm^2/equiv.
		T&F	
4.34	14.0	20.8	322
6.24	20.2	25.0	324
11.4	34.5	33.7	303
14.3	40.2	37.7	282
15.7	46.4	39.7	294
18.8	51.4	43.3	273
28.2	72.5	53.1	257
45.0	114.9	67.1	255

TABLE 4.2

Conductivity of Divalent Fluorides in HF

molality $\times 10^2$	κ mhos/cm$\times 10^3$	$\sqrt{I} \times 10^2$	Λ mhos cm^2/equiv.
		CaF_2	
2.11	10.7	25.2	254
2.5_1	12.4	27.4	247
3.2_5	15.3	31.2	235
4.6	20.1	37.3	217
5.5_7	23.6	40.9	212
6.9_1	27.9	45.5	202
8.1_7	30.7	49.5	188
8.5_3	32.2	50.6	189
10.4	38.3	55.9	183
10.6	36.9	56.4	174
14.2	46.7	65.3	164
14.6	48.2	66.3	164
saturated	50.6		

Table 4.2 (Continued)

molality $\times 10^2$	κ mhos/cm$\times 10^3$	$\sqrt{I}$ $\times 10^2$	Λ mhos cm^2/equiv.
		SrF_2	
4.43	21.5	36.5	243
6.45	28.9	44.0	224
6.51	29.4	44.2	226
8.5_1	36.1	50.5	212
8.9_5	37.7	51.8	210
12.3_2	47.8	60.8	194
13.0	49.5	62.5	190
21.8	71.5	80.9	164
23.4	75.5	83.9	161
28.7	86.6	92.8	151
31.4	92.4	97.1	147
42.9	104.	113.5	121
$51._1$	125.	123.8	122
$68._4$	145.	143.3	106

Table 4.2 (Continued)

molality $\times 10^2$	κ mhos/cm$\times 10^3$	$\sqrt{I} \times 10^2$	Λ mhos cm^2/equiv.
		BaF_2	
4.93	25.3	38.4	256
7.5_8	35.6	47.6	235
7.8_4	37.3	48.5	238
9.16	40.8	52.4	223
10.0	44.1	54.7	221
10.4_8	46.6	56.1	222
11.1_6	47.7	57.9	214
13.7	56.1	64.0	205
14.8_1	59.4	66.6	200
21.3	77.6	79.9	182
21.4	79.4	80.1	186
saturated	100.9		

Table 4.2 (Continued)

molality $\times 10^2$	κ mhos/cm$\times 10^3$	$\sqrt{I} \times 10^2$	Λ mhos cm^2/equiv.
		PbF_2	
2.95	14.2	29.7	240
4.61	20.2	37.1	219
6.2_9	25.8	43.4	205
6.62	26.6	44.5	201
9.8	35.9	54.2	183
10.1_7	36.2	55.2	178
saturated	48.0		

where ν_1 and ν_2 are the numbers of moles of cations and anions respectively formed from one mole of electrolyte, and z_1 and z_2 are the valencies of the cations and anions respectively. [90] Thus, for a di-univalent electrolyte I = 3m, while for a uni-univalent electrolyte I = m, i.e., the ionic strength and molality are identical.

The conductivities of the univalent fluorides increase in the order, LiF<NaF<KF<RbF<CsF≃T&F (Fig. 4.1). This is the same order as found for the alkali metal ion conductivities in water [91] and is the inverse order of their crystallographic radii. This order of conductivity in aqueous solutions has been attributed to a larger hydration sheath on the ions with a greater charge to radius ratio causing a reversal in the effective ionic size.

An approximate indication of the size of the solvated alkali metal ions is obtained by a comparison of their conductivities with those of the tetra-alkyl ammonium ions measured by Hulme (Table 4.3), [92] as ionic mobility depends inversely on ionic size. The tetra-alkyl ammonium ions, with their diffuse charge and outer sphere of methyl groups, are solvated only weakly if at all. Robinson and Stokes estimated the ionic radius of $(CH_3)_4N^+$ to be 3.47Å, $(C_2H_5)_4N^+$ to be 4.00Å and $(C_4H_9)_4N^+$ to be 4.94Å. [93] Their conductivities in HF solution increase in the order $(n\text{-}C_4H_9)_4N^+ < Li^+ \simeq (C_2H_5)_4N^+ < Na^+ < (CH_3)_4N^+ < K^+$ (Fig. 4.2). By comparison with the volume of the tetra-alkyl ammonium ions, a volume can be calculated for the solvated alkali metal ion,

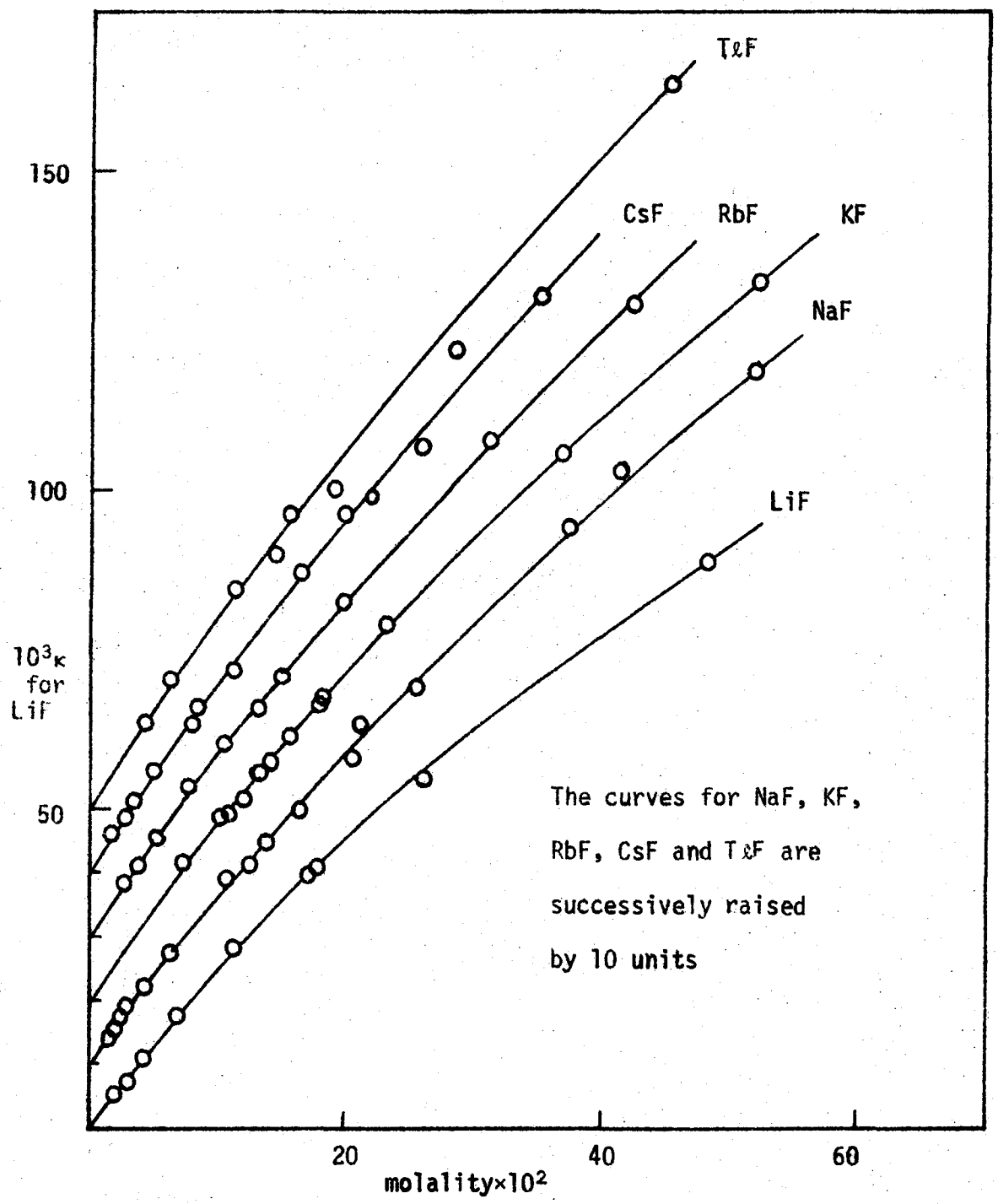

Figure 4.1 Specific Conductivity of Univalent Fluorides

TABLE 4.3

Conductivity of Tetra-alkyl Ammonium Fluorides in HF at 0°C [92]

molality×10^2	$10^3\kappa$	molality×10^2	$10^3\kappa$
$(CH_3)_4NF$		$(n\text{-}C_4H_9)_4NF$	
4.1	13.2	1.3	4.0
5.1	15.4	1.8	5.2
12.8	33.1	2.2	6.4
19.9	50.4	3.5	9.8
22.5	56.7	6.2	15.5
34.4	81.1	7.4	18.0
52.1	114.3	8.1	19.4
83.7	146.4	8.6	21.0
		10.6	23.9
$(C_2H_5)_4NF$		11.4	26.2
1.7	6.4	12.3	27.1
5.0	13.8	16.1	34.3
9.6	24.4	21.3	42.2
14.4	36.3	27.1	50.5
21.3	49.2		
25.4	57.5		
32.9	70.0		

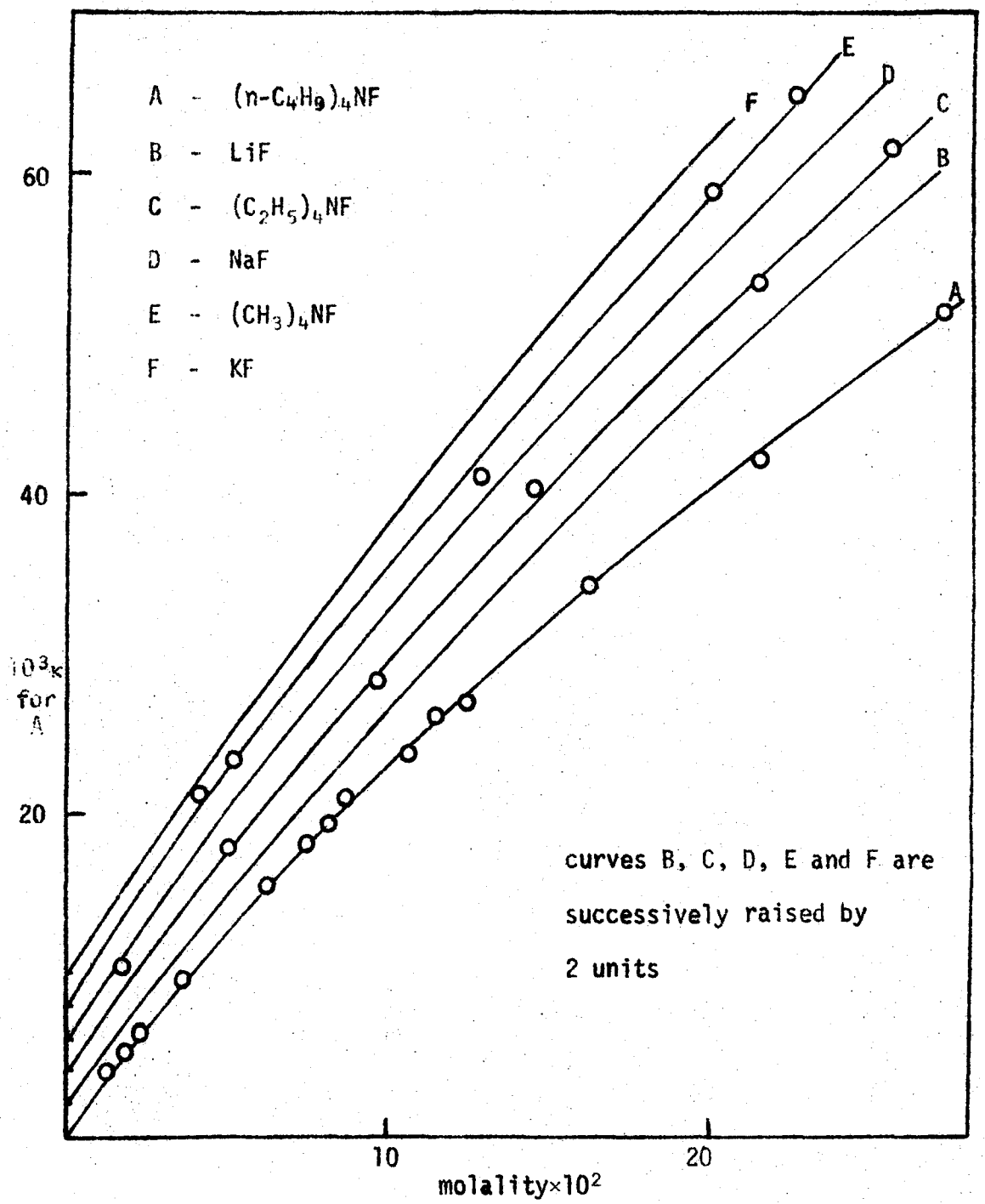

Figure 4.2 Specific Conductivity of Alkyl Ammonium Fluorides

and from this volume a rough estimate can be made of the average number of HF molecules in the solvation sphere by assuming they occupy their ordinary liquid volume of about 33$\mathring{A}^3$ at 0°C. The number of solvent molecules in the solvation sphere thus obtained are ~8 for Li^+, ~6 for Na^+ and ~5 for K^+.

The conductivities of KF determined in this work and by Kilpatrick and Lewis [19] do not have a common concentration range. Their data for NaF, however, do not agree with that found here and their conductivity values are greater at low concentrations, and lower at high concentrations. The curves cross at about 0.1 molal. The results found in this thesis are considered to be more reliable in view of their consistency with the other alkali fluorides measured.

Jache and Cady have determined the solubility of TℓF in HF to be about 2.6 molal at 11.9°C and about 2.0 molal at -7.8°C. [34] Clifford and Zamora concluded from emf measurements that TℓF is incompletely dissociated in HF. [88, 94] This conclusion is shown to be incorrect by the high conductivity of TℓF in HF, similar to that of CsF. If $Tℓ^+$ F^- is associated in HF, it is only to a very limited extent.

The conductivities of the divalent metal fluorides increase in the order, $PbF_2 \simeq CaF_2 < SrF_2 < BaF_2$ (Fig. 4.3). With the exception of Pb^{++}, this is again the inverse order of crystallographic radii. In aqueous solution, the limiting equivalent conductivity of Pb^{++} is about

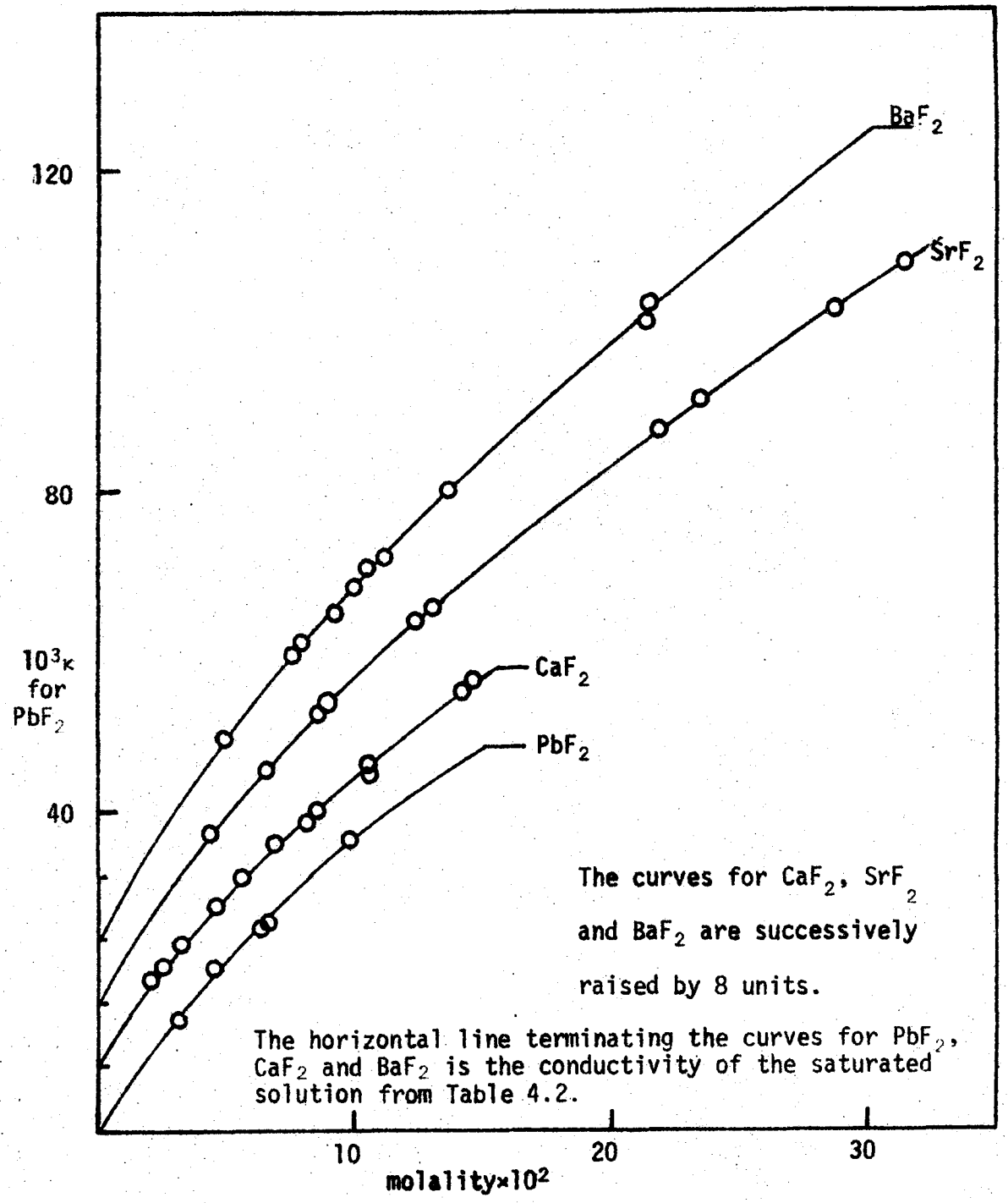

Figure 4.3 Specific Conductivity of Divalent Fluorides

10% greater than that of Ba^{++} and about 15% greater than that of Ca^{++}. [91] The lower observed conductivity in HF might be explained by some association to give PbF^{+}. Several workers have previously found this association to occur in aqueous solution using emf [95] and polarographic [96] methods.

The solubilities of calcium, barium and lead fluorides in HF were determined by extrapolating their specific conductance versus concentration curves to the conductance found for the saturated solutions (Fig. 4.3). The value for calcium fluoride of 0.160 molal at 0°C is in reasonable agreement with the value of 0.154 molal at 0°C found previously by Kongpricha and Clifford, [97] and is slightly higher than the value of 0.136 molal at -3.3°C found by Jache and Cady. [34] The solubility of 0.30 molal at 0°C found for barium fluoride is intermediate between the values of 0.27 molal at -3.3°C and 0.32 molal at 12.2°C found by Jache and Cady. [34] The solubility of 0.154 molal at 0°C found for lead fluoride is greater than the values found by Jache and Cady of 0.145 molal at -8.3°C and 0.107 molal at 12.4°C. [34] The solubilities of barium and lead fluorides in HF at 0°C had not been previously determined.

Fluoroanion Salts

The conductivities in HF of KPF_6, $KAsF_6$, $KSbF_6$, $NaSbF_6$ and KBF_4 were determined at 0°C and are tabulated in Table 4.4. The

TABLE 4.4

Conductivity of Fluoroanion Salts in HF

molality $\times 10^2$	κ mhos/cm$\times 10^3$	$\sqrt{m}$ $\times 10^2$	Λ mhos cm^2/equiv.
		KPF_6	
0.60	1.8	7.75	300
0.82	2.5	9.05	305
1.3_1	3.7	11.4	282
1.32	3.9	11.5	295
1.93	5.7	13.9	295
2.05	5.7	14.3	278
2.34	6.7	15.3	286
2.75	7.4	16.6	269
2.78	7.5	16.7	270
3.64	9.3	19.1	255
3.8_3	10.2	19.6	266
4.4_6	11.1	21.1	248
4.7_0	11.5	21.7	244
saturated	12.9		

Table 4.4 (Continued)

molality $\times 10^2$	κ mhos/cm$\times 10^3$	$\sqrt{m}$ $\times 10^2$	Λ mhos cm^2/equiv.
		$KAsF_6$	
1.39	4.1	11.8	295
1.52	4.8	12.3	316
1.80	5.2	13.4	289
2.30	6.5	15.1	282
2.5_6	7.2	16.0	281
3.40	8.8	18.4	259
3.9_9	10.7	20.0	268
4.1_8	10.6	20.4	253
6.2_3	14.6	25.0	234
saturated	17.7		

Table 4.4 (Continued)

molality $\times 10^2$	κ mhos/cm$\times 10^3$	$\sqrt{m}$ $\times 10^2$	Λ mhos cm^2/equiv.
		$KSbF_6$	
1.63	4.3	12.8	264
2.3_1	6.0	15.2	260
3.0_3	7.7	17.4	254
4.0_3	9.8	20.0	243
5.8_2	12.9	24.1	222
7.8_2	16.4	28.0	210
10.9	22.0	33.1	201
12.4	24.6	35.2	198
17.3	31.8	41.6	183
17.7	32.1	42.1	181
26.4	43.0	51.4	162

Table 4.4 (Continued)

molality $\times 10^2$	κ mhos/cm$\times 10^3$	$\sqrt{m}$ $\times 10^2$	Λ mhos cm^2/equiv.
		$NaSbF_6$	
1.19	3.2	10.9	269
1.7_9	4.4	13.3	246
2.35	5.8	15.3	247
3.1	7.3	17.7	234
3.8_2	8.9	19.6	233
5.4	12.0	23.4	220
8.8_7	19.0	29.8	214
12.3	24.5	35.1	199
17.8	32.3	42.2	181

Table 4.4 (Continued)

molality $\times 10^2$	κ mhos/cm$\times 10^3$		$\sqrt{m}$ $\times 10^2$	Λ mhos cm^2/equiv.
	0°C	20°C		0°C
		KBF_4		
2.5_5	6.6	8.1	15.9	259
4.7_2	11.0	13.3	21.7	233
5.1_2	11.9	14.5	22.6	232
6.0_9	14.3	17.1	24.7	235
7.4	16.3	19.8	27.1	221
8.6	19.0	23.0	29.4	220
10.5	21.9	26.7	32.3	210
10.7_6	22.6	27.2	32.8	210
12.9	26.3	31.7	35.9	203
13.7	27.5	33.4	37.0	200
18.0	34.3	41.2	42.4	191
$30._8$	51.2	61.5	55.4	166

conductivities of the KBF_4 solutions were also measured at 20.00±0.01°C in a regulated oil bath for purposes of comparison with the values previously determined by Kilpatrick et al. at that temperature. [56] It can be seen that their conductivities and those found in this work are in good agreement (Fig. 4.4).

The conductivity of KBF_4 at 20°C had been measured earlier by Kilpatrick and Luborsky, [48] but their values were too high and do not agree with those determined in this thesis and those determined later by Kilpatrick et al. [56] Kilpatrick and Luborsky compared their measured conductivity of KBF_4 with a conductivity calculated from other measurements for KBF_4 where the fluoroborate ion is not dissociated into fluoride ion and boron trifluoride. [48] The greater observed conductivity of KBF_4 was attributed to dissociation of BF_4^- to give the higher conducting fluoride ion.

$$BF_4^- \rightleftharpoons BF_3 + F^-$$

They calculated a dissociation constant for the BF_4^- ion in the range 10^{-2} to 10^{-3}.

$$k = [BF_3]\,[F^-] \,/\, [BF_4^-]$$

However, as their measured values for the conductivity of KBF_4 are high, it must be concluded that the dissociation constant calculated is much too high, and in fact, the BF_4^- ion is virtually undissociated in HF.

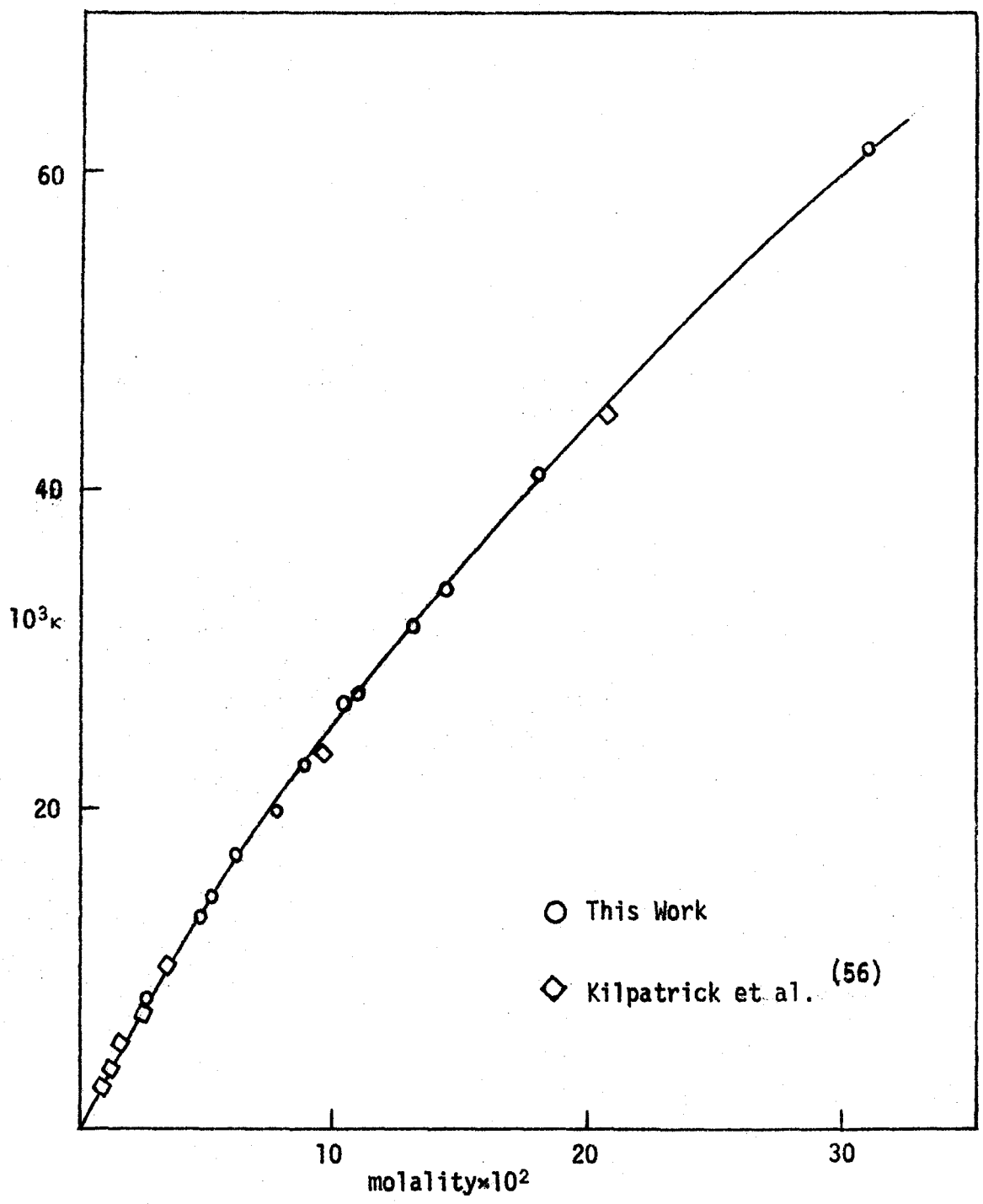

Figure 4.4 Specific Conductivity of KBF_4 at 20°C

Kilpatrick et al. did not comment on this dissociation constant in their later paper. (56)

Kilpatrick and Luborsky also measured the conductivity of BF_3 itself in HF and showed it to be a very weak acid. (47) The difference between the strong acceptor ability of BF_3 towards F^-, i.e. the low degree of dissociation of BF_4^-, and the very weak acid character of BF_3 in HF is accounted for by the very low degree of dissociation of HF itself. From the conductivity of pure HF and the equivalent conductances of the H_2F^+ and F^- ions (Tables 1.1 and 1.3) one can set an upper limit for the dissociation constant of HF at about 10^{-12}.

The conductivities of the fluoroanion salts at 0°C are all very similar with $NaSbF_6 < KSbF_6 \cong KBF_4 < KAsF_6 \cong KPF_6$ (Fig. 4.5). Both KPF_6 and $KAsF_6$ were found to have quite limited solubilities in HF, and their solubility was determined from the conductivity curves. KPF_6 gives a 0.053 molal and $KAsF_6$ a 0.079 molal solution in HF at 0°C at saturation. This compares with values of 0.0576 molal for KPF_6 and 0.2130 molal for $KAsF_6$ found by Netzer at 24°C. (98)

The conductivities of $NaSbF_6$ at 0°C were only determined by Kilpatrick and Lewis up to a concentration of 0.04 molal with only one point above 0.02 molal. The 0.04 molal point is about 18% below the curve found in this work and the other points are lower as well, though to a lesser amount and with a greater degree of scatter than the present measurements. The results determined in this thesis are considered to be more reliable, in view of their consistency with those found for the

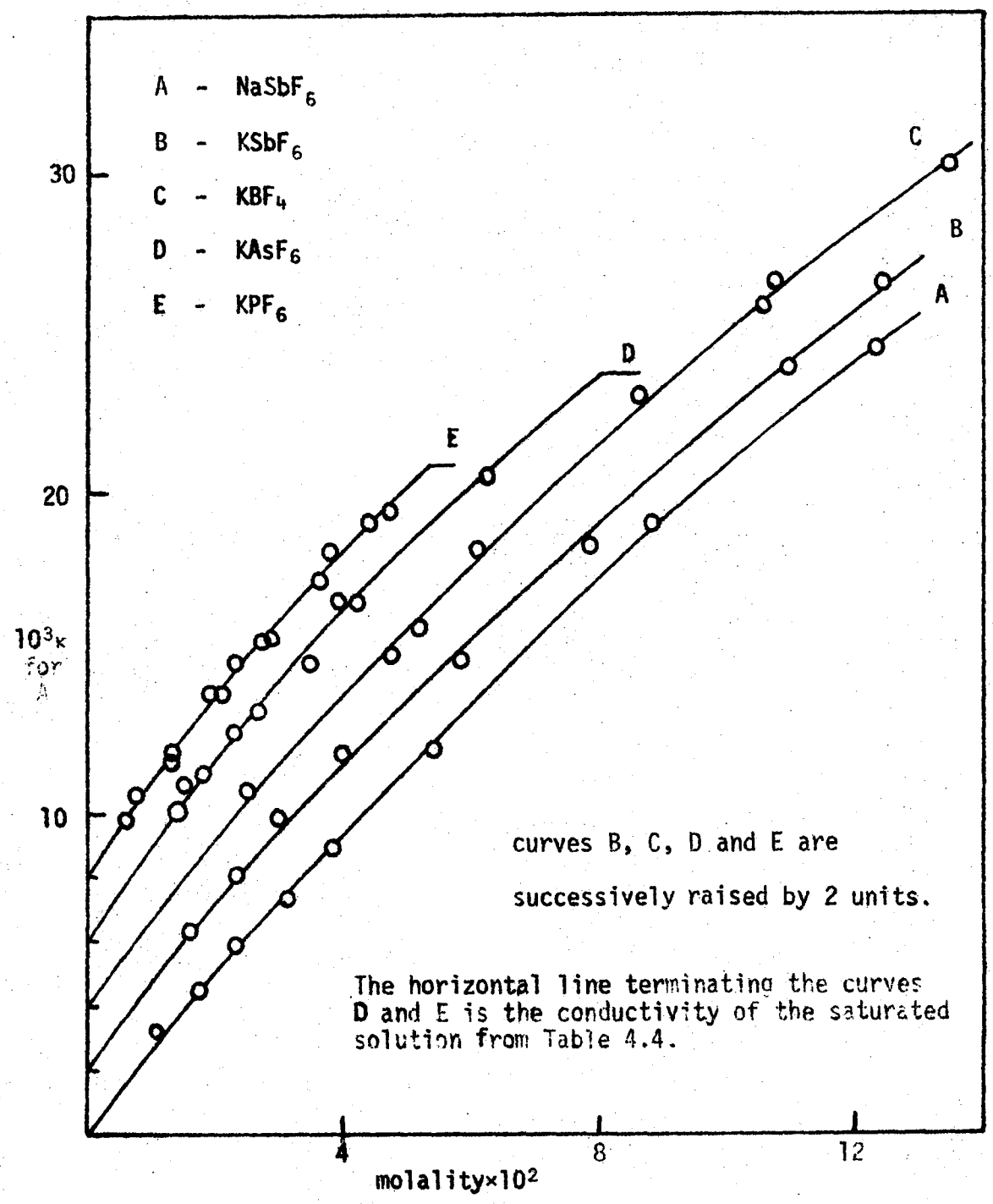

Figure 4.5 Specific Conductivity of Fluoroanion Salts

other salts measured. No previous conductivity measurements have been carried out on any PF_6^- or AsF_6^- salts in HF.

Predicted Conductivity Curves

The Onsager limiting law[90] describes the variation of the equivalent conductivity of an electrolyte with concentration for dilute solutions. It is of the form:

$$\Lambda = \Lambda o - A\sqrt{I}$$

where,

$$A = \frac{2.801\times10^6|z_1z_2|q\Lambda o}{(\varepsilon T)^{3/2}\,(1+\sqrt{q})} + \frac{41.25(|z_1|+|z_2|)}{\eta(\varepsilon T)^{1/2}}$$

and

$$q = \frac{|z_1z_2|}{(|z_1|+|z_2|)(|z_2|t_1^\circ + |z_1|t_2^\circ)}$$

t_1° and t_2° are the transport numbers, at infinite dilution, of the cation and anion respectively. For a 1:1 electrolyte q = 1/2. In the case of HF, lack of accurate transport number measurements means that q cannot be evaluated for other charge ratios. Inserting the values of the physical constants given for 0°C in table 1.1, the Onsager limiting law for HF becomes:

$$\Lambda = \Lambda o - (0.236\Lambda o + 212.8)\sqrt{I}$$

Molar units of concentration are normally used in this equation. However, the density of HF at 0°C is 1.002 grams/ml and there will be very little difference caused by using molal units. A modified form of the Onsager equation has been found to fit experimental data for aqueous solutions at higher concentrations. (90)

$$\Lambda = \Lambda o - \frac{A\sqrt{I}}{1 + \kappa a}$$

where

$$\kappa a = (8\pi Ne^2/1000\varepsilon kT)^{1/2}\, a\sqrt{I}$$

and, "a" is the mean diameter of the anion and cation. Therefore, a plot of Λ versus $\sqrt{I}$ for a 1:1 electrolyte in HF at 0°C is expected to have a limiting slope of $0.236\Lambda o + 212.8$.

Such plots are drawn for the univalent fluorides, divalent fluorides and salts in Figures 4.6, 4.7 and 4.8 respectively. The equivalent conductivities at infinite dilution (Λo) and limiting slopes are tabulated in table 4.5. Also given are the limiting slopes predicted by the Onsager law for the 1:1 electrolytes calculated from the observed Λo's. In every case the observed slope is considerably greater than the calculated one. Since the modified Onsager law

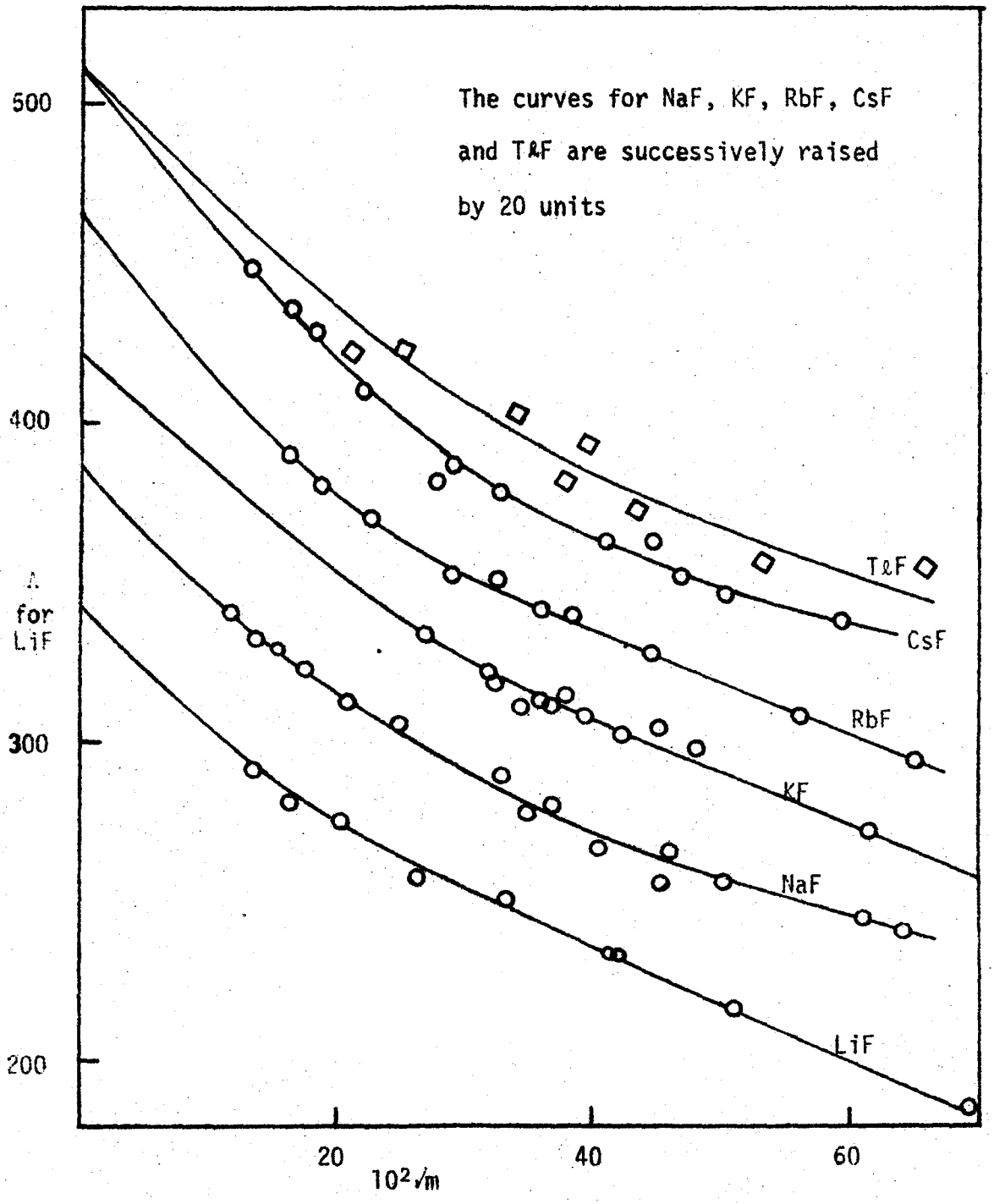

Figure 4.6 Equivalent Conductivity of Univalent Fluorides

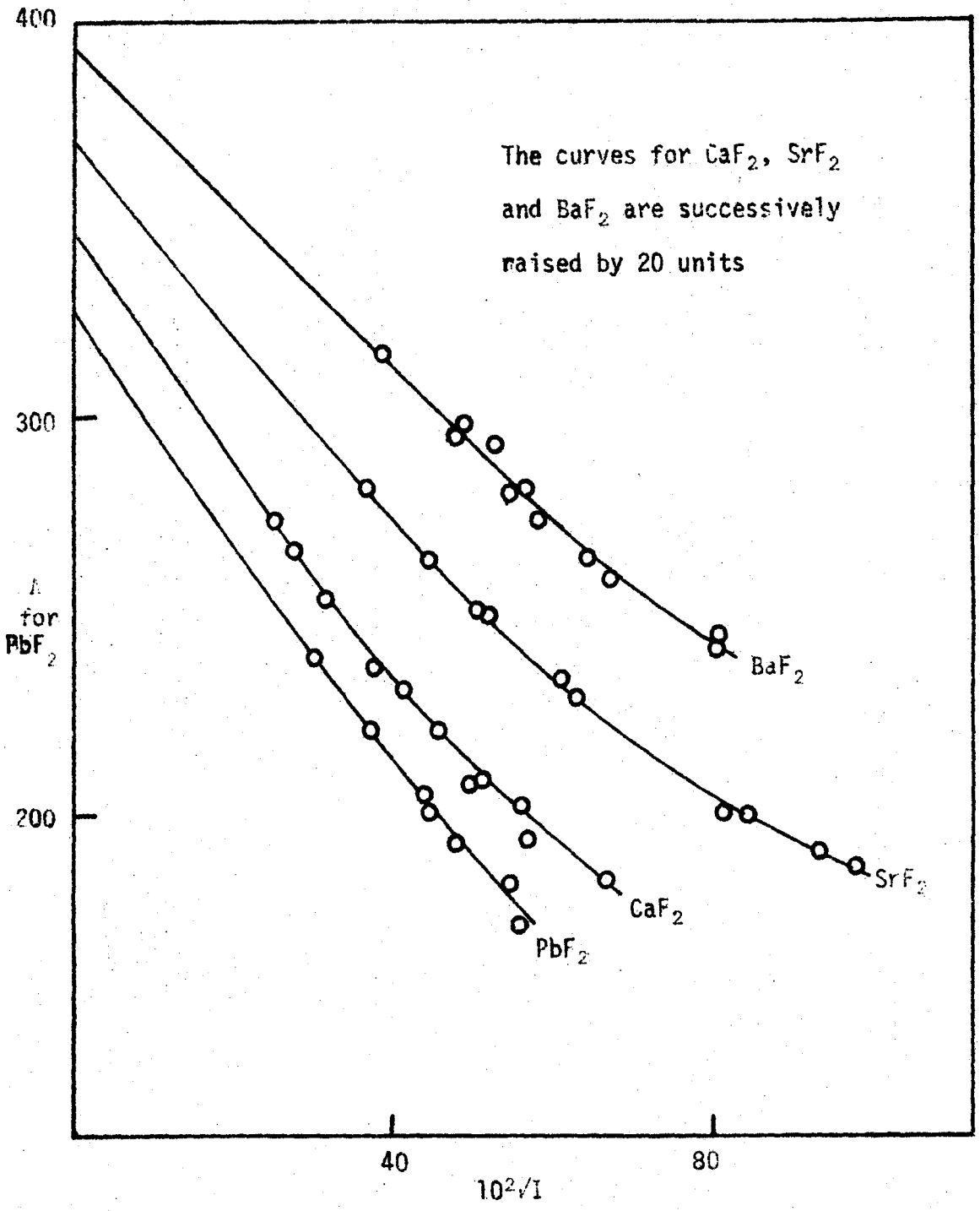

Figure 4.7 Equivalent Conductivity of Divalent Fluorides

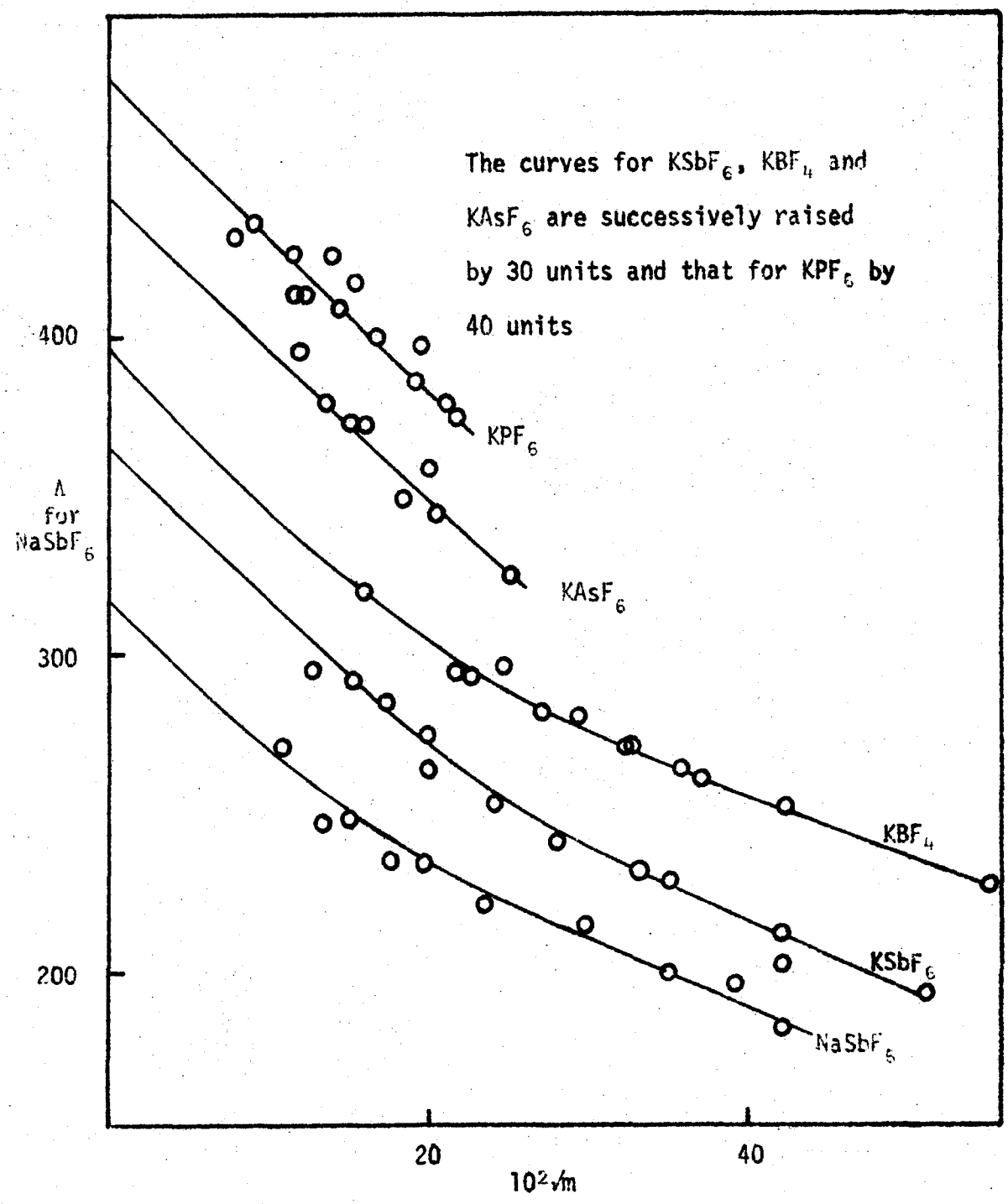

Figure 4.8 Equivalent Conductivity of Fluoroanion Salts

TABLE 4.5

Equivalent Conductivities in HF at 0°C

	Λ_o	Observed Slope	Predicted Onsager Slope
LiF	343	390	294
NaF	365	400	299
KF	382	350	303
RbF	405	480	308
CsF	430	460	314
T&F	410	380	309
CaF_2	330	320	-
SrF_2	330	240	-
BaF_2	335	230	-
PbF_2	328	320	-
KPF_6	352	520	296
$KAsF_6$	351	470	296
KBF_4	334	500	291
$KSbF_6$	334	480	291
$NaSbF_6$	317	470	287

predicts an even smaller decrease in conductivity than the limiting law for any value of "a", the modified law gives an even poorer agreement with the experimental data.

The shape of the equivalent conductivity curves were drawn to be consistent within a given class of electrolytes, i.e. univalent fluorides, divalent fluorides and salts. This is justified by the similarity of adjacent members of a group. The Λ_o values obtained in this way where very low concentration data were lacking form a self-consistent set. Although the conductivity curve for a given member of a set might be drawn to give a slope more in line with that predicted by the Onsager equation, for neither the univalent fluorides nor the fluoroanion salts can this be done for all set members. A conductivity behaviour which varies between such similar compounds is very difficult to justify.

Similar results have been found with other conductivity measurements in HF. Gillespie and Moss observed a Λ_o of 550 and slope of 450 for SbF_5 at 0°C as opposed to a calculated slope of 315. [20]

Kilpatrick et al. drew equivalent conductivity plots for KBF_4 and NO_2BF_4 which had a slope in agreement with those predicted by the Onsager limiting law. [56] However, they assumed the validity of the Onsager limiting law, and used it to calculate Λ_o's. From these values

of Λo, they drew the line with a slope calculated from the Onsager equation through their observed points. However, if the Onsager limiting law is initially ignored, when plotting their data, limiting slopes at infinite dilution of 520 and 450 are obtained for KBF_4 and NO_2BF_4 respectively, as opposed to their findings of 395 and 396.

The observed Λo versus $\sqrt{I}$ plots are also considerably steeper than predicted in the case of metal hydrogen sulfates dissolved in sulfuric acid. [89] This behaviour was attributed to the different conductivity mechanism occurring in these solutions as over 95% of the solution conductivity is due to a proton transfer mechanism. Gillespie and Moss postulated this as a reason for the difference between observed and calculated behaviour for solutions of SbF_5 in HF. [20] However, it can be seen that the differences between observed and predicted slopes are even greater in the case of fluoroanion salts where there are no ionic species present which conduct by a proton transfer mechanism (Table 4.5).

HF is not unique in having a slope considerably greater than predicted by the Onsager limiting law, even when ignoring solvents where a significant proton transfer conductivity occurs. The difference between the observed and predicted slope varies from -5% to +43% for some uni-univalent electrolytes in methanol [99] and differs by as much as +290% in the case of bi-univalent electrolytes in methanol. [99]

Determination of γ Values

Conductivity behaviour of dissolved solutes in sulfuric acid and fluorosulfuric acid is easily interpreted to calculate the extent of ionization of weak bases and, in conjunction with cryoscopy, to indicate the mode of reaction and ionization of dissolved solutes. This is because of the low mobility of all ions other than the characteristic solvent anion and cation (e.g. HSO_4^- and $H_3SO_4^+$ in sulfuric acid) which have abnormally high mobilities because they conduct by a proton transfer mechanism. If it is assumed that the contribution to the conductivity of all other ions can be neglected then the molal concentration of the abnormally conducting ion is determined by comparison with the conductivity plot of a standard strong acid or base. Dividing this concentration by the molality of the dissolved solute gives a "γ" value, i.e., the number of moles of the highly conducting species produced per mole of solute. Numerous examples of the use of γ values in interpreting solute behaviour have been given in recent reviews on sulfuric acid chemistry. [24, 100]

Similar γ values obtained from HF conductivity measurements must, however, be treated with caution. In contrast to sulfuric and fluorosulfuric acids, ions not derived from the solvent have high mobilities in HF. Therefore, care must be taken in choosing a comparison electrolyte. Ionic size is an important determinant of conductance. This is exemplified by the alkali fluorides where the difference in

equivalent conductivity at infinite dilution is more than 25% at the extremes of the series. An example of the difficulties of applying γ values is provided by the base, water, discussed in the next section.

Water

Since water is an important solute in its own right and as a reaction product in the ionization of many complex electrolytes, it is important therefore, to have a reliable value for its dissociation constant. Previous work showed it to be partially protonated, but there was some inconsistency in the dissociation constant. Conductivity measurements were carried out in an attempt to obtain a more reliable value of the dissociation constant.

The partially protonated water gives conducting solutions in HF at 0°C. (Table 4.6 and Figure 4.9).

$$H_2O + HF \rightleftharpoons H_3O^+ + F^-$$

The concentration of H_3O^+ for a given solution may in principle be determined by comparison with the conductivity of a solution of an alkali metal fluoride. It must be assumed that the mobility of the alkali metal cation of the comparison electrolyte and the mobility of H_3O^+ are the same. The H_3O^+ concentration for a given solution of H_2O in HF is then equal to the alkali metal fluoride concentration which gives a conductivity the same as that of the H_2O in HF solution.

TABLE 4.6

Conductivity of H_2O in HF

molality$\times 10^2$	$10^3\kappa$
3.6	10.3
5.3	14.1
7.9	17.3
13.4	28.5
18.2	35.8
23.2	42.3
$27._0$	47.4
29.5	50.3
34.6	56.3
$35._3$	57.3
$48._9$	72.0
$52._9$	74.4
68.	91.6

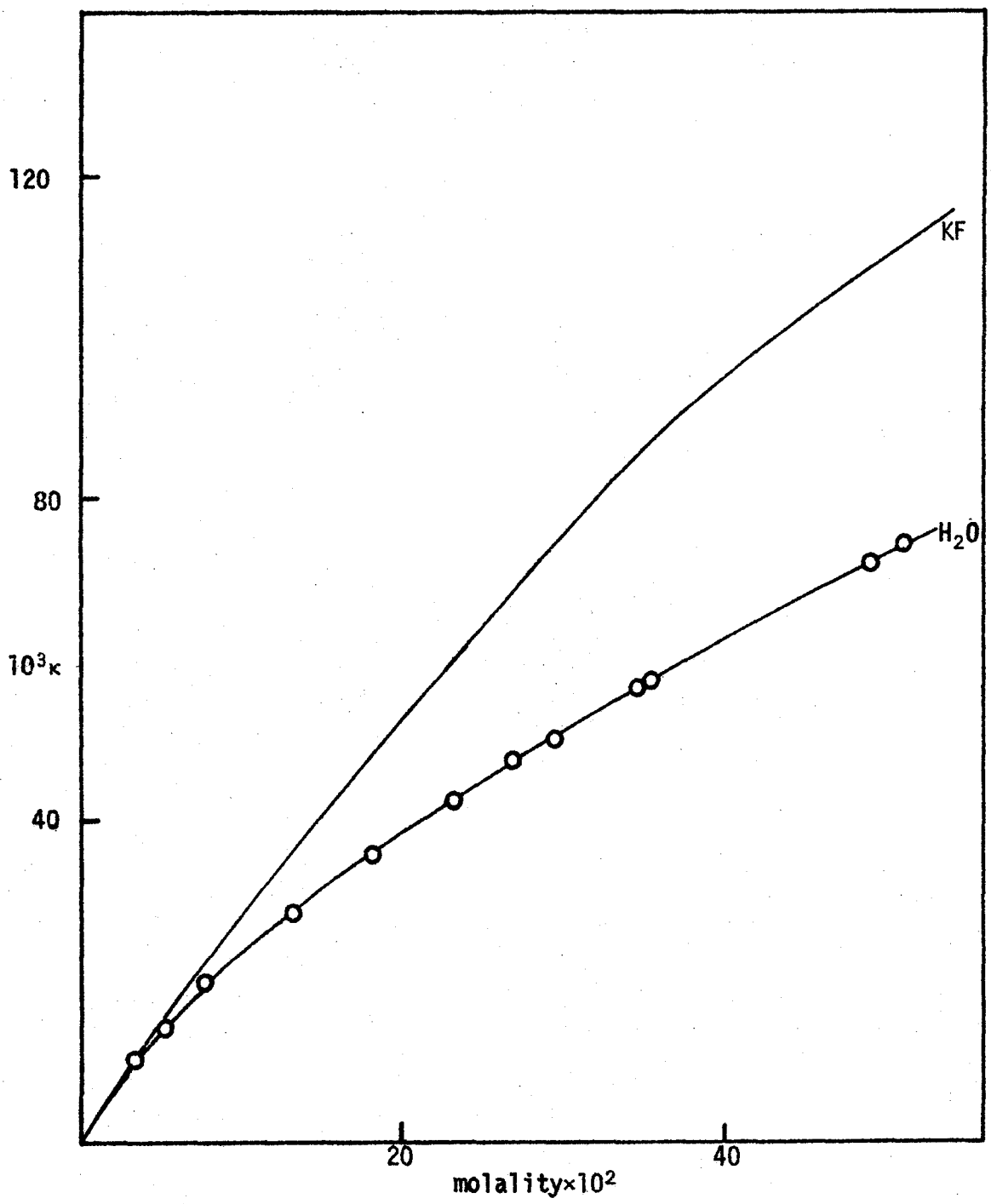

Figure 4.9 Specific Conductivity of H_2O

This alkali metal fluoride concentration may be obtained by interpolation from the conductivity curve of the alkali metal fluoride. From this concentration, γ, the number of moles of H_3O^+ ion produced per mole of H_2O may be obtained and the dissociation constant can then be calculated. However, it can be seen (Table 4.7) that the dissociation constant depends on the alkali metal fluoride used for comparison, from an average of 0.73 for LiF to 0.28 for CsF. A dissociation constant calculation was not carried out on the lowest three water conductivities measured because of the relatively large uncertainty in the small differences used in calculating the dissociation constant. Lithium fluoride is not a proper comparison, because at low concentrations H_2O gives solutions with a higher conductivity than LiF indicating H_3O^+ has a mobility greater than Li^+. The radius of the H_3O^+ ion will probably not differ greatly from that of the NH_4^+ ion which has a radius of 1.48Å according to Phillips and Williams [101] and 1.43Å according to Cotton and Wilkinson. [102] This compares with a crystal radius of 1.48Å for Rb^+ and 1.33Å for K^+. [101] Hence, we assume that Rb^+ or K^+ are the best comparison electrolytes and the best value for the dissociation constant is ~0.34. This compares with 0.55 at infinite dilution found by Kongpricha and Clifford at 0°C. [97] This value was obtained by extrapolation from data obtained on solutions with ionic strengths in the range 0.64 to 0.41 and so could be inaccurate. The actual values found for the dissociation constant ranged from 0.25 to

TABLE 4.7

Dissociation Constant of H_2O in HF at 0°C

$[H_2O]_{total}$ molality×10^2	comparison electrolyte	Dissociation Constant LiF	NaF	KF	RbF	CsF
$52._9$					0.38	0.30
$48._9$					0.39	0.32
$35._3$		0.75	0.54	0.37	0.34	0.30
34.6		0.78	0.52	0.36	0.33	0.30
29.5		0.74	0.51	0.36	0.32	0.28
$27._0$		0.74	0.51	0.35	0.31	0.28
23.2		0.68	0.48	0.34	0.30	0.27
18.2		0.70	0.47	0.34	0.28	0.27
13.4		0.75	0.48	0.32	0.28	0.24
average		0.73	0.50	0.35	0.34	0.28

to 0.34. Kongpricha and Clifford also extrapolated to infinite dilution Fredenhagen's boiling point rise data at ∿20°C and conductivity data at -15°C to obtain ionization constants of 0.19 and 0.15 respectively. In contrast, Humphreys found from cryoscopic measurements at ∿-83°C that water is completely protonated. (11)

In view of the difficulties experienced above in connection with comparison electrolytes, it cannot be claimed that the present value for the dissociation constant is of great accuracy. However, it would appear that there is an increase in the dissociation constant with decreasing temperature and it is probably very large at low temperature. A useful extension of the present work would be to determine the conductivity of water and comparison electrolytes over a temperature range.

Ionic Mobility Calculations

In view of the uncertainty of the transport number determinations of Kilpatrick and Luborsky, it was desirable to attempt to obtain equivalent ionic conductivities (λ_o's) by examination of the Λ_o's found in this work. (Table 4.5).

It is assumed that the F^- and H_2F^+ ions have abnormally high ionic conductivities that are greater than those of any other ions. Upper and lower limits for the λ_o of F^- can then be set at 330 and 215. The maximum is based on the Λ_o of 330 for CaF_2, assuming all the

conductivity is due to the F^- ion. The minimum of 215 is dictated by the Λo of 430 for CsF. If the λo for F^- is set any lower the mobility of the F^- ion would be less than that of Cs^+. Gillespie and Moss found a value of 550 for the Λo of H_2F^+ SbF_6^-. [20] The H_2F^+ ion must have a minimum λo of 275 or it would not have an abnormal mobility compared to SbF_6^-. Then λo of SbF_6^- is 275 and one obtains a value of 59 for the λo of K^+ in $KSbF_6$. However, this value of λo for K^+ gives a λo value for PF_6^- in KPF_6 of 293, which is greater than the λo of H_2F^+ and is thus not allowed on the basis of our first assumption. The minimum value of H_2F^+ must thus be adjusted to 284. From this one can calculate a maximum λo of 266 for SbF_6^- and a minimum λo of 68 for K^+. Thus the maximum λo of F^- must be decreased to 314. However, in all cases where a proton transfer mechanism occurs, the cation mobility is greater than that of the anion. [23, 89, 91] To meet this requirement, the λo of H_2F^+ must be adjusted to a minimum of 299 and the λo of F^- must be adjusted to a maximum of 299. From the minimum λo of 215 for F^-, a maximum λo of 383 can be calculated for H_2F^+. The λo's of H_2F^+ and F^- are related in that they must total 598. Summarizing then for F^-, $215<\lambda o<299$; and for H_2F^+, $384>\lambda o>299$.

In order to proceed further another assumption must be made. The H_2F^+ and F^- ions should be of similar size to the H_3O^+ and OH^- ions. One would expect that in media of similar viscosity the normal mobility ratios H_2F^+/F^- and H_3O/OH^- would be the same. If one assumes that the

abnormal mobility ratios for H_2F^+/F^- and H_3O^+/OH^- are the same as well, then one can calculate the H_2F^+ and F^- mobilities. Water at 100°C (η=0.283) [102a] has a viscosity slightly higher than HF at 0°C (η=0.256). [7] The λ_o's of 630 for H_3O^+ and 450 for OH^- at 100°C gives a cation/anion mobility ratio of 1.4. Setting the mobility ratio of H_2F^+/F^- at 1.4, one can calculate λ_o = 250 for F^- and λ_o = 350 for H_2F^+. Using these values, λ_o's can then be calculated for the other ions from the measured limiting equivalent conductivities (Table 4.8). The value of 1.4 for the H_2F^+/F^- mobility ratio happens to be very similar to the ratios for the characteristic solvent cations and anions in H_2SO_4 [89] and HSO_3F, [23] but this could be entirely coincidental.

TABLE 4.8

Equivalent Ionic Conductivities

	λ_o^+		λ_o^-
H_2F^+	350	F^-	250
Li^+	90	PF_6^-	220
Na^+	115	AsF_6^-	220
K^+	130	SbF_6^-	205
Rb^+	155	BF_4^-	205
Cs^+	180		
$T\ell^+$	160		
Ca^{++}	80		
Sr^{++}	80		
Ba^{++}	85		
Pb^{++}	80		

CHAPTER V

ADDUCTS OF SF_4 - THE SF_3^+ CATION

Introduction

Sulfur tetrafluoride has been shown to form stable 1:1 complexes with a number of fluoride acceptors. [103, 104] $SF_4 \cdot BF_3$ is a white solid which sublimes at room temperature and has a dissociation pressure of one atmosphere at 56°C, [105] in marked contrast to the physical properties of the two components (SF_4 m.pt. -121, b.pt. -40; BF_3 m.pt. -127, b.pt. -101). [106] Vapour density measurements and infra-red spectra show that it is completely dissociated in the gas phase. [107] $SF_4 \cdot AsF_5$ is more stable, the dissociation pressure reaching one atmosphere at about 180°C. [78] $SF_4 \cdot SbF_5$ melts to a colourless liquid at 245°C. [78]

Bartlett and Robinson originally proposed a donor-acceptor structure for these adducts. [104] However, Cotton and George have argued against this formulation [108] and suggested instead the ionic structure $SF_3^+ BF_4^-$. Although they obtained evidence for the BF_4^- ion from IR spectra in KBr discs and Nujol mulls, they could not rule out the possibility that it originated by hydrolysis. [107] Seel and Detmer also found a characteristic infra-red absorbtion ascribable to BF_4^- in solid $SF_4 \cdot BF_3$, and of greater importance, they observed

absorbtions at 908 cm^{-1} and 940 cm^{-1}, which by comparison with the isoelectronic PF_3, were assigned to the SF_3^+ ion. (105)

The ^{19}F nmr spectrum of the AsF_3-SF_4 system shows only one type of fluorine environment due to a rapid exchange of fluorine atoms. (109) Oppegard et al. pointed out that association and dissociation of a simple donor-acceptor adduct would not provide a mechanism for exchange of fluorine atoms bonded to arsenic with those bonded to sulfur, while the ionic formulation SF_3^+ AsF_4^- would do so. However, they observed no exchange between SF_4 and SiF_4, which forms the stable $SiF_6^=$ ion and this led them to suggest the possibility of a fluorine bridged structure.

Intermolecular exchange in SF_4 has also been shown by ^{19}F nmr to be catalyzed by BF_3. (110) At 70°C, an 8% solubility of BF_3 (or the BF_3 - SF_4 complex) in liquid SF_4 was found.*

In a subsequent paper, Bartlett and Robinson strongly favoured the ionic formulation over a fluorine bridged structure. (78) The main argument was the nonexistence of interaction between SF_4 and CsF or NO_2F. However, the compounds $CsSF_5$ (111) and $(CH_3)_4NSF_5$ (112) have since been prepared. Bartlett obtained an x-ray powder photograph of $SF_4 \cdot SbF_5$ and found it to be simple cubic, with one molecule

* The single fluorine peak had a chemical shift for this solution to low field of SF_4 rather than to higher field as expected. It was pointed out that though the shift of F on B is to high field of SF_4, the shift of the complex was not known. However, it is shown in this work that the chemical shift of SF_3^+ is also to high field of SF_4. No explanation for these results can be made by the author of this thesis.

per unit cell, noting that the symmetry is suggestive of the ionic formulation SF_3^+ SbF_6^-. They also determined that the stability of the adducts increased in the order $BF_3<AsF_5<SbF_5$ and showed that the weaker fluoride acceptor can be displaced from the adduct by the stronger one. They, as well as earlier workers, [78, 105, 113] measured the enthalpy of dissociation of solid $SF_4 \cdot BF_3$ to gaseous SF_4 and BF_3, and by comparison with the enthalpies of dissociation of the alkali fluoroborates $CsBF_4$, $RbBF_4$ and KBF_4, showed that it was consistent with an ionic formulation (Table 5.1). However, it should be noted that $CH_3CN \cdot BF_3$, which has a donor-acceptor structure, [114] has an enthalpy of dissociation on going from the solid adduct to gaseous CH_3CN and BF_3 very similar to that of $SF_4 \cdot BF_3$ (Table 5.1). Donor-acceptor complexes of the weaker Lewis acid PF_5 with $(CH_3)_2O$, $(CH_3)_2S$ and $(CH_3)_2Se$ also have similar enthalpies of dissociation. The much lower values found for the adducts $(CH_3)_2O \cdot BF_3$ and $(C_2H_5)_2O \cdot BF_3$ are for the dissociation of the gaseous complexes. [115]

Calvert and Morton have obtained single crystal x-ray data on $SF_4 \cdot BF_3$. [116] Finding a strong similarity between the observed crystallographic data and the data for $NH_4^+IO_3^-$, they ascribe to it the ionic formulation $SF_3^+BF_4^-$.

Azeem investigated the bonding in $SF_4 \cdot BF_3$ by ^{18}F exchange and IR spectroscopy. [117] He measured the amount of ^{18}F exchanged

between $S^{18}F_4$ and BF_3, and SF_4 and $B^{18}F_3$ on formation of the complex and subsequent decomposition by a suitable donor molecule as a function of temperature. He found that at low temperatures there was less exchange than expected for an ionic structure, and that the amount of exchange was best interpreted in terms of a fluorine bridged structure such as that below:

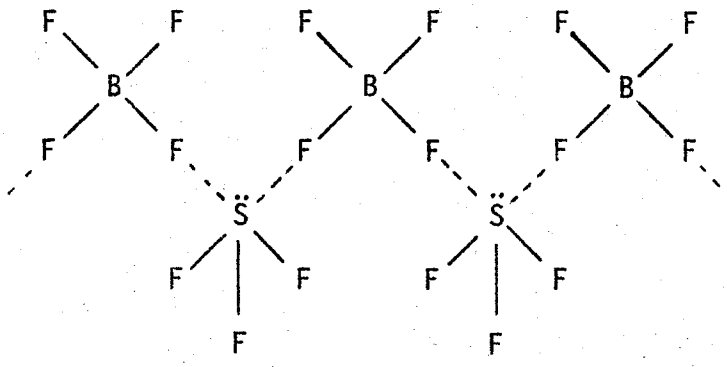

Subsequent to the investigations reported here, Evans and Long observed the Raman spectrum of molten $SF_4 \cdot SbF_5$ and assigned it on the basis of the ionic model $SF_3^+SbF_6^-$. (121)

Vibrational Spectra of the Solid Adducts

Raman spectra were obtained for the adducts $SF_4 \cdot BF_3$, $SF_4 \cdot PF_5$ $SF_4 \cdot AsF_5$ and $SF_4 \cdot SbF_5$. It was found that spectra obtained at a temperature of -70°C and lower were of better quality than those run at room temperature. There are probably two reasons for this:

1) The more volatile of the adducts have an appreciable vapour pressure at room temperature. Localized heating by the laser beam

caused the solid to slowly sublime out of the beam path, since the tube had been evacuated in the sample preparation. This was shown by a slow decline in intensity of the spectra obtained, and a subsequent recovery of intensity on slightly repositioning the sample tube. This drop in intensity did not occur at low temperature;

2) The low temperature spectra were also sharper than those run at room temperature. A much larger number of molecules will be in a first excited vibrational level at the higher temperature, and absorbtions due to transitions from this level will be observed. However, due to anharmonicity, the energy absorbed will differ slightly from that in transitions from the ground state, consequently, a broadening of the Raman band occurs. All spectra reported here were run at low temperature.

a) $SF_4 \cdot SbF_5$

The Raman spectrum of solid $SF_4 \cdot SbF_5$ is given in Table 5.2. Also included for purposes of comparison is the spectrum obtained by Evans and Long for the molten complex.

The hexafluoroantimonate ion belongs to the point group O_h and therefore has six normal modes of vibration $\nu_1(A_{1g})$, $\nu_2(E_g)$, $\nu_3(T_{1u})$, $\nu_4(T_{1u})$, $\nu_5(T_{2g})$ and $\nu_6(T_{2u})$ of which ν_1, ν_2 and ν_5 are Raman active and ν_3 and ν_4 are IR active. PF_3 has C_{3v} symmetry and therefore has four normal modes of vibration $\nu_1(A_1)$, $\nu_2(A_1)$, $\nu_3(E)$ and $\nu_4(E)$ all of which are both infra-red and Raman active. Thus, for a

TABLE 5.2

Raman Spectrum of $SF_4 \cdot SbF_5$

Solid			Melt*	
Relative intensity	Frequency shift (cm^{-1})	Assignment	Frequency shift (cm^{-1})	Assignment *
26	288	ν_5 SbF_6^-	291	ν_5 SbF_6^-
5	411	ν_4 SF_3^+	356	ν_4 SF_3^+
11	529	ν_2 SF_3^+		
19	554	ν_2 SbF_6^-	568	ν_2 SbF_6^-
20	582			
100	652	ν_1 SbF_6^-	645	ν_1 SbF_6^-
24	680	ν_3 SbF_6^-	690	ν_2 SF_3^+
sh	928	ν_1, ν_3 SF_3^+	922	ν_3 SF_3^+
66	943		943	ν_1 SF_3^+
sh	955			

* reference 121

purely ionic structure, only seven lines are expected in the Raman spectrum. However, if the structure is of a type similar to that shown below, in which fluorine bridging is occurring to some extent, the symmetry of the ions is lowered.

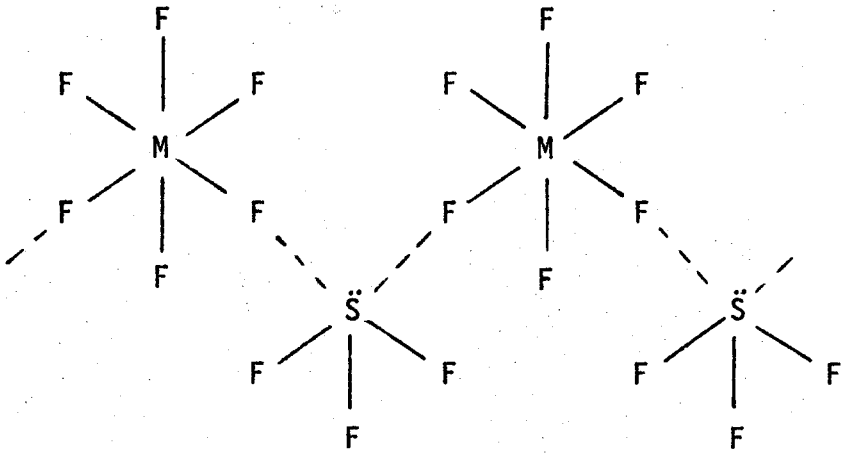

In the case of SF_3^+, this means that the degenerate lines can be split, while for the anion the Raman forbidden, infra-red active lines can become Raman active in addition to splitting. The extent to which this occurs will depend on the degree of fluorine bridging. In the extreme case of strong fluorine bridge bonds, the ionic structure will be strongly perturbed and the spectrum will not be interpretable by comparison to SbF_6^- and PF_3.

It can be seen that the spectrum of the solid adduct can be assigned by comparison with previous assignments for SbF_6^- [122] (Table 5.3) and PF_3 [123] (Table 5.8). The assignments for SbF_6^- agree

TABLE 5.3

Vibrational Frequencies of the SbF_6^- ion, cm^{-1}

Raman	$\nu_1(A_{1g})$	$\nu_2(E_g)$	$\nu_3(T_{1u})$	$\nu_4(T_{1u})$	$\nu_5(T_{2g})$
$LiSbF_6$ solid *	668	558			294
$KSbF_6$ solid †	664	583			298 270
$KSbF_6$ solution in DMF ¶	645	572			279
SeF_3SbF_6 molten ¶	645	550			290
SF_3SbF_6 molten ¶	645	568			291
Infra-red					
$KSbF_6$ solid ¶			660		
$LiSbF_6$ solid *			669	350	

* reference 122

† this work

¶ reference 121

reasonably well with those of Evans and Long except that ν_2 and ν_5 are found to be doublets and the weak line at 680 cm^{-1} is attributed to ν_3 which is formally forbidden instead of to the SF_3^+ ion. It is assumed that the splitting of ν_2 and ν_5 and observation of ν_3 in the Raman spectrum arise from some lowering of symmetry of the SbF_6^- in the crystal probably as a result of fluorine bridging with SF_3^+.

The bands observed at 928, 943, 529 and 411 cm^{-1} are assigned by comparison with the spectrum of the isoelectronic molecule PF_3 [123] to ν_3, ν_1, ν_2 and ν_4 respectively of the SF_3^+ ion (Table 5.2). A shoulder on the ν_3 band is apparent at 955 cm^{-1} and this is consistent with some reduction of symmetry as a consequence of fluorine bridging. The splitting of ν_3 of SF_3^+ and ν_2 and ν_5 of SbF_6^- can not be ascribed to in and out of phase vibrations occurring where more than one molecule is present in the unit cell, as the unit cell of $SF_4 \cdot SbF_5$ has been shown to contain only one molecule. [78]

The assignment of SF_3^+ differs from that proposed by Evans and Long [121] on two points:

1) The weak band at 529 cm^{-1} rather than the band at 690 cm^{-1} is assigned to ν_2; this latter band which was observed at 680 cm^{-1} being assigned to ν_3 of SbF_6^-. Although ν_3 should be forbidden, it is reasonable to assume that it is weakly allowed in the melt as well as in the crystal because of fluorine bridging. This assignment is confirmed by the fact that no line at 680 cm^{-1} is found in the spectra

of $SF_4 \cdot BF_3$ and $SF_4 \cdot PF_5$ although both contain the SF_3^+ ion. Evans and Long themselves regarded the assignment of the 690 cm^{-1} band to ν_2 as rather unsatisfactory.

2) The ν_4 band is found at 411 cm^{-1} rather than 356 cm^{-1}. This is confirmed by the observation of bands having frequencies close to this value in all the other SF_3^+ compounds that were studied (Table 5.8).

b) $\underline{SF_4 \cdot BF_3}$

The Raman spectrum of $SF_4 \cdot BF_3$ is given in Table 5.4. Also given is the complementary IR spectrum observed by Azeem. [124] The tetrafluoroborate anion belongs to the point group T_d and therefore, has four normal modes of vibration all of which are active in the Raman $\nu_1(A)$, $\nu_2(E)$, $\nu_3(T_2)$ and $\nu_4(T_2)$ and only ν_3 and ν_4 are active in the infra-red. Thus, for a purely ionic structure only eight bands are expected in the Raman spectrum and six in the infra-red. If fluorine bridging occurs, the symmetry of the ions will be lowered. Forbidden bands can appear in the Raman spectrum and splitting can occur in the Raman and infra-red spectra.

An assignment of the observed bands in the Raman and infra-red spectra can be made in terms of the ionic model $SF_3^+BF_4^-$ using the previous assignments for BF_4^- (Table 5.5) and PF_3 (Table 5.8). However, the forbidden infra-red frequencies ν_1 and ν_2 appear with reasonable intensity and ν_2 appears as a doublet. In addition, ν_3 for SF_3^+ is split in the Raman spectrum. The occurrence of the forbidden bands and

TABLE 5.4

Raman and Infra-red Spectra of $SF_4 \cdot BF_3$

Relative Intensity	Frequency shift (cm^{-1})	Frequency (cm^{-1})	Relative* Intensity	Assignment
23	357	357	w	ν_2 BF_4^-
		370	w	
21	414	409	m	ν_4 SF_3^+
6	529	520	vs	ν_2 SF_3^+
7	546	536	vs	ν_4 BF_4^-
		753	m	ν_1 BF_4^-
43	770	773	m	
46	913	910	vs	ν_1, ν_3 SF_3^+
sh	921			
100	939	935	vs	
		1035-1090	vs, br	ν_3 BF_4^-
		1140	s	

* s = strong, m = medium, w = weak, v = very, br = broad

TABLE 5.5

Vibrational Frequencies for the BF_4^- ion, cm^{-1}

		$\nu_2(E)$	$\nu_4(T_2)$	$\nu_1(A_1)$	$\nu_3(T_2)$
Raman					
Aqueous $NaBF_4$	*	369	541	786	1100
	†	353	524	769	984 1016
	¶	358	530	767	
KBF_4 solid	¶	358	529 536	773	
Infra-red					
KBF_4	§		525 536	773	1038 1063 1078
$NaBF_4$	T		516 527	779	1036 1078

* reference 125

† reference 126

¶ this work

§ reference 127

T reference 128

the additional splittings can be attributed to a lowering of the symmetry of both ions in the crystal probably as a result of fluorine bridging.

c) $\underline{SF_4 \cdot PF_5}$

The vibrational spectrum of this compound has not been previously studied. The Raman spectrum of the solid is given in Table 5.6. The PF_6^- ion belongs to the point group O_h, as does the SbF_6^- ion, and the comments about $SF_4 \cdot SbF_5$ apply here. The spectrum of the $SF_4 \cdot PF_5$ adduct can be assigned on the basis of the ionic structure $SF_3^+PF_6^-$ making use of previous assignments for PF_6^- (122) and PF_3. The observed spectrum due to PF_6^- is very similar to that of SbF_6^- and again indicates a lowering of symmetry. Thus it can be seen that ν_5 and ν_2 are split into doublets and the forbidden ν_3 vibration appears weakly at 815 cm^{-1}. As in all the other compounds studied, ν_3 of SF_3^+ is split into a doublet. These observations are consistent with some fluorine bridging between the ions SF_3^+ and PF_6^-.

d) $\underline{SF_4 \cdot AsF_5}$

The vibrational spectrum of this compound has not been previously studied. The Raman spectrum of the solid is given in Table 5.7. Again, the AsF_6^- ion belongs to the O_h point group, as do the PF_6^- and SbF_6^- ions and the comments about those adducts apply here as well. The spectrum can be assigned on the basis of the ionic structure $SF_3^+AsF_6^-$ making use of previous assignments for AsF_6^- (122)

TABLE 5.6

Raman Spectrum of $SF_4 \cdot PF_5$

Relative intensity	Frequency shift (cm^{-1})	Assignment	KPF_6 * Raman shift (cm^{-1})	KPF_6 * Infra-red Frequency (cm^{-1})
13	408	ν_4 SF_3^+		
5	463	ν_5 PF_6^-	477	
14	479			
10	531	ν_2 SF_3^+		
19	558	ν_2 PF_6^- or ν_2, ν_4 PF_6^-		558
8	580		580	
90	748	ν_1 PF_6^-	751	
5	815	ν_3 PF_6^-		830
21	929	ν_1, ν_3 SF_3^+		
100	954			
sh	964			

* reference 122

TABLE 5.7

Raman Spectrum of $SF_4 \cdot AsF_5$

Relative intensity	Frequency shift (cm^{-1})	Assignment	$CsAsF_6$ * Frequency shift (cm^{-1})
36	379	ν_5 AsF_6^-	372
11	411	ν_4 SF_3^+	
7	530	ν_2 SF_3^+	
35	563	ν_2 AsF_6^-	576
10	587		
76	686	ν_1 AsF_6^-	685
19	926	ν_1, ν_3 SF_3^+	
100	945		
sh	960		

* reference 122

and PF_3. Again, it is noted that ν_2 for AsF_6^- and ν_3 for SF_3^+ are split indicating probable fluorine bridging. The frequencies assigned to SF_3^+ in all four compounds have been summarized in Table 5.8. The good agreement between the observed frequencies gives further confirmation of the correctness of the assignment.

Conductivity Measurements

The two adducts, $SF_4 \cdot BF_3$ and $SF_4 \cdot SbF_5$ give solutions in anhydrous HF which have conductivities that are closely similar to, although slightly lower than, those of KBF_4 and $KSbF_6$ (Table 5.9 and Fig. 5.1, 5.2). It can be concluded therefore, that the two adducts are fully ionized in solution in HF, e.g.:

$$SF_4 \cdot BF_3 \xrightarrow{HF} SF_3^+ + BF_4^-$$

Solutions of SF_4 also have a moderate conductivity although this is considerably smaller than that of the fully ionized BF_3 and SbF_5 adducts. At 0°C, pure liquid SF_4 has an equilibrium vapour pressure of five atmospheres. In view of this, there is probably an appreciable vapour pressure of SF_4 above the HF solution. The shape of the conductivity curve obtained on diluting a solution of SF_4 supports this.

$$SF_4 \text{ (in HF solution)} \rightleftharpoons SF_4 \text{ (vapour phase)}$$

TABLE 5.8

Vibrational Frequencies for the SF_3^+ ion and PF_3, cm^{-1}

	$\nu_1(A_1)$	$\nu_2(A_1)$	$\nu_3(E)$	$\nu_4(E)$
PF_3 *	892	487	860	344
$SF_3 \cdot BF_4$	939	529	913	414
$SF_3 \cdot PF_6$	954	531	929	408
$SF_3 \cdot AsF_6$	945	530	926	411
$SF_3 \cdot SbF_6$	943	529	928	411

* reference 123

TABLE 5.9

Conductivities of Solutions

of $SF_4 \cdot BF_3$ and $SF_4 \cdot SbF_5$ in HF

$SF_4 \cdot BF_3$		$SF_4 \cdot SbF_5$	
Concentration (molal)	$\kappa \times 10^2$ (mhos/cm)	Concentration (molal)	$\kappa \times 10^2$ (mhos/cm)
0.0522	1.109	0.0305	0.714
0.0935	1.806	0.0546	1.169
0.126	2.455	0.0698	1.548
0.138	2.446	0.0732	1.457
0.155	2.67	0.0945	1.806
0.177	2.97	0.119	2.231
0.192	3.16	0.143	2.507
0.263	4.08	0.220	3.471
0.561	7.21	0.308	4.415
0.839	8.83		
0.840	9.01		
1.238	11.09		

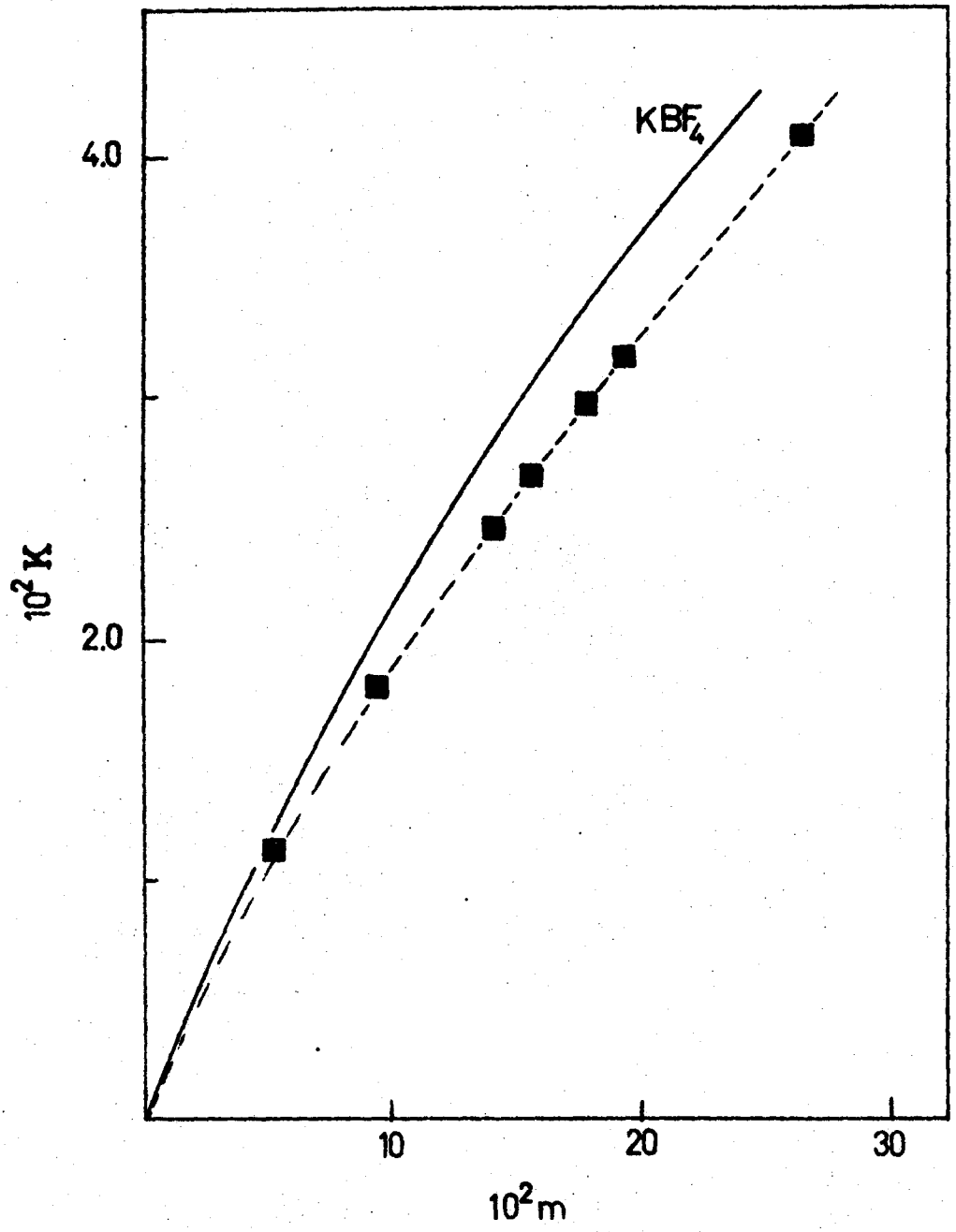

Figure 5.1 Conductivity of $SF_4 \cdot BF_3$

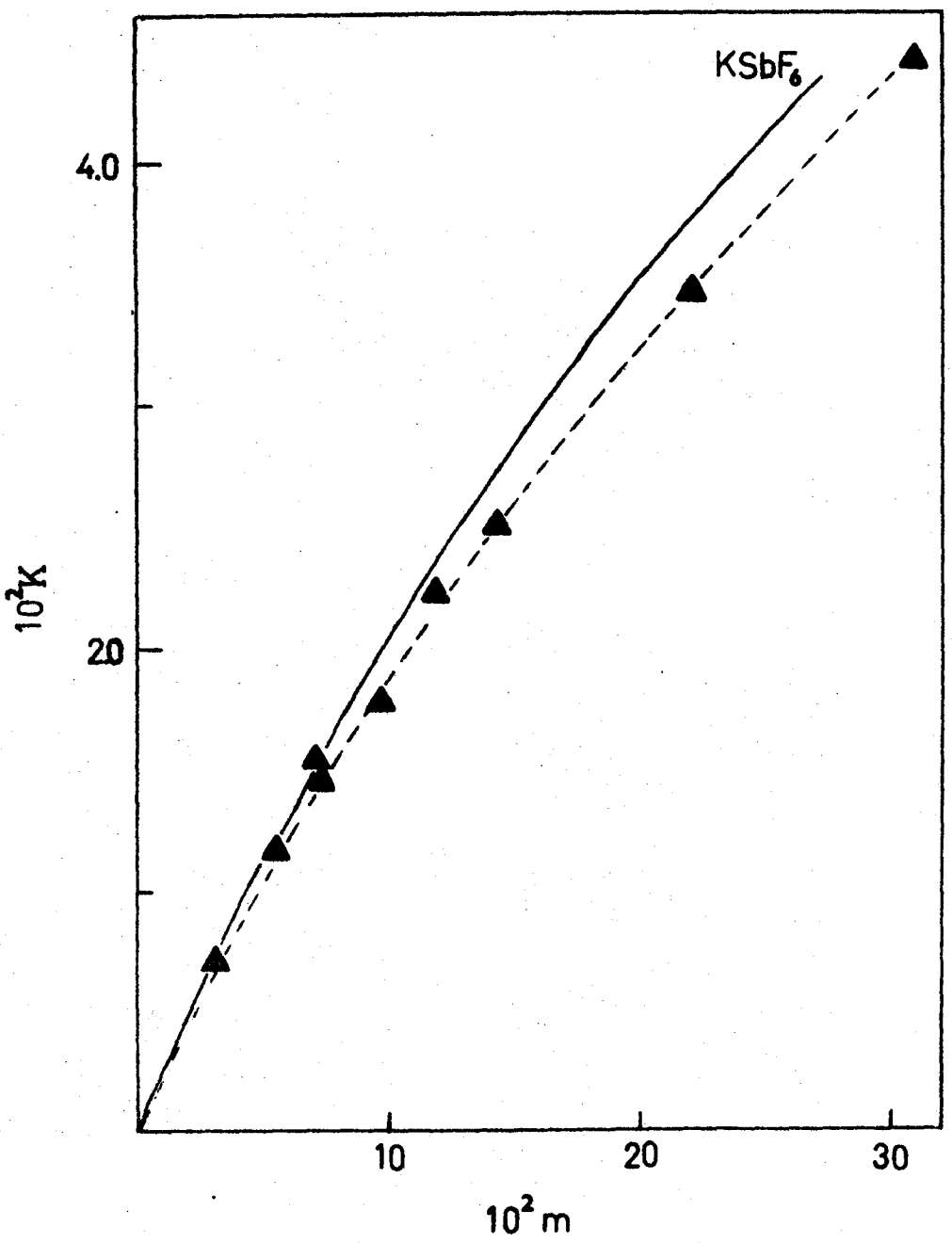

Figure 5.2 Conductivity of $SF_4 \cdot SbF_5$

However, there is an interaction between them, as shown by the conductivity, and the presence of only one liquid phase in the more concentrated solutions of SF_4 in HF, where sufficient SF_4 was present to be in the liquid state under pressure.

Therefore, to obtain the true concentration of SF_4 in solution an extrapolation technique was used. As the conductivity cell is filled with successive increments of HF, the volume of vapour space decreases towards zero. At the same time, the dilution reduces the concentration of SF_4 in solution. Both factors will push the equilibrium to the left. When no vapour space is left, that is, the conductivity cell is completely filled, the calculated concentration would be the same as the true concentration. However, it is not only difficult, but also dangerous to fill the conductivity cell completely. The observed conductivity was plotted against the molality calculated assuming complete dissolution of the SF_4 and the curve was extrapolated to the molality corresponding to the completely filled cell. The concentration for this point was calculated from the known weight of SF_4 taken and the volume of the cell, taking the density of liquid HF as 1.00 g/ml. In this way, one point on the SF_4 in HF conductivity curve was obtained from each dilution run.

Initially, the SF_4 and then the first increment of HF were condensed in with liquid nitrogen. Subsequent increments of HF were condensed in with a dry ice-trichloroethylene slush bath. An infra-red

spectrum of the SF_4 used at a known pressure showed it to contain 5% SOF_2 by comparison of the band intensity with a sample of pure SOF_2 at a known pressure. As conductivity measurements showed that SOF_2 does not give conducting solutions in HF, this affected the measurements only to the extent that the weight of SF_4 taken had to be corrected for the amount of impurity present. The dilution runs are summarized in Table 5.10 and the extrapolations illustrated in Figure 5.3. The final conductivity curve is illustrated in Figure 5.4.

It can be concluded that SF_4 behaves as a partially ionized weak base in solution in anhydrous HF.

$$SF_4 + HF \rightleftharpoons SF_3^+ + HF_2^-$$

The results shown in Figures 5.1 and 5.2 show that the mobility of the SF_3^+ ion must be similar to that of the K^+ ion. Hence, by comparing the observed conductivity of SF_4 with that of KF at any given temperature, one can obtain the degree of dissociation and hence the equilibrium constant for its ionization.

$$K = \frac{[SF_3^+][HF_2^-]}{[SF_4]}$$

This was found to be $4\pm2\times10^{-2}$ at 0°C.

TABLE 5.10

Conductivity of SF_4 in HF

Run # 113 corrected weight SF_4 = 0.523 gm cell volume = 27.0 ml

weight of HF	nominal molality	$10^3\kappa$
7.15	0.67	37.7
10.78	0.45	31.8
14.08	0.34	28.2
18.08	0.27	26.3

extrapolated molality = 0.18

extrapolated conductivity = 23

dissociation constant = 5.5×10^{-2}

Run # 114 corrected weight SF_4 = 0.188 gm cell volume = 23.8 ml

weight of HF	nominal molality	$10^3\kappa$
7.34	0.24	20.7
10.50	0.17	16.4
14.69	0.12	14.0
20.38	0.085	11.4

extrapolated molality = 0.07

extrapolated conductivity = 11

dissociation constant = 2.6×10^{-2}

TABLE 5.10 (Continued)

Run # 115 corrected weight SF_4 = 0.723 gm cell volume = 27.0 ml

weight of HF	nominal molality	$10^3\kappa$
6.90	0.97	44.1
13.52	0.49	34.5
23.33	0.29	26.2

extrapolated molality = 0.25

extrapolated conductivity = 24

dissociation constant = 4.0×10^{-2}

Run # 116 corrected weight SF_4 = 0.107 gm cell volume = 23.8 ml

weight of HF	nominal molality	$10^3\kappa$
8.48	0.12	14.4
14.07	0.07	10.5
20.13	0.05	8.2

extrapolated molality = 0.04

extrapolated conductivity = 7

dissociation constant = 1.9×10^{-2}

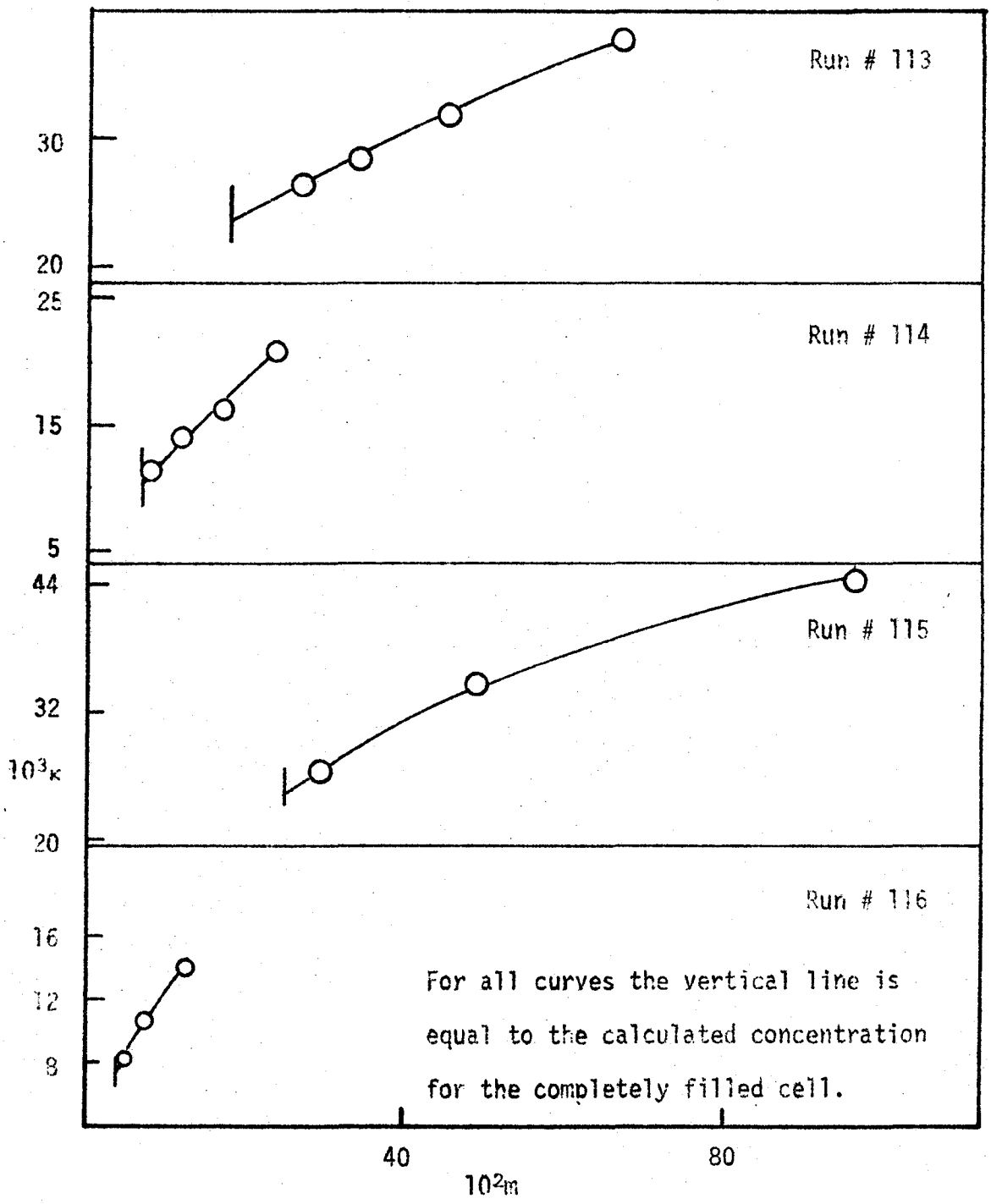

Figure 5.3 Conductivity of SF_4 - Dilution Runs

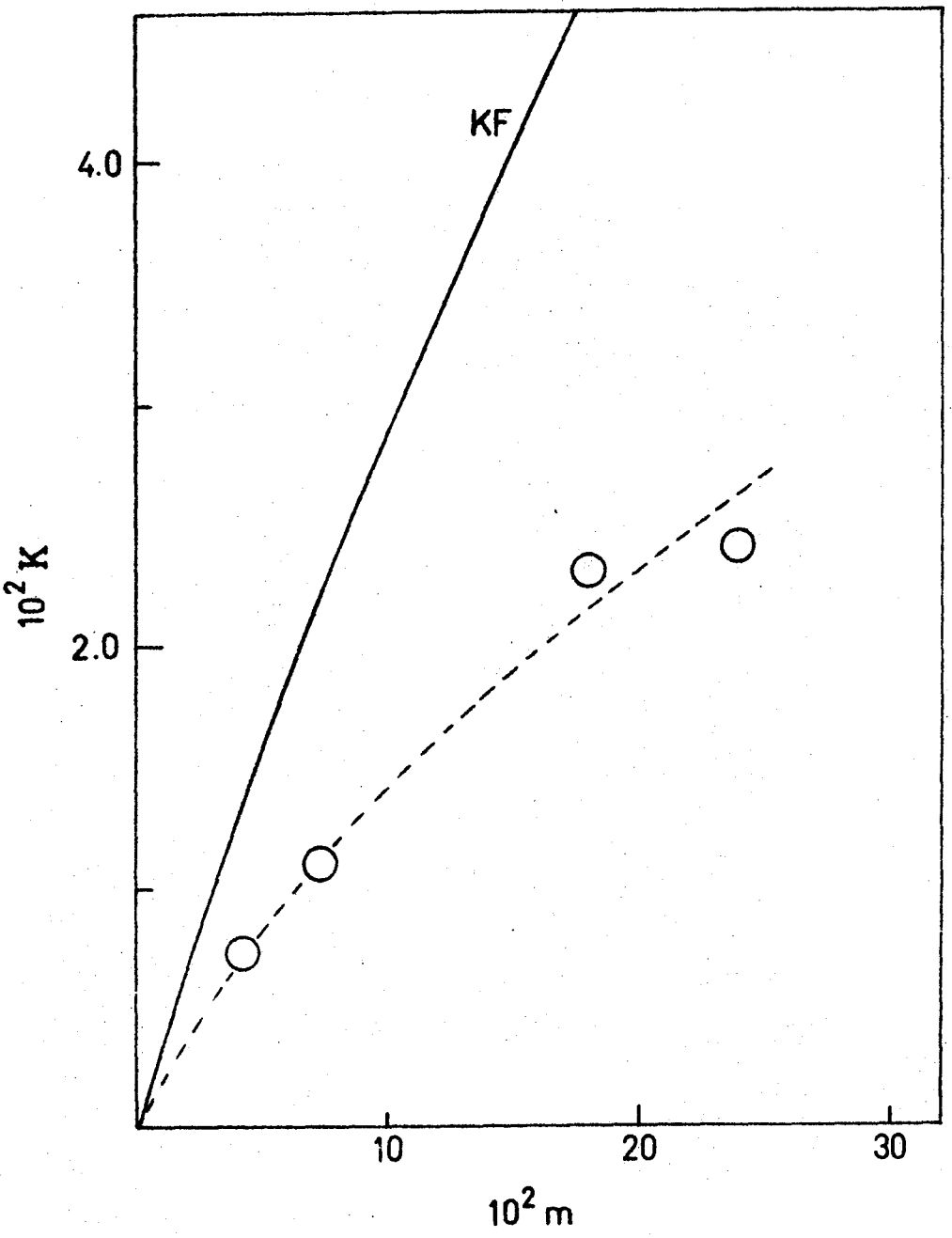

Figure 5.4 Conductivity of SF_4

NMR Spectra

The ^{19}F nmr spectrum of $SF_4 \cdot BF_3$ in HF gave only a single broad peak at room temperature. On cooling, this peak narrows and a second smaller peak appears to lower field. Similar behaviour was observed for $SF_4 \cdot SbF_5$ and $SF_4 \cdot AsF_5$ (Table 5.11). The low field peak has very nearly the same chemical shift* in each case (-25 to -30 ppm from $CFC\ell_3$) and is in the fluorine on sulfur region of the spectrum. This peak is attributed to the SF_3^+ ion. The high field peak is due to the anion BF_4^-, SbF_6^- or AsF_6^- exchanging with the solvent.

The width of the SF_3^+ peak is dependent both on the temperature and the acidity of the HF. Hydrogen fluoride is normally slightly basic, (i.e. there is an excess of F^- ion) due to water impurity. In all solutions where no steps were taken to acidify the HF, the SF_3^+ peak was visible only on cooling. The SF_3^+ peak is too broad to be observed at room temperature, presumably because of exchange of fluorine with the solvent. Even in a neutral solution, the SF_3^+ peak is still not visible in the room temperature spectra. Neutrality is shown by the observation of the coupling between the proton and fluorine in the HF solvent. (129)

Additions of a small amount of fluoride ion to solutions of $SF_4 \cdot BF_3$ resulted in the appearance of a new peak at +153.5 ppm from $CFC\ell_3$ and the simultaneous disappearance of the peak assigned to SF_3^+ which could not then be observed even at low temperatures. The new

* Chemical shift (δ) = $10^6(\nu_{CFC\ell_3} - \nu_s)/\nu_{CFC\ell_3}$ where $\nu_{CFC\ell_3}$ and ν_s are the resonant frequencies of $CFC\ell_3$ and the sample respectively.

TABLE 5.11

^{19}F Chemical Shifts of SF_4 Adducts in HF (ppm from $CFCl_3$)

Solute	T (°C)	Chemical Shift SF_3^+	HF	Anion	
$SF_4 \cdot BF_3$	25	-	195.3	-	
	0	-	195.3	-	
	-50	-26.7	194.2	-	
	-70	-25.9	193.2	-	
	-90	-25.5	191.3	-	
$SF_4 \cdot BF_3 + KBF_4$	-30	-26.9	194.5	-	
	-50	-26.1	194.5	-	
$SF_4 \cdot BF_3 + KF$	0	-	191.6	153.5	
	-30	-	190.0	152.9	(BF_4^-)
	-50	-	189.7	153.5	
$SF_4 \cdot BF_3 + NH_4F$	-55	-	175.8	151.7	
$SF_4 \cdot AsF_5$*	25	-30.5	191.7	-	
$SF_4 \cdot 2AsF_5$	25	-29.2	181.3	-	
	- 5	-28.4	180.6	-	
	-30	-27.5	181.5	-	
	-60	-26.8	178.3	-	
$SF_4 \cdot SbF_5$	-60	-27.1	198	-	
	-90	-26	195.4	-	
$SF_4 \cdot 2SbF_5$	-85	-27.6	191.1	124.3	(SbF_6^-)
				95.2	
				120.7	($Sb_2F_{11}^-$)
				142.6	

* Slight excess of AsF_5.

peak is due to BF_4^- (cf. the shift of +153.6 ppm observed for a solution of KBF_4 in HF). The addition of fluoride represses the exchange of fluoride between BF_4^- and the solvent

$$BF_4^- + HF \rightleftharpoons BF_3 + HF_2^-$$

while at the same time promoting the exchange between SF_3^+ and the solvent

$$SF_3^+ + HF_2^- \rightleftharpoons SF_4 + HF$$

Addition of a slight excess of AsF_5 to the $SF_4 \cdot AsF_5$ solution gave an SF_3^+ peak which was observable, although rather broad, even at room temperature. Cooling the sample caused the peak to narrow. Addition of one mole of AsF_5 per mole of $SF_4 \cdot AsF_5$ gave a sharp SF_3^+ peak even at room temperature. As AsF_5 is an acid in HF, it will repress the exchange between SF_3^+ and the solvent, by the removal of fluoride ions through which the exchange occurs. No AsF_6^- peak was observed in any of the spectra presumably because of exchange of fluoride with the solvent and quadrupole relaxation of the ^{75}As nucleus.

For the solutions of $SF_4 \cdot SbF_5$ a peak at -27.1 ppm which may be attributed to SF_3^+ was obtained at low temperature in addition to a peak due to the solvent. No peak was observed from SbF_6^-, presumably because of partially relaxed coupling to ^{121}Sb (I=5/2) and ^{127}Sb (I=7/2)

and exchange with the solvent giving a very broad spectrum which could not be detected above the base line noise. Addition of SbF_5 to this solution however, gave ^{19}F nmr signals which could be attributed to $Sb_2F_{11}^-$ and SbF_6^-. (20)

It is noted that there is a solvent shift for $Sb_2F_{11}^-$ in SO_2 of 3.6 ppm for the bridging fluorine, and 10 to 11 ppm in the peripheral fluorines (Table 5.12). This is attributed to some ion-pair formation on going from HF (ε = 175 at -73°C) (7) to SO_2 (ε = 24.6 at -68.8°C), (131) which draws off some of the shielding electron density. The peripheral fluorines, through which ion pair formation would occur, show a greater shift than the bridging fluorine, which will take no direct part in the ion pairing.

A solution of SF_4 in HF gave only a single resonance at all temperatures showing that exchange is occurring which is consistent with the conductimetric evidence for incomplete ionization of SF_4 in HF.

Summary

The Raman spectra of the solid 1:1 adducts of SF_4 with BF_3, PF_5, AsF_5 and SbF_5 can be assigned in terms of the ionic model $SF_3^+ MF_6^-$ (MF_4^-) but there is some perturbation of the spectra due to fluorine bridging. Similar fluorine bridging has been found in $SeF_3^+ Nb_2F_{11}^-$ (132) and $BrF_2^+ SbF_6^-$ (133) where structures have been determined by x-ray crystallography. In the latter compound, an ionic

TABLE 5.12

^{19}F shift in $Sb_2F_{11}^-$ from $CFC\ell_3$ in ppm

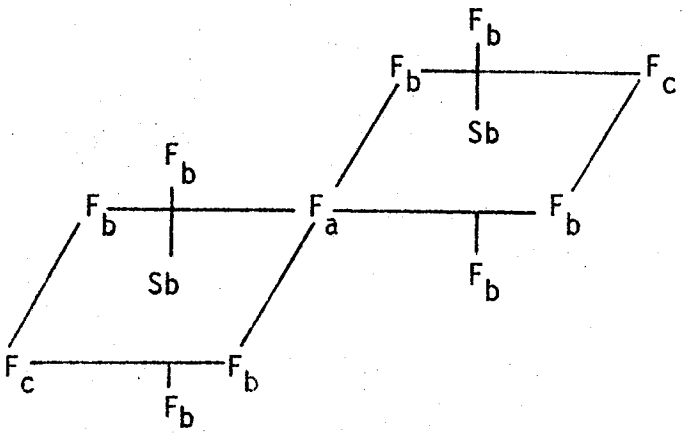

	F_a	F_b	F_c
$SF_4 \cdot SbF_5 + SbF_5$ in HF	95.2	120.7	142.6
SbF_5 in HF	93.0	120.1	141.8
$CsSb_2F_{11}$ in SO_2 *	89.4	109.1	131.2
Solvent shift from HF to SO_2	3.6	11.0	10.6

* reference 130

formulation was found to be a reasonable approximation to the structure. There was some contribution from fluorine bridging to the endless chain structure of alternate BrF_2^+ and SbF_6^- groups.

In hydrogen fluoride solution, both conductivity and ^{19}F nmr measurements indicate complete ionization to SF_3^+ and MF_6^- (MF_4^-). SF_4 is a weak base which only partly ionizes to give SF_3^+ and HF_2^-.

CHAPTER VI

ADDUCTS OF SOF_4 - THE SOF_3^+ CATION

Introduction

Solid 1:1 complexes between SOF_4 and SbF_5, AsF_5 or BF_3 were first prepared by Seel and Detmer. [105] They proposed an ionic structure for these compounds, e.g., $SOF_3^+SbF_6^-$, but they gave no experimental evidence in support of this. No other investigations of these complexes have been reported. It was of interest to obtain structural information on these adducts as no mixed oxide fluoride cations were known when this investigation was begun. However, recently several workers have shown the existence of a mixed oxide fluoride cation of nitrogen, NOF_2^+. [59] An ionic formulation for the SOF_4 adducts would also be a direct contrast to the donor-acceptor structure found for complexes of several other sulfur-oxygen-fluorine compounds, SOF_2, CH_3SO_2F and SO_2, with SbF_5 [79] and AsF_5. [134]

Raman Spectra of the Solid Adducts

The vibrational spectra of $SOF_4 \cdot AsF_5$ have not been previously studied. The Raman spectrum of the solid at -80°C is given in Table 6.1 The AsF_6^- ion, belonging to the point group O_h, has three Raman active vibrations. The details of the spectra of octahedral species have been discussed in Chapter V. The SOF_3^+ ion is isoelectronic with

TABLE 6.1

Raman Spectrum of $SOF_4 \cdot AsF_5$

Relative intensity	Frequency shift (cm^{-1})	Assignment	$CsAsF_6$ * Raman shift (cm^{-1})	$CsAsF_6$ * Infra-red Frequency (cm^{-1})
2	367	ν_4 AsF_6^-		
36	373	ν_5 AsF_6^-	372	
4	384	ν_4 AsF_6^-		392
16	391	ν_6 SOF_3^+		
4	402	ν_4 AsF_6^-		
12	497	ν_5 SOF_3^+		
4	513	ν_3 SOF_3^+		
24	585	ν_2 AsF_6^-	576	
100	689	ν_1 AsF_6^-	685	
24	706	ν_3 AsF_6^-		689
100	911	ν_2 SOF_3^+		
10	1057	ν_4 SOF_3^+		
10	1063			
14	1529	ν_1 SOF_3^+		
8	1538			

* reference 122

NSF_3 and POF_3 and its spectrum can be assigned by comparison with the already known spectra of these compounds. They belong to the C_{3v} point group and have six normal modes of vibration, $\nu_1(A_1)$, $\nu_2(A_1)$, $\nu_3(A_1)$, $\nu_4(E)$, $\nu_5(E)$ and $\nu_6(E)$ all of which are Raman and infra-red active. Thus, for an ionic structure, nine lines are expected in the Raman spectrum. However, if there is some degree of fluorine bridging between the ions, as was the case with the $SF_3^+MF_6^-$ compounds, the symmetry of the ions is lowered. In the case of AsF_6^-, this means that the Raman forbidden infra-red active lines can become Raman active, and in addition, the degenerate lines can be split, while for SOF_3^+ the degenerate lines can be split. The extent to which this occurs will depend on the degree of fluorine bridging.

It can be seen that the spectrum of the solid adduct can be assigned by comparison with previous assignments for NSF_3, [135] POF_3 [136] (Table 6.4) and AsF_6^- (Table 6.1). Both Raman forbidden vibrations of AsF_6^-, ν_3 and ν_4, have become active and in addition ν_4 appears as three lines indicating a complete removal of degeneracy for this band.

The bands observed at 1538 and 1529, 911, 513, 1063 and 1057, 497 and 391 cm^{-1} are assigned to ν_1, ν_2, ν_3, ν_4, ν_5 and ν_6 respectively. The assignment of ν_3 and ν_5 is opposite to that in POF_3. ν_3 is assigned to the higher frequency S-F bending mode and ν_5 to the lower frequency mode. However, this corresponds to the order of assignment in NSF_3 which is better for comparison of these particular vibrations.

In addition, in a series of compounds of similar C_{3v} symmetry; $OPC\ell_3$, $OPBr_3$, $OVC\ell_3$ and SPF_3, the frequency of ν_3 is greater than ν_5 in every case. (137) Final assignment of these vibrations must depend, however, on detailed force constant calculations which are beyond the scope of this work. The ν_4 band of SOF_3^+ is split indicating some removal of degeneracy. This, together with the removal of degeneracy for the AsF_6^- vibrations, is consistent with fluorine bridging between the ions. The ν_1 vibration of SOF_3^+ also is split. A possible reason for this splitting is the occurrence of in-phase and out-of-phase vibrations of two or more SOF_3^+ groups per unit cell.

The SO stretching frequency of 1533 cm^{-1} in SOF_3^+ AsF_6^- is the highest that has been observed. In comparison, an SO stretching frequency of 1379 cm^{-1} has been observed for SOF_4 (138) and the average of the symmetric and assymetric stretches in SO_2F_2 is 1385 cm^{-1}. (139) Gillespie and Robinson have calculated force constants for a number of SO bonds from their stretching frequencies by assuming there is negligible coupling between the vibration of the SO group and the other vibrations of the molecule and then treating the SO group as a simple diatomic molecule. (140) Their results were in reasonable agreement with more precise values obtained by other workers. A similar calculation on SOF_3^+ yields a force constant of 14.7 mdyne/Å. For comparison, Gillespie and Robinson's value for the force constant of SOF_4 is 11.7 mdyne/Å and that for SO_2F_2 is 12.0 mdyne/Å. The authors further found

a linear relationship between log k_{SO} and log r_{SO}, where k_{SO}, and r_{SO} are the stretching force constant and bond length respectively, and a linear relation between k_{SO} and the SO bond order. Using their relationships, one can calculate a bond length of 1.38Å and a bond order of 2.3 for SOF_3^+. This would make the SO bond in SOF_3^+ the shortest known. The bond length in SO_2F_2 has been found by microwave spectroscopy to be 1.405Å. (141)

This high bond order can be accounted for if it is assumed that the bonding can be described by the resonance structures I and II.

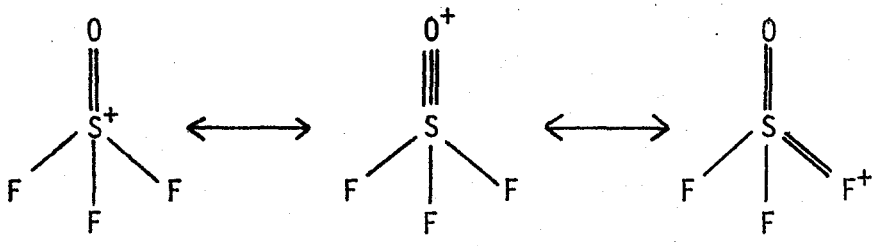

I II III

A similar high bond order of 2.2 has been found for the PO bond in the isoelectronic POF_3 molecule. (142) The SF assymmetric and symmetric stretching frequencies of 1063 and 911 cm^{-1} are also the highest that have been observed for any SF bond. Presumably there is also some contribution from structures such as III. The effect of a positive charge on sulfur on the SF stretching frequency is also illustrated by the increase in frequency on going from SF_4 to SF_3^+ (Table 6.2).

TABLE 6.2

Sulfur Fluorine Stretching Frequencies

	ν_{asym}	ν_{sym}
SOF_2	808	748
SOF_4	928	821
$SOF_3^+ AsF_6^-$	1060	911
SF_4	738	723
SF_6	940	775
$SF_3^+ SbF_6^-$	943	928

The Raman spectrum of $SOF_4 \cdot SbF_5$ has been obtained by Dean [143, 144] (Table 6.3). It can be assigned on the basis of the ionic structure $SOF_3^+ SbF_6^-$ making use of previous assignments for NSF_3 and SbF_6^-. The forbidden band ν_3 of SbF_6^- is Raman active, and in addition, it is split showing a complete removal of degeneracy consistent with fluorine bridging. In addition, ν_1 is again split. The agreement between the observed frequencies for SOF_3^+ in the AsF_5 and SbF_5 complexes of SOF_4 give further confirmation of the correctness of the assignment. (Table 6.4)

NMR Spectra of the Adducts

$SOF_4 \cdot AsF_5$ is a white solid at room temperature. It was prepared in an nmr tube on the vacuum line by condensing together SOF_4 and AsF_5, taking one or the other in excess in an attempt to dissolve some adduct. Some SO_2F_2 and SOF_2 were also present as impurities in the SOF_4. The ^{19}F nmr spectra of the resulting solutions were run over a range of temperatures. However, the adduct proved to have a very small solubility and was undetectable by nmr in either of the components. When excess SOF_4 was present, no peak due to AsF_5 was visible and in addition the SOF_4 peak was not broadened or shifted when compared to SOF_4 itself (δ_{CFCl_3} = -77 ppm) indicating there is no detectable exchange occurring between solvent SOF_4 and SOF_4 in the adduct. When excess AsF_5 was present, no peak due to SOF_4 was visible.

TABLE 6.3

Raman Spectrum of $SOF_4 \cdot SbF_5$

Relative Intensity	Frequency shift (cm^{-1})	Assignment	$LiSbF_6$* Raman shift (cm^{-1})	$LiSbF_6$* Infra-red Frequency (cm^{-1})
3	83	lattice modes		
2	94			
2	109			
<1	121			
3	234			
41	291	ν_5 SbF_6^-	294	350 (ν_3)
12	387	ν_6 SOF_3^+		
9	508	ν_5 SOF_3^+		
2	535	ν_3 SOF_3^+		
12	577	ν_2 SbF_6^-	558	
100	647	ν_1 SbF_6^-	668	
sh	655, 657, 661	ν_3 SbF_6^-		669
41	909	ν_2 SOF_3^+		
6	1063	ν_4 SOF_3^+		
6	1532	ν_1 SOF_3^+		
6	1540			

* reference 122

TABLE 6.4

SOF_3^+ Vibrational Frequencies

$SOF_3 \cdot AsF_6$	$SOF_3 \cdot SbF_6$	POF_3 *	NSF_3 †	Assignment
391	387	345	342	ν_6 δ(SO)
497	508	485	429	ν_5 δ(SF)
513	535	473	521	ν_3 δ(SF)
911	909	873	775	ν_2 ν_s(SF)
1057, 1063	1063	990	811	ν_4 ν_{as}(SF)
1529, 1538	1532, 1540	1415	1815	ν_1 ν(SO)

* reference 136

† reference 135

Small peaks due to SO_2F_2 and SOF_2 were observed in all solutions. The SOF_2 peak shifted in solutions containing excess AsF_5, indicating complex formation (see Chapter VII). The insolubility of the complex in excess AsF_5 or in the SOF_2 and SO_2F_2 present with the SOF_4 contrasts with the solubility of other AsF_5 complexes in sulfur-oxide-fluorides. (134)

Similarly, Dean found from a ^{19}F nmr study that $SOF_4 \cdot SbF_5$ was completely insoluble in $SO_2C\ell F$ at low temperatures. (144) Again this contrasts with the findings for other SbF_5 complexes in $SO_2C\ell F$. (79)

Mixtures of SOF_4 and BF_3 were prepared in a similar manner to those of SOF_4 and AsF_5. However, in contrast to the behaviour of mixtures with AsF_5 which contained a white solid at all temperatures, a white solid appeared in the mixtures containing BF_3 only on cooling. ^{19}F nmr showed no evidence for association of SOF_4 and BF_3 in the liquid phase, either by broadening of peaks, shift of peak position, or the appearance of new peaks. In addition to the peaks due to SO_2F_2 and SOF_2 only two peaks were seen, those of SOF_4 and BF_3, with the same chemical shifts as that of the pure compounds. Cooling the solution only caused a decrease in the peak intensities. The behaviour can be explained by an equilibrium between a solid complex and the dissociated components in the liquid phase.

$$SOF_4 \text{ (liquid)} + BF_3 \text{ (liquid)} \rightleftharpoons SOF_4 \cdot BF_3 \text{ (solid)}$$

This equilibrium is similar to the dissociation of solid $SF_4 \cdot BF_3$, which sublimes and is completely dissociated in the gas phase.

$$SF_4 \text{ (gas)} + BF_3 \text{ (gas)} \rightleftharpoons SF_3^+ BF_4^- \text{ (solid)}$$

However, in the present case the stability of the complex is low enough to show dissociation within the liquid range of the two components.

No complex formation between SOF_4 and PF_5 has been previously reported. Solutions of the two components gave ^{19}F nmr spectra similar to those found for SOF_4 and BF_3. Only lines due to SOF_4 and PF_5 were visible. In addition, the coupling constant J_{PF} was unchanged from that in pure PF_5. Cooling the solutions resulted in formation of a white solid and a decrease in intensity of the nmr peaks. The behaviour can be explained by the equilibrium:

$$SOF_4 \text{ (liquid)} + PF_5 \text{ (liquid)} \rightleftharpoons SOF_4 \cdot PF_5 \text{ (solid)}$$

Raman spectra of SOF_4 and BF_3, and SOF_4 and PF_5 in the liquid phase showed strong lines attributable to the two components. There were in addition some weak lines, some of which may be due to SO_2F_2 and some of which may be weak lines of SOF_4. There were, however, no strong lines which could be attributed to a complex. On cooling the sample until solid formation occurred, new lines appeared in the spectra, though those previously seen still remained. Annealing the sample at dry ice temperature for a week resulted in an increase in intensity of

the new lines, while the original lines of SOF_4 and BF_3 or PF_5 decreased in intensity. Further storage time in dry ice caused the spectral change to progress further. However, on storage in liquid nitrogen, no changes occurred in a given spectrum. In all cases the sample was transferred from the storage container to Raman sample dewar without being allowed to warm. The spectra were not assignable on a simple $SOF_3^+PF_6^-$ (BF_4^-) formulation, and no further attempts to assign them were carried out. However, on the basis of the spectral behaviour one can say that both BF_3 and PF_5 do form complexes with SOF_4, but they are much weaker than those with AsF_5 or SbF_5. Apparently a slow polymerization takes place at low temperatures during the annealing period. This explanation is consistent with the freezing and melting behaviour of the samples. There was no definite freezing or melting point. Solid and liquid phases were in contact in a sample tube over a considerable range of temperature. Storing the samples at dry ice temperature for one hour did not cause them to solidify. However, after several days complete solidification occurred.

Solutions in HF

a) Conductivity

$SOF_4 \cdot AsF_5$ dissolved in HF to give solutions with a conductivity similar to that of $SF_3^+BF_4^-$ and $SF_3^+SbF_6^-$ (Table 6.5 and Fig. 6.1). It can be concluded therefore that the adduct is completely ionized in

TABLE 6.5

Conductivity of Solutions

of $SOF_4 \cdot AsF_5$ in HF

Concentration (molal)	$\kappa \times 10^2$ (mhos/cm)
0.0871	1.76
0.1105	2.11
0.157	2.75
0.202	3.30
0.234	3.67
0.318	4.53
0.405	5.24

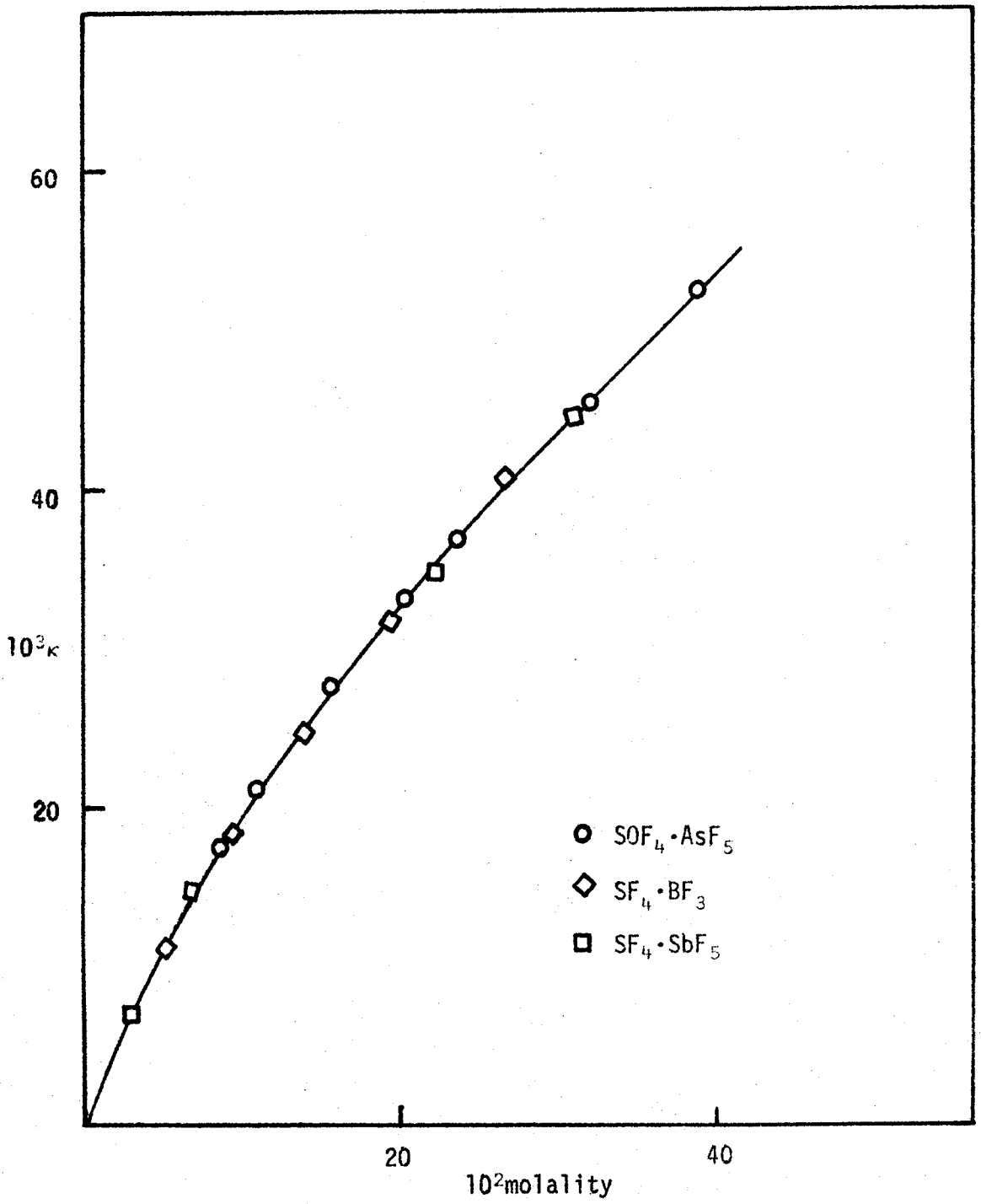

Figure 6.1 Conductivity of $SOF_4 \cdot AsF_5$

solution.

$$SOF_4 \cdot AsF_5 \xrightarrow{HF} SOF_3^+ + AsF_6^-$$

An approximately 0.5 molal solution of SOF_4 in HF had a very low conductivity, (of the order of 10^{-3} mhos/cm) indicating that it behaves as a very weak electrolyte.

b) NMR Spectra

The ^{19}F nmr spectrum of SOF_4 in HF at room temperature gave a single resonance at -75 ppm from $CFC\ell_3$ in addition to the solvent resonance. Rapid exchange between SOF_4 and HF did not occur. The spectrum of $SOF_4 \cdot AsF_5$ in HF had two signals in addition to a broad solvent peak, a very weak peak at $\delta_{CFC\ell_3}$ = -75 ppm which can be assigned to SOF_4 and a strong peak at $\delta_{CFC\ell_3}$ = -32 ppm which is assigned to SOF_3^+ (Table 6.6). The chemical shift of +43 ppm for F on S on going from SOF_4 to SOF_3^+ is in the same direction and of similar magnitude to the shift of ~+30 ppm found for F on S on going from SF_4 to SF_3^+.

On cooling the solution, the solvent peak broadened and split into a doublet which at -40° had a splitting of 526 Hz which did not increase on further cooling. This splitting is due to proton fluorine spin-spin coupling in the HF molecule. The value of J_{HF} observed is very slightly larger than that of 521 Hz obtained previously by Mackor and Maclean for liquid HF. [129] This splitting can only be observed

TABLE 6.6

^{19}F Chemical Shifts of SOF_4 Adducts in HF (ppm from $CFC\ell_3$)

$SOF_4 \cdot AsF_5$

T°C	HF			SOF_3^+	SOF_4
	δ	width (Hz)	J_{HF} (Hz)	δ	δ
0	+193.4	900	-	-32.9	-75.0
-13	+197.3	300	-	-32.8	-74.7
-20	+198.3	290	-	-32.4	-74.8
-30	+196.9		513	-32.0	
-40	+195.2		526	-31.7	
-50	+196.0		518	-31.7	
-60	+195.8		525	-31.8	
-70	+195.1		523	-32.1	

$SOF_4 \cdot SbF_5$

0	+198.1	292	-	-32.3	-75.5
-10	+199.0	530	-	-32.3	-75.2
-20	+198.2		428	-32.1	-75.2
-30	+198.2		500	-32.1	-75.2
-40	+196.8		518	-32.3	-75.0
-50	+197.0		527	-32.1	-74.9
-70	+196.0		522	-32.1	-74.9
-80	+195.5		527	-32.1	-74.6

Table 6.6 (Continued)

$SOF_4 \cdot AsF_5$ + KF

T°C				SOF_3^+	SOF_4	SO_2F_2
	δ	width (Hz)	J_{HF} (Hz)	δ	δ	δ
0	+192.5	310	-	-32.7	-75.4	-29.2
-10	+200.1	530	-	-33.6	-75.9	-29.5
-20	+196.9		407	-32.3	-74.8	-29.2
-30	+197.6		481	-32.0	-74.8	-28.9
-50	+197.4		495	-31.8	-74.7	-29.0
-70	+196.2		502	-31.9	-75.0	-29.2
-80	+194.8		504	-32.1	-74.7	-29.4

$SOF_4 \cdot AsF_5$ + AsF_5

+20	+176.3	-	-33.1	-	
+10	+175.1	-	-32.8	-	
0	+175.2	-	-32.7	-	
-10	+173.7	-	-32.9	-	
-30	+179.4	-	-32.6	-	
-40	+181.4	-	-32.6	-	

when the HF solution is exactly neutral. At the neutral point $[H_2F^+]$ = $[HF_2^-]$ and the total number of ions formed by dissociation of the solvent is at a minimum. (129) Both the fluoride ion and the acidium ion catalyze chemical exchange in HF which collapses the doublet. Even at neutrality, the solution must be cooled to slow exchange and allow resolution of the doublet. The separation of the doublet was observed at -40°C which is a higher temperature than found previously.

Normally the minute traces of water that are present in HF produce a slight excess of HF_2^- that is sufficient to collapse the proton-fluorine coupling. Observation of the very weak SOF_4 peak indicates the mechanism by which this trace of HF_2^- is removed by reaction with SOF_3^+.

$$SOF_3^+ + HF_2^- \longrightarrow SOF_4 + HF$$

The spectrum of a solution of $SOF_4 \cdot AsF_5$ in HF containing an excess of AsF_5 did not show the SOF_4 peak and the solvent signal was a sharp singlet (Table 6.6). The excess of acidium ion resulting from the ionization of the acid, AsF_5, reacted with any SOF_4 present and also catalyzed the exchange in the solvent thus causing complete collapse of the proton fluorine coupling.

$$SOF_4 + H_2F^+ \longrightarrow SOF_3^+ + 2\ HF$$

The SOF_4 peak increased in intensity relative to the SOF_3^+ peak in a solution of $SOF_4 \cdot AsF_5$ containing added KF. The SOF_3^+ peak

remained visible even at room temperature (Table 6.6). In addition, a small peak appeared at -29 ppm which can be assigned to SO_2F_2. This SO_2F_2 is formed by hydrolysis of SOF_4. Even though KF had been added, the J_{HF} coupling was still visible. If it had remained in solution as F^-, chemical exchange would be expected to completely wash out observation of the coupling. The observation of proton fluorine coupling and the increase in intensity of the SOF_4 peak indicates that practically all the fluoride was removed by reaction with SOF_3^+. The system SOF_3^+/SOF_4 appears to act as a buffer in the HF solvent system, maintaining the solution at neutrality, i.e. $[H_2F^+] = [HF_2^-]$.

No other observation of buffering action in the HF solvent system appears to be known. Maclean and Mackor, in their initial observation of proton fluorine coupling in HF, were effectively trying to buffer the solvent at neutrality with BF_3/BF_4^-, though they did not state this as such. [129] However, their results show that the BF_3/BF_4^- system does not act as a buffer at the neutral point in HF. This is not to say that this system will not function as a buffer in HF, probably on the acid side of neutrality, but it has not yet been demonstrated. Indeed, buffering by an external solute in either of the other common strong acid systems, sulfuric or fluorosulfuric acids, is apparently not known. In these other acid solvents, however, there is a built-in weak buffering action due to the solvent self-dissociation.

A solution of $SOF_4 \cdot SbF_5$ in HF gave a very similar spectrum to

that of $SOF_4 \cdot AsF_5$ (Table 6.6). A signal due to fluorine on the MF_6^- anion was not observed for either solution, presumably because of partially relaxed coupling to ^{75}As (I = 3/2) for AsF_6^- and ^{121}Sb (I = 5/2) and ^{127}Sb (I = 7/2) giving a very broad spectrum which could not be detected above the base line noise. Similar results were also obtained on solutions of SF_4 adducts in HF, where signals due to the AsF_6^- and SbF_6^- anions were not seen.

Summary

The Raman spectra of the solid 1:1 adducts of SOF_4 with AsF_5 and SbF_5 can be assigned in terms of the ionic model $SOF_3^+ MF_6^-$ but there is some perturbation of the spectra, probably due to fluorine bridging. Similar results were observed for the adducts of SF_4 with AsF_5, SbF_5, PF_5 and BF_3. The SO bond in SOF_3^+ is the strongest sulfur oxygen bond known and is presumably therefore the shortest.

In hydrogen fluoride solution, conductivity and ^{19}F nmr measurements indicate complete ionization to $SOF_3^+MF_6^-$. The system SOF_3^+/SOF_4 acts as a buffer in the HF solvent system, maintaining it at the neutral point, i.e. $[H_2F^+] = [HF_2^-]$.

CHAPTER VII

DONOR-ACCEPTOR COMPLEXES OF SULFUR-OXIDE-FLUORIDES

Introduction

Thionyl fluoride, SOF_2, was present as an impurity to the extent of 5% in the sulfur tetrafluoride used in this work. It results from the hydrolysis of SF_4, and separation of the two compounds is very difficult because of their similar physical properties (SOF_2 m.pt. -129°C, b.pt. -44°C; SF_4 m.pt. -121°C b.pt. -40°C). [106] A chemical method of purification has been proposed, based on the formation of a complex of lower volatility between SF_4 and BF_3, while SOF_2 does not form such a complex and can be pumped off. [145] The SF_4 is subsequently recovered by decomposition of $SF_4 \cdot BF_3$ by a suitable donor which forms a stronger complex with BF_3. However, it was desirable to further investigate the lack of reactivity of SOF_2 to the fluoride acceptors used in this work in order to eliminate any possiblity of interference in the observations on SF_4 adducts. This was particularly important since the fluoride ion acceptors are also strong Lewis acids and might co-ordinate to the lone pair electrons on the oxygen atom of SOF_2. During the course of this investigation, other similar compounds were also investigated. Interaction with fluoride acceptors was investigated by observing nmr spectra of solutions of the fluoride acceptors in the

various sulfur oxide-fluorides.

Work on addition compounds of PF_5, AsF_5 and SbF_5 among others has been reviewed by Webster up to December, 1964. [146] Addition compounds of BF_3 have been reviewed by Greenwood and Martin [188] and by Stone. [147] Although evidence has been obtained for stable complexes of AsF_5 with relatively strong Lewis bases such as CH_3CN, [148] $(CH_3)_3N$ and $(CH_3)_2O$, [149] except for a study of AsF_5-SO_2 in which it was concluded that no complex formation occurred [150] there has been no investigation of the possiblity of complex formation with very weak bases. Similarly, though complex formation between PF_5 [120, 149] and BF_3 [151] with relatively strong bases has been studied, there has been no investigation of the possibility of complex formation with relatively weak bases. From freezing point studies, Booth has demonstrated the existence of solid 1:1 complexes of BF_3 with SO_2 [151] and SOF_2 [152] although there is considerable dissociation above the melting point.

Concurrent with this investigation, Dean investigated the ^{19}F nmr of SbF_5 and the weak bases SO_2ClF, SO_2 and CH_3SO_2F. He showed them to form 1:1 and 2:1 SbF_5-base complexes. [79] Prior to that the complex $SbF_5 \cdot SO_2$ had been characterized both in solid state and solution. (154)

The Complex $SbF_5 \cdot SOF_2$

SbF_5 dissolves in excess SOF_2 at room temperature and the ^{19}F nmr spectrum shows two broad lines, one in the F on S region and

one in the F on Sb region. At lower temperatures these peaks can be resolved. The spectrum at -100°C of a solution with SbF_5:SOF_2 = 1:23 shows two peaks in the F on S region, one at -73.5 ppm due to solvent SOF_2 and a second smaller peak at -46.7 ppm. In the F on Sb region, there is a doublet at +102.3 ppm and a quintet at +138.4 ppm of relative intensities 4:1. Together this doublet and quintet constitute an AX_4 spectrum due to four equivalent fluorines coupled to a fifth fluorine. The coupling constant J_{FF} is 92 Hz. The peak at -46.7 ppm has a relative intensity of 2, and is assigned to F on SOF_2 complexed by SbF_5. Thus, it can be seen that a 1:1 complex between SOF_2 and SbF_5 is present. From the nmr spectrum, the structure below can be assigned with four fluorines <u>cis</u> and one <u>trans</u> to SOF_2, all arranged in an octahedral configuration about the antimony.

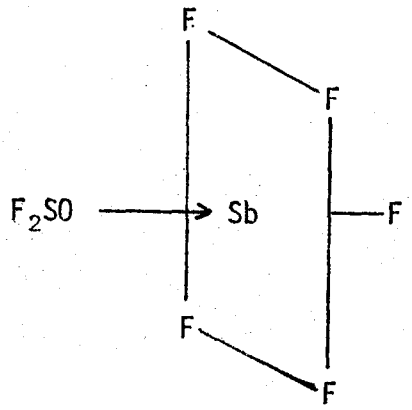

The chemical shift and coupling constant agree quite well with that found for SbF_5 in the complex $SbF_5 \cdot SO_2$ (F_{cis} = +105 ppm, F_{trans} = +137 ppm, J_{FF} = 100 Hz).[154] An X-ray structural determination shows the SO_2 to be co-ordinated to SbF_5 through oxygen to complete the octahedron around antimony.

On warming to -40°C, the complexed SOF_2 peak is still visible. However, on further warming to -15°C, the complexed SOF_2 peak disappears and the solvent, SOF_2 peak becomes broader. In a 1:2.7 SbF_5:SOF_2 solution, the peak due to complexed SOF_2 is still visible at 0°C, though it merges with the main peak at room temperature. No peak due to a 2:1 $SbF_5 \cdot SOF_2$ complex was visible down to -50°C, the freezing point of the sample.

A 1:0.96 SbF_5:SOF_2 sample showed only two peaks at room temperature at -55.0 ppm (F on S) and +112.1 ppm (F on Sb). These could not be resolved as the sample froze immediately with very slight cooling. The F on Sb peak had a chemical shift the same as the average value for F_{cis} and F_{trans}. However, the F on S peak has a value intermediate between free and complexed SOF_2. This can be explained by formation of a 2:1 $SbF_5 \cdot SOF_2$ complex tying up SbF_5 and leaving free SOF_2. Dean has investigated solutions of SbF_5 and SOF_2 in SO_2ClF, and has observed the formation of a 2:1 complex.[79] The F on S peak in this complex only shifts a further 2.3 ppm to high field beyond that of the 1:1 complex. Comparison with the 26.8 ppm shift between the 1:1

complex and free SOF_2 shows that by tying up SbF_5 in the 2:1 complex, the resultant free SOF_2 will leave the average chemical shift of F on S at an intermediate value between free and complexed SOF_2.

The complex is not stable when dissolved in anhydrous HF. The ^{19}F nmr spectrum of SOF_2 with an excess of SbF_5 in HF showed only a single F on S peak with the same chemical shift as that for SOF_2 itself in HF. Apparently SbF_5 extracts a fluoride ion from HF more readily than it forms a co-ordinate bond with SOF_2.

Complexes with AsF_5

a) The AsF_5-SO_2F_2 System

No complex formation occurs between AsF_5 and SO_2F_2 even at -140°C. The ^{19}F spectrum of a 1:4.25 AsF_5:SO_2F_2 sample showed only a single F on S peak with the same chemical shift as that found for pure SO_2F_2. The F on As peak was very broad (more than 1000 Hz at -35°C) as for pure AsF_5, and in contrast to the findings for AsF_5 with stronger donors which form complexes. This result is not surprising as SO_2F_2 does not form any complex with SbF_5. [79] In fact, in solution in SO_2F_2, SbF_5 forms fluorine bridged chains as in liquid SbF_5, rather than complex with SO_2F_2. It is known from vibrational spectroscopy that AsF_5 is monomeric in the liquid as well as the gas phase [46] so that in this case the formation of polymeric fluorine bridged chains does not compete with the formation of an $AsF_5 \cdot SO_2F_2$ complex. Since

no interaction occurs, SO_2F_2 was used as a solvent for the other potential bases that were studied, in order to obtain the nmr spectra at temperatures down to the freezing point of SO_2F_2 (-135.8°C). (155)

b) The AsF_5-SOF_2-SO_2F_2 System

In addition to the SO_2F_2 solvent peak, only two lines were visible in the ^{19}F nmr spectrum at all temperatures and for varying concentrations. The peak due to fluorine on SOF_2 was a sharp singlet. The chemical shift varied over a range of 22 ppm from near that of uncomplexed SOF_2 when the sample was at +6°C to near that of SOF_2 complexed by SbF_5 for a sample at -100°C containing excess AsF_5, (Table 7.1) The F on As peak was much narrower than for the AsF_5 solution in SO_2F_2. The chemical shift changed from near that of AsF_5 in SO_2F_2 (+63 ppm at -35°C) for a sample at +20°C to near the average value for F on As in the complex $C_5H_5N \cdot AsF_5$ for a sample at -100°C containing excess SOF_2.*

These results can be explained by assuming that, by analogy with the SbF_5-SOF_2 system, a 1:1 complex is formed, but that in this case it is rather labile and is in equilibrium with its components.

$$AsF_5 + SOF_2 \rightleftharpoons AsF_5 \cdot SOF_2$$

* $C_5H_5N \cdot AsF_5$ $F_{equatorial}$ = +41.0 ppm F_{apical} = +82.7 ppm
$F_{average}$ = +45.3 ppm (from Ref. 148)

TABLE 7.1

^{19}F Shift in AsF_5-SOF_2-SO_2F_2 from $CFCl_3$ in ppm

Sample Composition

AsF_5:SOF_2:SO_2F_2	1:0.56:3.2			1:0.79:3.8		
	SOF_2	AsF_5		SOF_2	AsF_5	
T°C	δ	δ	width*	δ	δ	width*
6	-70.6	+62.5	240	-71.5	+62.9	250
- 6	-69.6	+61.7	230	-71.1	+62.0	160
- 28	-66.6	+59.0	130	-66.8	+58.8	110
- 51	-58.8	+57.7	130	-59.8	+55.2	75
- 76	-52.0	+57.0	75	-54.0	+52.5	60
-100†	-48.6	+58.1	75	-50.8	+57.8	50
-125	-46.2	+57.5	60	-45.7	+57.3	50

AsF_5:SOF_2:SO_2F_2	1:2.3:6.2		
6	-71.1	+61.0	185
- 6	-71.1	+59.5	110
- 28	-69.6	+56.9	110
- 51	-65.9	+51.8	110
- 76	-63.3	+49.4	50
-100†	-62.0	+48.7	25

* Width of AsF_5 peak at half height in Hz

† At -100°C shift of pure SOF_2 = -73.5 ppm
and shift of F on S in $SbF_5 \cdot SOF_2$ = -46.7 ppm

At room temperature, the equilibrium lies far to the left, shifting to the right on cooling. The rate of formation and dissociation of the new complex must be very rapid, as the F on SOF_2 peak remained narrow even at -125°C.

The sharpness of the F on As peak is indicative of a much greater rate of quadrupole relaxation of the coupling between ^{75}As (I = 3/2) and ^{19}F than in AsF_5 in SO_2F_2. This is expected as the electric field gradient about the arsenic will be greater in the complexed molecule than in uncomplexed AsF_5 in which the very rapid intramolecular exchange of fluorine (pseudo-rotation) causes a rapid averaging of the electric field gradient to a very low value. In complexed AsF_5, there is a more symmetric octahedral arrangement of bonds about arsenic, but five are strong As-F bonds, while the sixth is the weak As - O complex bond. The resultant electric field gradient is likely to be much larger than for the AsF_5 molecule.

c) <u>The AsF_5-$SO_2C\ell F$ System</u>

In addition to the peak of SO_2F_2 present as an internal reference, only two single lines are visible in the ^{19}F nmr spectrum at all temperatures observed (Table 7.2). As in the AsF_5-SOF_2-SO_2F_2 system, the F on As peak was shifted downfield from that of AsF_5 in SO_2F_2, and its width was much less than for AsF_5 and decreased with decreasing temperature again indicating that there is an interaction

TABLE 7.2

^{19}F Shift in AsF_5-$SO_2C\ell F$ from $CFC\ell_3$ in ppm*

T°C	$SO_2C\ell F$	AsF_5	
		Shift	Width[¶]
+30[†]	-97.7	+61.0	100
-20	-97.2	+58.8	84
-35	-97.1	+57.5	88
-51	-96.8	+56.5	88
-68	-96.6	+55.2	80
-85	-96.3	+53.9	56
-100	-96.0	+52.8	44
-125		+52.0	46

* Converted from SO_2F_2 internal reference

($\delta_{SO_2F_2} = \delta_{CFC\ell_3} + 31.0$ ppm)

[¶] Width of AsF_5 peak at half height in Hz

[†] Shift of $SO_2C\ell F$ with SO_2F_2 at 30°C = -97.7 ppm

with the $SO_2C\ell F$. However, even with a large excess of $SO_2C\ell F$, the AsF_5 peak did not shift as far as in the SOF_2 samples. These observations would indicate an equilibrium lying farther to the left than that with SOF_2.

$$AsF_5 + SO_2C\ell F \rightleftharpoons AsF_5 \cdot SO_2C\ell F$$

This is in agreement with the finding that $SO_2C\ell F$ is a weaker base than SOF_2 towards SbF_5.[79]

d) The AsF_5-SO_2-SO_2F_2 System

In addition to the SO_2F_2 solvent peak only a single sharp F on As peak was seen in the spectrum of a 1:2.0:5.7 AsF_5-SO_2-SO_2F_2 sample (Table 7.3). The chemical shift as a function of temperature, and width of the peak are quite similar to that found for AsF_5 complexed to SOF_2. In this case though, even at room temperature, the F on As resonance is not as close to uncomplexed AsF_5 as it is in an SOF_2 sample of similar ratio, indicating an equilibrium shifted farther to the right than that with SOF_2. This is consistant with the previous finding that SO_2 is a stronger base than SOF_2. [79]

$$AsF_5 + SO_2 \rightleftharpoons AsF_5 \cdot SO_2$$

It is not unexpected to find that SO_2 interacts with AsF_5, since it has been shown that it forms a solid 1:1 complex with the even weaker Lewis

TABLE 7.3

^{19}F Shift of AsF_5 in AsF_5-SO_2-SO_2F_2 from $CFC\ell_3$ in ppm*

T°C	Shift	Width (Hz)
6	+57.8	55
- 6	+56.3	55
-28	+53.2	50
-51	+51.0	50
-76	+49.9	50
-100	+49.6	48

* Measured from solvent SO_2F_2 and converted to $CFC\ell_3$ using

$\delta_{CFC\ell_3} = \delta_{SO_2F_2} - 31.0$ ppm

acid BF_3, though with considerable dissociation above the freezing point. (152)

e) The AsF_5-CH_3SO_2F-SO_2F_2 System

In addition to the SO_2F_2 solvent peak only two lines are visible in the ^{19}F nmr spectra at all temperatures and for varying concentrations. The chemical shift of the lines, the coupling constant J_{HF} in CH_3SO_2F, and the width of the F on As line indicates that complex formation is occurring. However, unlike the AsF_5-SOF_2 samples, the lines do not markedly shift with varying temperature (Tables 7.4 and 7.5).

The position of F on CH_3SO_2F shifts upfield in the complex, further even than in the $SbF_5 \cdot CH_3SO_2F$ complex (+2.1 ppm). The F on S peak is split into a 1:3:3:1 quartet because of coupling to the methyl protons. The coupling constant J_{HF} in CH_3SO_2F increases from 5.3 Hz for uncomplexed CH_3SO_2F to 6.5 Hz for the complex $AsF_5 \cdot CH_3SO_2F$. This again parallels the behaviour of $SbF_5 \cdot CH_3SO_2F$ for which J_{HF} increases to 6.8 Hz.(134) With less than a stoichiometric amount of AsF_5 the changes in the chemical shift and J_{HF} were correspondingly less. For samples containing large amounts of CH_3SO_2F, SO_2 was added in order to ensure that the system remained homogeneous. This SO_2 did not have any effect on the spectra showing that it is a weaker base than CH_3SO_2F towards AsF_5 as it also is towards SbF_5. (79) Similar changes in chemical shifts and coupling constants were observable in the proton

TABLE 7.4

^{19}F Shift of CH_3SO_2F in ppm*

Sample Composition					
$AsF_5:CH_3SO_2F:SO_2F_2$	1:0.65:8.5				
	T°C	J_{HF}(Hz)	δ	J_{HF}(Hz)	δ
	-28	6.3	+3.63		
	-35	6.7	+3.68		
	-59	6.7	+3.75		
	-68	6.3	+3.77		
$AsF_5:CH_3SO_2F:SO_2F_2:SO_2$	1:0.96:2.0:2.7			1:1.2:4.3:2.8	
	- 6	6.2	+3.49		
	-12	6.5	+3.50	6.0	+3.42
	-20	6.3	+3.52	6.2	+3.40
	-28	6.2	+3.61	6.0	+3.47
	-35	6.3	+3.65	6.2	+3.42
	-43	6.5	+3.63	6.2	+3.43
	-51	6.3	+3.61		
	-59	6.3	+3.58	6.3	+3.38
	-68	6.3	+3.56	6.3	+3.40
	-76	6.5		6.2	
	-85	6.5		6.3	

* Shift from CH_3SO_2F in SO_2F_2 (1:15) at the same temperature, both originally measured from solvent SO_2F_2.

TABLE 7.5

^{19}F Shift of F in AsF_5 Complexed to CH_3SO_2F from $CFC\ell_3$ in ppm*

Sample Composition $AsF_5:CH_3SO_2F:SO_2F_2:SO_2$	T°C	δ	Width (Hz)
1:0.65:8.5:0	- 51	+50.9	45
	- 68	+53.9	45
1:0.96:2.0:2.7	- 59	+50.6	38
	- 68	+50.0	42
	- 85	+49.8	30
1:1.2:4.3:2.8	- 28	+49.3	45
	- 51	+50.9	35
	- 76	+50.5	70
	-100	+41.5	250

* Measured from solvent SO_2F_2 and converted using

$\delta_{SO_2F_2} = \delta_{CFC\ell_3} + 31.0$ ppm

spectra, (Table 7.6). The proton resonance shifts farther to lower field for the complex with SbF_5 than with AsF_5, presumably due to the greater electron withdrawing ability of SbF_5. This is similar to earlier findings with complexes of stronger bases with PF_5 and AsF_5.[149]

The ^{19}F spectrum of CH_3SO_2F in SO_2F_2 had a second quartet of peaks in addition to those due to F on ^{32}S in CH_3SO_2F. This second set was due to F on ^{34}S (I = 0) and had an isotope shift from the main peaks. The intensity of the satellite peaks compared to the main peaks (4.5%) was in good agreement with the natural abundances of ^{32}S (95.06%) and ^{34}S (4.18%). The isotope shift ($\Delta\delta_{^{34}S - ^{32}S}$) is 0.046 ppm, which at the magnetic field strength used in this experiment (equivalent to a fluorine resonance frequency of 56.4 MHz.) is 2.6Hz. This is almost exactly half the J_{HF} coupling constant in CH_3SO_2F and so the satellite peaks were observed nearly midway between the main peaks because of the spectral resolution obtained. The main peak width was 0.3Hz at half height. Fluorine satellite peaks in CH_3SO_2F have been observed previously by Gillespie and Quail, but they were not as well resolved.[156] They obtained an isotope shift of 0.043±0.004 ppm for the average of thirty runs. Satellite peaks were not observed in the solutions of CH_3SO_2F containing AsF_5. The signal to noise ratio was lower, and the main peaks were slightly broader than in the AsF_5 free solution. However, the resolution was still more than adequeate to measure the J_{HF} coupling.

TABLE 7.6

^1H Shift of CH_3SO_2F from TMS in ppm

Sample Composition	T°C	δ	J_{HF}(Hz)
$CH_3SO_2F:SO_2F_2$ 1:15			
	+30	-2.50	5.0
	-20	-2.61	5.5
	-37	-2.50	5.5
	-55	-2.70	5.5
	average	-2.58	5.3
$AsF_5:CH_3SO_2F:SO_2F_2:SO_2$ 1:0.96:2.0:2.7			
	+30*	-3.13	6.4
	-20	-3.36	6.0
	-37	-3.30	6.5
	-55	-3.25	6.5
	average	-3.26	6.3

* CH_3SO_2F in $SbF_5 \cdot CH_3SO_2F$ J_{HF} = 6.8 Hz δ = 3.71 at +30°C

The absence of changes in the chemical shift and in the coupling constant with temperature indicate that the CH_3SO_2F is essentially fully complexed even at +20°C. However, there is still a very labile exchange occurring as evidenced by the single CH_3SO_2F peak, and the lack of any fine structure in the AsF_5 peak (Table 7.5).

Complexes with PF_5

As in the case of SbF_5 and AsF_5, no complex formation is observed between PF_5 and SO_2F_2 even at -140°C. The ^{19}F nmr spectrum of a 1:4.4 PF_5:SO_2F_2 sample showed only a single F on S peak with the same chemical shift as that found for pure SO_2F_2. The F on P peak was split into a doublet by phosphorus-fluorine coupling. The chemical shift of 100.1 ppm from solvent SO_2F_2 (+69.1 ppm from $CFC\ell_3$) and coupling constant of 933 Hz are in agreement with previously found values of PF_5 in an inert solvent [44] and as a neat liquid. [157] The chemical shift and coupling constant were identical at -140 and -100°C. Since no interaction occurs, SO_2F_2 was used as a solvent for the other potential bases that were studied.

PF_5 and excess base dissolved in SO_2F_2 were studied at -120°C by locking on to the SO_2F_2 solvent peak and measuring the shifts from SO_2F_2. There was no change in the chemical shift or in the coupling constant J_{PF} on addition of SOF_2, SO_2 or CH_3SO_2F to the SO_2F_2 solution of PF_5. In addition, the position of F on SOF_2 or CH_3SO_2F did not shift.

Unlike the case of AsF_5, no complex formation occurs, indicating that PF_5 is too weak an acid to complex with these very weak bases. Even if the complex were very labile and only an average F on P environment were observed instead of an AX_4 pattern, as is the case with AsF_5, a change in the coupling constant would be expected.

The change in coupling constant from free PF_5 is observed for the complex $CH_3CN \cdot PF_5$, which at +25°C shows only a doublet in the ^{19}F spectrum (J_{PF}=770Hz). [148] Similarly, $(CH_3)_2O \cdot PF_5$ shows only 2 broad fluorine resonance signals at 25°C, due to coupling between P and F. The broadness is due to rapid exchange between free and complexed PF_5, resulting in an average fluorine environment being observed. At low temperature, a pair of doublets and a pair of quintets are seen. This is an AX_4 spectrum from an octahedral $PF_5 \cdot$base complex split by PF coupling with J_{PF} apical = 777 Hz and J_{PF} equatorial = 820 Hz. [149]

The ^1H spectrum of CH_3SO_2F and PF_5 in SO_2F_2 at 25°C showed no change in J_{HF} (5.2 Hz) or chemical shift (-2.5 ppm from TMS) compared to CH_3SO_2F in SO_2F_2.

Summary

The previously unreported complex $SbF_5 \cdot SOF_2$ has been observed and a strucutre similar to that for $SbF_5 \cdot SO_2$ was proposed. AsF_5 was also found to form a complex with SOF_2 and also with SO_2ClF, SO_2 and CH_3SO_2F, but they are very labile which suggests that AsF_5 is a weaker Lewis acid than SbF_5. Sulfuryl fluoride was found to act as an inert

diluent for AsF_5. The donors considered were found to have the following order of base strength towards AsF_5:

$$CH_3SO_2F > SO_2 > SOF_2 > SO_2C\ell F > SO_2F_2$$

This is the same order of base strength that had been previously found towards SbF_5. The Lewis acid PF_5 is too weak to form complexes with any of the bases studied. The Lewis acids have the following order of acid strength towards the bases used in this work:

$$SbF_5 > AsF_5 > BF_3 > PF_5$$

CHAPTER VIII

ADDUCTS OF SeF_4 - THE SeF_3^+ CATION

Introduction

Selenium tetrafluoride is expected to resemble sulfur tetrafluoride in its chemical properties and in fact, selenium tetrafluoride forms adducts with fluoride ion acceptors that are apparently similar to the sulfur tetrafluoride adducts. Peacock first prepared the adduct with SO_3 and suggested for it the ionic structure, $SeF_3^+SO_3F^-$. (158) Bartlett and Robinson prepared adducts with BF_3, AsF_5 and SbF_5 and suggested that they all contain the SeF_3^+ ion. (104) An x-ray structural determination on $SeF_4 \cdot 2NbF_5$ found the ionic structure $SeF_3^+Nb_2F_{11}^-$ giving the first direct evidence for the SeF_3^+ ion. (132) However, considerable interaction through fluorine bridging was observed between the SeF_3^+ and $Nb_2F_{11}^-$ ions. Evans and Long have interpreted the Raman spectra of the molten adducts with AsF_5 and SbF_5 in terms of the ionic structures $SeF_3^+MF_6^-$.

Subsequently Gillespie and Whitla showed that the structure of the adduct of SeF_4 and SO_3 can best be described in terms of a polymeric bridged fluorosulfate structure for the solid and the melt, which is broken down in solution to form mainly a dimeric species. (159) They also examined adducts of SeF_4 with BF_3 and some group V pentafluorides,

concluding that although the adducts are best formulated as having ionic structures, the ions interact strongly by fluorine bridging. (160) The fluorine bridging was found to persist in the molten state and to some extent in solution.

Solutions of SeF_4 in HF

SeF_4 dissolves in HF to give solutions which conduct (Table 8.1), though to a considerably lesser degree than similar solutions of SF_4. SeF_4 is presumably ionizing as a weak base.

$$SeF_4 + HF \rightleftharpoons SeF_3^+ + HF_2^-$$

By comparison with the conductivity curve of KF, the concentration of ionic species for a given solution was obtained from the conductivity of the solution. The dissociation constant for SeF_4 in HF was then calculated. The value found ranged from 2×10^{-4} to 6×10^{-4} (Table 8.1) The dissociation constant was about the same when the other alkali metal fluorides were used as comparison electrolytes. It is not clear why the dissociation constant varies in this way. Thus, SeF_4 is a weaker base in HF than SF_4 by two orders of magnitude. This is in agreement with the findings of Whitla that $SeF_4 \cdot PF_5$ could not be prepared (80), in contrast to the ease of preparation of $SF_4 \cdot PF_5$.

^{19}F nmr of SeF_4 in HF showed only a single broad line at all temperatures. The chemical shift was intermediate between pure HF and

TABLE 8.1

Conductivity of SeF_4 in HF

molality	κ mhos/cm $\times 10^3$	dissociation constant $\times 10^4$
0.184	2.0	2.0
0.289	2.9	3.6
0.425	3.8	2.9
0.466	4.0	3.2
0.620	5.2	4.2
1.119	8.0	5.7

pure SeF_4, at about the position expected for a weighted average for the relative numbers of fluorines in SeF_4 and HF. Rapid exchange between SeF_4 and HF presumably occurs through the formation of the SeF_3^+ ion.

Solutions of $SeF_4 \cdot BF_3$ in HF

$SeF_4 \cdot BF_3$ gives conducting solutions in HF, but the conductivity is not as great as solutions of KBF_4 or $SF_3^+ BF_4^-$. (Table 8.2 and Fig. 8.1) It is presumably only partly dissociated in solution.

$$SeF_4 \cdot BF_3 \rightleftharpoons SeF_3^+ + BF_4^-$$

This result is in agreement with the behaviour of $SeF_4 \cdot BF_3$ in the lower dielectric constant solvent nitrobenzene, where it gives a low conductivity comparable with that of the weak electrolyte $A\ell C\ell_3$. (160) Cryoscopic measurements on $SeF_4 \cdot BF_3$ in nitrobenzene similarly show it to be incompletely dissociated. (160) By comparison of the conductivity of $SeF_4 \cdot BF_3$ in HF with that of KBF_4, the concentration of ionized species in solution can be found, and from this the dissociation constant can be calculated (Table 8.2). It is not clear why the dissociation constant varies with concentration in the manner it does. If fluorine bridged chains were forming, the dissociation constant would be expected to decrease with increasing concentration. KBF_4 could be a poor comparison electrolyte. Comparison with $SF_3^+BF_4^-$, the only other BF_4^- salt measured

TABLE 8.2

Conductivity of $SeF_4 \cdot BF_3$ in HF

molality $\times 10^2$	κ mhos/cm$\times 10^3$	dissociation constant
3.9	5.2	0.019
4.9	6.4	0.023
6.9	8.6	0.036
9.6	11.2	0.048
26.5	24.0	0.10
34.4	28.5	0.10
47.2	35.2	0.12

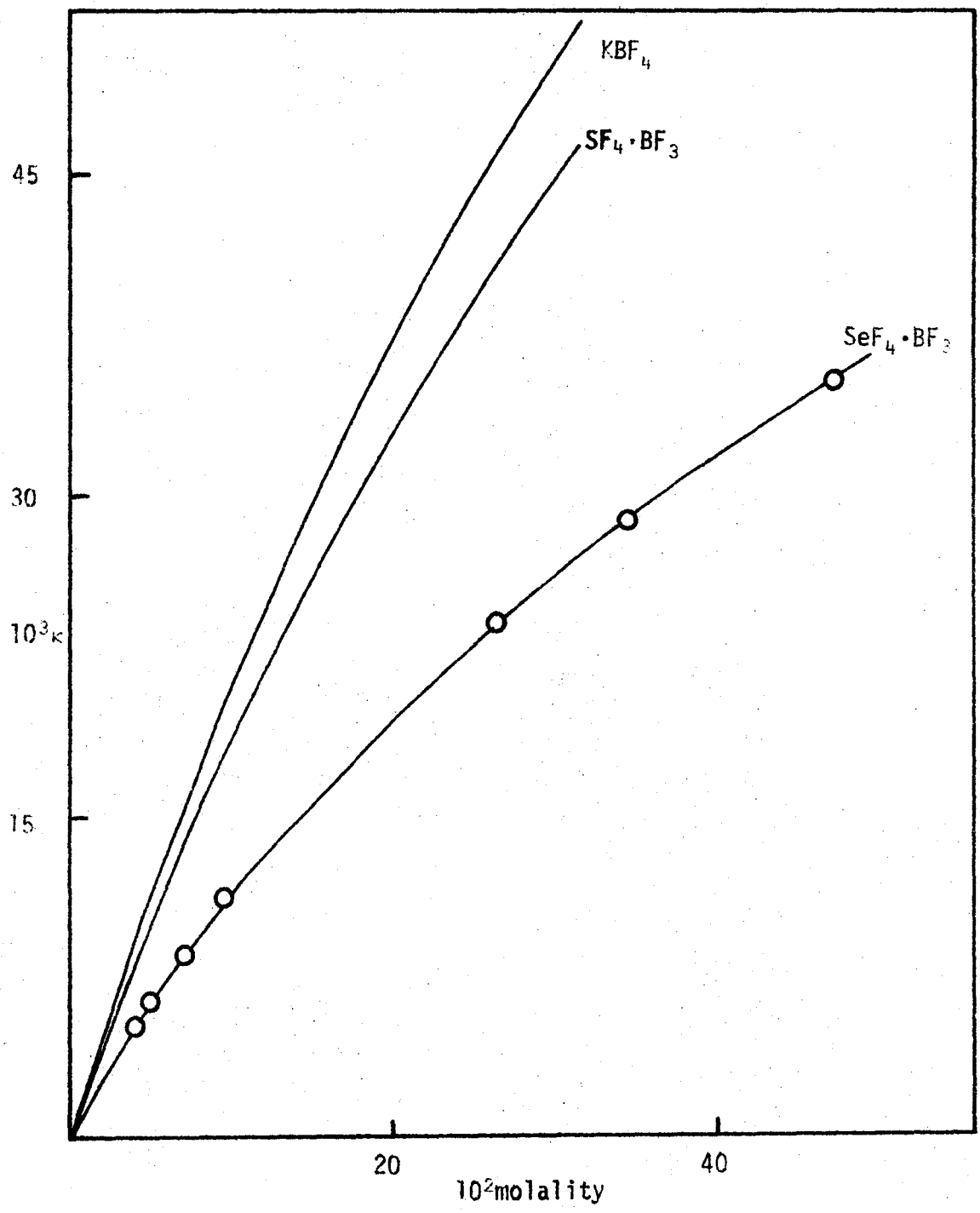

Figure 8.1 Conductivity of $SeF_4 \cdot BF_3$

results in a greater variation in the dissociation constant at the higher concentrations as well. It is possible that formation of the unionized weak base SeF_4 is occurring to some extent in the dilute solutions.

^{19}F nmr of solutions of $SeF_4 \cdot BF_3$ in HF at -40°C and lower showed, in addition to the solvent HF peak, only a single peak due to BF_4^- at +152 ppm from $CFC\ell_3$. On addition of excess BF_3, the peak due to BF_4^- disappeared and a new peak which is assigned to SeF_3^+ appeared at -6.0 ppm from $CFC\ell_3$. Exchange of fluorine between BF_4^- and the solvent can take place through BF_3.

$$BF_3 + 2HF \rightleftharpoons BF_4^- + H_2F^+$$

However, since there is no free fluoride ion present when there is excess BF_3, any SeF_4 is converted to SeF_3^+, and the rate of exchange of fluorine in SeF_3^+ with fluorine in HF through SeF_4 is greatly decreased.

The change in chemical shift of +18.8 ppm from that measured for pure SeF_4 (-24.8 ppm from $CFC\ell_3$) is in the same direction and of similar magnitude to that found for F on S on going from SF_4 to SF_3^+ ($\sim$+30 ppm) and from SOF_4 to SOF_3^+ (+43 ppm). The correctness of the assignment to fluorine on selenium is shown by the observation of two satellite peaks due to coupling of ^{19}F to the magnetic isotope ^{77}Se (I = 1/2) present in 7.5% abundance. The coupling constant $J_{^{77}SeF}$, measured at both 94.1 MHz and 56.4 MHz, was found to be 1212.6±0.2 Hz

at -80°C. It is interesting to note that this coupling constant is intermediate between those found for other Se(IV) compounds and those found for Se(VI) compounds (Table 8.3). [161] The isotope shift from F on ^{77}Se to F on ^{80}Se was found to be +0.012±0.004 ppm for the average of ten measurements. This is of similar magnitude to the selenium isotope effect on the fluorine chemical shift previously observed (Table 8.3). [162]

Summary

Selenium tetrafluoride was shown to have a base strength in hydrogen fluoride two orders of magnitude lower than sulfur tetrafluoride. The adduct $SeF_4 \cdot BF_3$ was found to be only partly dissociated, similar to its behaviour in nitrobenzene, and in contrast to the fully ionized $SF_4 \cdot BF_3$. The ion SeF_3^+ was observed by ^{19}F nmr and the coupling constant and isotope shift for $^{77}SeF_3^+$ was compared to that found in other fluorine compounds of selenium.

TABLE 8.3

Coupling Constants and Isotope Shifts of some Selenium - Fluorine Compounds

Coupling Constants [161]

		$J_{^{77}SeF}$ (Hz)
Se(IV)	$SeOFC\ell$	647
	$SeOF_2$	837
	SeF_3^+	1212.6
Se(VI)	SeF_6	1421
	$HSeO_3F$	1453
	SeO_2F_2	1584

Isotope Shifts [162]

	$\Delta\delta^{77}Se - {}^{80}Se$ (ppm)
$SeOF_2$	0.009±0.005
SeF_3^+	0.012±0.004
SeF_6	0.021±0.004
$HSeO_3F$	0.016±0.005
SeO_2F_2	0.020±0.005

CHAPTER IX

CONCLUSIONS

Although hydrogen fluoride is an important and reasonably well studied solvent there has never been an extensive systematic study of the electrical conductivities of solutions of simple electrolytes. An attempt has been made in this work to provide this basic data for solutions of alkali and alkaline earth metal fluorides and some other simple salts. This information is important as it forms the basis for using conductivity measurements to study the behaviour of a variety of electrolytes in hydrogen fluoride. In addition, the information obtained is of importance in its own right. Comparison of the conductivities for the alkali and alkaline earth metal fluorides gives relative values for the equivalent ionic conductivities of the cations which are of interest in comparison with water and other solvents. The order of these conductivities was in fact found to be the same as in water, i.e. Li<Na<K<Rb<Cs and Ca<Sr<Ba. By making some reasonable assumptions tentative values were assigned for the equivalent ionic conductivities of a series of cations and anions. The equivalent ionic conductivities of the anions PF_6^-, AsF_6^-, SbF_6^- and BF_4^- were found to be very similar.

Further conductivity measurements at even lower solute concentrations would be of great value, to decrease the extrapolation distance

in the Λ versus $\sqrt{m}$ plots. However, the extremely corrosive and hygroscopic nature of the solvent and the great hygroscopicity of some of the solutes studied make these measurements a very difficult undertaking. At very low solute concentrations, the conductivity of the water impurity is a significant fraction of the solution conductivity. The problem is not one of obtaining acid of very low conductivity, but rather one of preventing the acid from picking up minute traces of moisture when transferred from the test cell to the conductivity cell.

The low weight of solute required, tens of milligrams or less, makes the accurate preparation of low concentration solutions difficult as well. The solutes must be weighed out and transferred in a dry box. For best results, the drybox should be designed around a precision analytical balance and be reserved exclusively for the manipulation of nonvolatile substances. Thus, a further stage of sophistication is needed to obtain accurate conductivity measurements on low concentration solutions. A step in this direction was achieved in this work with the development of the type II conductivity cell. One of its advantages is a greater volume which enables a solution of lower concentration to be prepared for a given weight of solute.

The equivalent ionic mobilities obtained in this work enable the equivalent conductivity at infinite dilution to be calculated for any combination of the ions studied. Measurements on these combinations, i.e. fluoroanion salts of metals other than potassium, should be carried out as a check on the equivalent ionic mobilities determined in this

work. This would also test the assumption that the cation/anion mobility ratio for hydrogen fluoride is the same as that in water. If this assumption proved to be wrong, enough data should then be available to calculate a self-consistent set of equivalent ionic conductivities.

Values of "γ" for hydrogen fluoride solutions are not as useful as they are for the other strong acid solvents, because of the high mobility of ions other than the characteristic solvent cation and anion. However, when care is taken to use a proper comparison electrolyte, they can be used in the calculation of dissociation constants and the elucidation of ionization schemes. Such a method of study of more complex electrolytes by conductivity measurements has been established. Examples of the use of this method are provided by the study of sulfur tetrafluoride, thionyl tetrafluoride and selenium tetrafluoride and their adducts with fluoride acceptors.

Sulfur tetrafluoride and selenium tetrafluoride are the first non-metallic fluorides which have been definitely shown to have an appreciable basicity in hydrogen fluoride. In addition, thionyl tetrafluoride has been shown to be a weak base, but no dissociation constant was calculated for it in hydrogen fluoride.

These three tetrafluorides are fully ionized in hydrogen fluoride in the presence of fluoride ion acceptors. The adducts of these tetrafluorides with fluoride ion acceptors have been studied by conductivity and fluorine nuclear magnetic resonance spectroscopy. Confirmation

of the ionization has been obtained from Raman spectra of the solid adducts. These spectra have been interpreted on the basis of ionic structures, but there is interaction between the ions through fluorine bridging. The sulfur and selenium tetrafluorides have been shown to give the trifluorosulfur(IV) and trifluoroselenium(IV) cations respectively in hydrogen fluoride solution. Thionyl tetrafluoride ionizes to give the previously unknown trifluorosulfur(VI) oxide cation and buffer action in hydrogen fluoride has been demonstrated for the first time, by the system SOF_3^+/SOF_4.

Areas which deserve further study are the hydrogen fluoride solutions of the halogen fluorides. It is known that the halogen fluorides; chlorine trifluoride, bromine trifluoride and bromine pentafluoride give weakly conducting solutions in hydrogen fluoride, but their mode of ionization has not been investigated. They also form adducts with fluoride acceptors, but a cationic derivative has been proven for only two of them. An x-ray crystallographic structure of the adduct of bromine trifluoride with antimony pentafluoride shows it to contain the BrF_2^+ cation. Vibrational spectra of adducts of chlorine trifluoride with fluoride acceptors show the existence of the ClF_2^+ cation. However, no studies of their behaviour in hydrogen fluoride have been reported. Iodine pentafluoride forms adducts with both fluoride acceptors and fluoride donors. Structural studies have not been carried

out on the adducts with fluoride acceptors. Vibrational spectra of the adducts with fluoride donors have been interpreted on the basis of the IF_6^- anion. It would be of great interest to determine if iodine pentafluoride will ionize as a base in hydrogen fluoride to give a cationic iodine species, or if it will ionize as an acid to give an anionic iodine species. Adducts of iodine heptafluoride with fluoride acceptors are also known, and their vibrational spectra have been interpreted on the basis of the IF_6^+ cation, but again no solution studies have been carried out on them.

Xenon hexafluoride gives conducting solutions in hydrogen fluoride, but its mode of ionization is not known. Xenon hexafluoride also forms adducts with both fluoride acceptors and fluoride donors. An x-ray crystallographic study of the adduct with platinum pentafluoride has shown it to contain the XeF_5^+ cation. The structures of the adducts with fluoride donors have not been studied. A study of the solutions of xenon hexafluoride and its adducts in hydrogen fluoride is necessary to determine how they ionize.

Adducts of fluoride acceptors with sulfur-oxide-fluoride compounds other than thionyl tetrafluoride have also been studied in this work and have been found to be donor-acceptor complexes rather than ionic compounds. The most stable complex studied, the complex between antimony pentafluoride and thionyl fluoride, was found to dissociate

in hydrogen fluoride solution. The solvent hydrogen fluoride is a stronger donor towards antimony pentafluoride than is thionyl fluoride. The difference in behaviour between thionyl tetrafluoride and the other sulfur-oxide-fluoride compounds is a sharp contrast. However, when the symmetry of the molecules is considered a consistent pattern emerges. Both sulfur and selenium tetrafluorides go from C_{2V} symmetry, with a pseudo-trigonal bipyramid structure where one axial position is occupied by a lone pair of electrons, to a pseudo-tetrahedral structure in the cation. Thionyl tetrafluoride also goes from a trigonal bipyramid structure of C_{2V} symmetry to a tetrahedral structure in the cation. Thionyl fluoride, however, already has a pseudo-tetrahedral structure. Loss of a fluoride ion would give a bent SOF^+ molecule. Formation of a donor-acceptor complex by thionyl fluoride through donation of the lone pair of electrons on oxygen allows a pseudo-tetrahedral arrangement to be retained about sulfur. Similarly, sulfuryl chlorofluoride has a tetrahedral arrangement of atoms about sulfur. Loss of fluoride ion would give a trigonal planar $SO_2C\ell^+$ ion. However, a tetrahedral arrangement about sulfur is retained on formation of a donor-acceptor complex. It appears that a tetrahedral arrangement about the central atom is more stable. These observations provide a basis for classification and prediction of the behaviour of sulfur and selenium compounds in their reactions with Lewis acids.

References

1. R. J. Gillespie and D. J. Millen. Quart. Rev. 2, 227 (1948).

2. M. L. Kilpatrick, M. Kilpatrick and J. G. Jones. J. Phys. Chem. 69, 2248 (1965).

3. A. J. Rudge. The Manufacture and Use of Fluorine and its Compounds. Oxford University Press. 1962.

4. S. Nagase. Fluorine Chemistry Reviews. 1, 77 (1967).

5. Reference 3, Chapter 7.

6. J. H. Simons. Fluorine Chemistry, Vol. I. chapter 7. Academic Press. 1950.

7. H. H. Hyman and J. J. Katz, in Non-Aqueous Solvent Systems. T. C. Waddington, (Ed.), Academic Press. 1965. p.47-81.

8. M. Kilpatrick and J. G. Jones, in The Chemistry of Non-Aqueous Solvents. Vol. II. J. J. Lagowski, (Ed.), Academic Press. 1967.

9. The Chemistry and Chemical Technology of Fluorine reprinted from Encyclopedia of Chemical Technology, 2nd Ed. Vol. IX, Interscience Publishers. 1966. p.506-847.

10. G. Olah. Friedel Crafts and Related Reactions. Vol. I, Interscience Publishers. 1963.

11. D. A. Humphreys. Ph.D. Thesis. McMaster University. 1969.

12. A. Netzer. Private Communication.

13. M. E. Peach and T. C. Waddington in Non-Aqueous Solvent Systems. T. C. Waddington (Ed.), Academic Press. 1965. p.85.

14. Handbook of Chemistry and Physics. 48th Edition. The Chemical Rubber Co. 1967.

15. Reference 7, p.59.

16. M. Atoji and W. N. Lipscomb. Acta Cryst. 7, 173 (1954).

17. M. L. N. Sastri and D. F. Hornig. J. Chem. Phys. 39, 3497. (1963).

18. J. H. Simons. Fluorine Chemistry. Vol. I. Academic Press. 1950. p.229.

19. M. Kilpatrick and T. J. Lewis. J. Am. Chem. Soc. 78, 5186 (1956).

20. R. J. Gillespie and K. C. Moss. J. Chem. Soc. (A). 1170, (1966).

21. J. H. Simons. Fluorine Chemistry. Vol. I. Chapter 6. Academic Press. 1950.

22. J. Barr, R. J. Gillespie and R. C. Thompson. Inorg. Chem. 3, 1149 (1964).

23. R. C. Thompson, J. Barr, R. J. Gillespie, J. B. Milne and R. A. Rothenbury. Inorg. Chem. 4, 1641 (1965).

24. R. J. Gillespie in Inorganic Sulfur Chemistry, G. Nichless (Ed.) Chap. 16. Elsevier Publishing Publishing Company. 1969.

25. M. D. Campbell. Ph.D. Thesis, Purdue University. (Dissn. Abs. 26 (5), 2457).

26. K. Fredenhagen, G. Cadenbach and W. Klatt. Z. physik. Chem. A 164, 176 (1933).

27. F. P. Del Greco and J. W. Gryder. J. Phys. Chem. 65, 922 (1961).

28. W. Klatt. Z. anorg. allgem. Chem. 222, 225 (1935).

29. W. Klatt. Z. anorg. allgem. Chem. 222, 289 (1935).

30. M. Kilpatrick and F. E. Luborsky. J. Am. Chem. Soc. 75, 577 (1953).

31. D. A. McCaulay and A. P. Lien. J. Am. Chem. Soc. 73, 2013 (1951).

32. D. A. McCaulay and A. P. Lien. J. Am. Chem. Soc. 77, 5579 (1955).

33. M. Kilpatrick, J. A. S. Bett and M. L. Kilpatrick. J. Am. Chem. Soc. 85, 1038 (1963).

34. A. W. Jache and G. H. Cady. J. Phys. Chem. 56, 1106 (1952).

35. G. P. Rutledge, R. L. Jarry and W. Davis Jr. J. Phys. Chem. 57, 541 (1953).

36. R. L. Jarry, F. D. Rosen, C. F. Hale and W. Davis Jr. J. Phys. Chem. 57, 905 (1953).

37. B. Frlec and H. H. Hyman. Inorg. Chem. 6, 1596 (1967).

38. H. Selig and E. L. Gasner. J. Inorg. Nucl. Chem. 30, 658 (1968).

39. H. Selig and B. Frlec. J. Inorg. Nucl. Chem. 29, 1887 (1967).

40. A. F. Clifford, H. C. Beachell and W. M. Jack. J. Inorg. Nucl. Chem. 5, 57 (1957).

41. D. A. McCauley, W. S. Higley and A. P. Lien. J.Am. Chem. Soc. 78, 3009 (1956).

42. H. H. Hyman, L. A. Quarterman, M. Kilpatrick and J. J. Katz. J. Phys. Chem. 65, 123 (1961).

43. H. H. Hyman, T. J. Lane and T. A. O'Donnell. 145th meeting ACS Abstracts p. 63T.

44. S. Brownstein. Can. J. Chem. 47, 605 (1969).

45. P. A. W. Dean, R. J. Gillespie and R. Hulme. Chem. Comm. 990 (1969).

46. L. C. Hoskins and R. C. Lord. J. Chem. Phys. 46, 2402 (1967).

47. M. Kilpatrick and F. E. Luborsky. J. Am. Chem. Soc. 76, 5865 (1954).

48. M. Kilpatrick and F. E. Luborsky. J. Am. Chem. Soc. 76, 5863 (1954).

49. C. Maclean and E. L. Mackor. Disc. Faraday Soc. 34, 165 (1962).

50. D. A. McCaulay and A. P. Lien. J. Am. Chem. Soc. 75, 2411 (1953).

51. M. T. Rogers, J. L. Speirs, M. B. Panish and H. B. Thomson. J. Am. Chem. Soc. 78, 936 (1956).

52. M. T. Rogers, J. L. Speirs and M. B. Panish. J. Am. Chem. Soc. 78, 3288 (1956)

53. M. T. Rogers, J. L. Speirs and M. B. Panish. J. Phys. Chem. 61, 366 (1957).

54. R. J. Gillespie and M. J. Morton. Inorg. Chem. in press.

55. K. O. Christe and W. Sawodny. Inorg. Chem. 6, 313 (1967).

56. M. L. Kilpatrick, M. Kilpatrick and J. G. Jones. J. Am. Chem. Soc. 87, 2806 (1965).

57. K. O. Christe, J. P. Guertin, A. E. Pavalth and W. Sawodny. Inorg. Chem. 6, 533 (1967).

58. W. E. Tolberg, R. T. Rewick, R. S. Stringham and M. E. Hill. Inorg. Chem. 6, 1156 (1967).

59. C. A. Wamser, W. B. Fox, B. Sukornick, J. R. Holmes, B. B. Stewart, R. Juurik, N. Vanderkooi and D. Gould. Inorg. Chem. 8, 1249 (1969).

60. J. K. Ruff. Inorg. Chem. 5, 1791 (1966).

61. A. R. Young II, and D. Moy. Inorg. Chem. 6, 178 (1967).

62. B. Frlec and H. H. Hyman. J. Inorg. Nucl. Chem. 29, 2124 (1967).

63. J. G. Malm, H. Selig, J. Jortner and S. R. Rice. Chem. Rev. 65, 199 (1965).

64. N. Bartlett, F. Einstein, D. F. Stewart and J. Trotter. Chem. Comm. 551, (1966).

65. J. Binenboym, H. Selig and J. Shamir. J. Inorg. Nucl. Chem. 30, 2863 (1968).

66. E. G. Hill and A. P. Sirkar. Proc. Roy. Soc. London, A 83, 130 (1909).

67. K. Fredenhagen and G. Cadenbach. Z. anorg. allgem. Chem. 178, 289 (1929).

68. K. Fredenhagen and G. Cadenbach. Z. physik. Chem. A 146, 245 (1930).

69. J. Simons. J. Am. Chem. Soc. 46, 2179 (1924).

70. M. E. Runner, G. Balog and M. Kilpatrick. J. Am. Chem. Soc. 78, 5183 (1956).

71. J. Shamir and A. Netzer. J. Sci. Instr. 1, 770 (1968).

72. H. Canterford and T. A. O'Donnell in Techniques of Inorganic Chemistry. H. B. Johassen and A. Weissberger, (Eds.) Vol. VII. Interscience. 1968. p.273.

73. R. F. Barrow, E. A. N. S. Jeffries and J. M. Swinstead. Trans. Faraday Soc. 51, 1650 (1955).

74. W. Kwasnik, in Handbook of Preparative Inorganic Chemistry. Vol. I. G. Brauer, (Ed.) Academic Press. 1963. p.234.

75. H. M. Dess and R. W. Parry. J. Am. Chem. Soc. 79, 1589 (1957).

76. W. A. Mazeika and H. M. Neuman. Inorg. Chem. 5, 309 (1966).

77. P. A. Van der Muellen and H. L. Van Mater. Inorg. Syn. 1, 24 (1939).

78. N. Bartlett and P. L. Robinson. J. Chem. Soc. 3417 (1961).

79. P. A. W. Dean and R. J. Gillespie. J. Am. Chem. Soc. 91, 7260 (1969).

80. W. A. Whitla. Ph.D. Thesis. McMaster University. 1964.

81. W. C. Smith and V. A. Engelhardt. J. Am. Chem. Soc. 82, 3838 (1960).

82. R. C. Thompson. Ph.D. Thesis. McMaster University. 1962.

83. R. E. Dodd and P. L. Robinson. Experimental Inorganic Chemistry. Elsevier Publishing Company. 1954. p.219.

84. G. Jones and B. C. Bradshaw. J. Am. Chem. Soc. 55, 1780 (1933).

85. L. A. Quarterman, H. H. Hyman and J. J. Katz. J. Phys. Chem. 61, 912 (1957).

86. P. J. Hendra and E. J. Loader. Chem. and Ind. 718 (1968).

87. S. K. Freeman and D. O. Landon. The Spex Speaker. Vol. VIII, #4.

88. A. F. Clifford, W. D. Pardieck and M. W. Wadley. J. Phys. Chem. 70, 3241 (1966).

89. R. H. Flowers, R. J. Gillespie, A. E. Robinson and C. Solomons. J. Chem. Soc. 4327 (1960).

90. R. A. Robinson and R. H. Stokes. Electrolyte Solutions. Academic Press, Inc. 1954. p.138.

91. R. A. Robinson and R. H. Stokes. Electrolyte Solutions. 2nd ed. Academic Press, Inc. 1959. appendices 6.1 & 6.2.

92. R. Hulme and R. J. Gillespie. unpublished results

93. Reference 90, p. 121.

94. A. F. Clifford and E. Zamora. Trans. Faraday Soc. 57, 1963 (1961).

95. E. Bottari and L. Ciavatta. J. Inorg. Nucl. Chem. 27, 133 (1965).

96. S. S. Mesaric and D. N. Hulme. Inorg. Chem. 2, 788 (1963).

97. S. Kongpricha and A. E. Clifford. J. Inorg. Nucl. Chem. 18, 270 (1961).

98. A. Netzer. Ph.D. Thesis. Hebrew University of Jerusalem. 1969.

99. D. A. MacInnes. The Principles of Electrochemistry. Dover Publications, Inc. 1961. Chapter 19.

100. R. J. Gillespie and E. A. Robinson, in Non-Aqueous Solvent Systems. T. C. Waddington, (Ed.), Academic Press. 1965.

101. C. S. G. Phillips and R. J. P. Williams. Inorganic Chemistry. Vol. I. Oxford University Press. 1965. p.152.

102. F. A. Cotton and G. Wilkinson. Advanced Inorganic Chemistry. Interscience Publishers. 2nd ed. 1966. p.334.

102a. Reference 91, appendix 1.1.

103. P. L. Robinson and G. J. Westland. J. Chem. Soc. 4481, (1956).

104. N. Bartlett and P. L. Robinson. Chem. and Ind. 1351 (1956).

105. F. Seel and O. Detmer. Z. anorg. allgem. Chem. 301, 113 (1959)

106. R. D. W. Kemmitt and D. W. A. Sharp, in Adv. Fluorine Chem. M. Stace, J. C. Tatlow and A. G. Sharpe, (Eds.), Butterworths. 1965. p.142.

107. F. A. Cotton and J. W. George. J. Inorg. Nucl. Chem. 7, 397, (1958).

108. F. A. Cotton and J. W. George. J. Chem. Phys. 28, 994 (1958).

109. A. L. Oppegard, W. C. Smith, E. L. Muetterties and V. A. Englehardt. J. Am. Chem. Soc. 82, 3836 (1960).

110. E. L. Muetterties and W. D. Phillips. J. Chem. Phys. 46, 2861 (1967).

111. C. W. Tullock, D.D. Coffman and E. L. Muetterties. J. Am. Chem. Soc. 86, 357 (1964).

112. R. Tunder and B. Siegel. J. Inorg. Nucl. Chem. 25, 1097 (1963).

113. F. A. Cotton and J. W. George. J. Inorg. Nucl. Chem. 12, 386 (1966).

114. L. J. Hoard, T. B. Owen, A. Buzzel and O. N. Salmon. Acta Cryst. 3, 130 (1950).

115. A. W. Laubengayer and G. R. Finlay. J. Am. Chem. Soc. 65, 884 (1943).

116. L. D. Calvert and J. R. Morton. Acta Cryst. 17, 613 (1964).

117. M. Azeem. Ph.D. Thesis. McMaster University. 1965.

118. N. N. Greenwood and R. L. Martin. Quart. Rev. 8, 1 (1954).

119. A. W. Laubengayer and D. S. Sears. J. Am. Chem. Soc. 67, 164 (1945).

120. I. K. Gregor. Chem. and Ind. 385, (1965).

121. J. A. Evans and D. A. Long. J. Chem. Soc. (A) 1688 (1968).

122. G. M. Begun and A. C. Rutenberg. Inorg. Chem. 6, 2212 (1967).

123. M. K. Wilson and S. R. Polo. J. Chem. Phys. 20, 1711 (1952).

124. M. Azeem, M. Brownstein and R. J. Gillespie. Can. J. Chem. 47, 4159 (1969).

125. J. O. Edwards, G. C. Morisson, V. F. Ross and J. W. Schultz. J. Am. Chem. Soc. 77, 266 (1955).

126. J. Gobeau and W. Bues. Z. anorg. allgem. Chem. 268, 221 (1952).

127. N. N. Greenwood. J. Chem. Soc. 3811 (1959).

128. G. L. Cote and H. W. Thompson. Proc. Roy. Soc. A 210, 217 (1951).

129. C. Maclean and E. L. Mackor. Proc. XI Colloq. Ampere North Holland Publishing Co. Eindhoven. (1962). p.571.

130. J. Bacon, P. A. W. Dean and R. J. Gillespie. Can. J. Chem. 47, 1655 (1969).

131. A. Vierk. Z. anorg. allgem. Chem. 261, 279 (1950).

132. A. J. Edwards and G. R. Jones. Chem. Comm. 346 (1968).

133. A. J. Edwards and G. R. Jones. J. Chem. Soc. (A) 1467 (1969).

134. M. Brownstein and R. J. Gillespie. J. Am. Chem. Soc. in press.

135. H. Richert and O. Glemser. Z. anorg. allgem. Chem. 307, 328 (1961).

136. H. S. Gutowsky and A. D. Liehr. J. Chem. Phys. 20, 1652 (1952).

137. H. Siebert. Anwendungen der Schwingungsspektroskopie in der Anorganischen Chemie, Springer-Verlag. 1966.

138. R. L. Goggin, H. L. Roberts and L. A. Woodward. Trans. Faraday Soc. 57, 1877 (1961).

139. R. J. Gillespie and E. A. Robinson. Can. J. Chem. 39, 2171 (1961).

140. R. J. Gillespie and E. A. Robinson. Can. J. Chem. 41, 2074 (1963).

141. D. R. Lide, D. E. Mann and R. M. Friston. J. Chem. Phys. 26, 734 (1954).

142. E. A. Robinson. Can. J. Chem. 41, 3021 (1963).

143. M. Brownstein, P. A. W. Dean and R. J. Gillespie. Chem. Comm. 9 (1970).

144. M. Brownstein, P. A. W. Dean and R. J. Gillespie. J. Chem. Soc. (A). to be published.

145. N. Bartlett and P. L. Robinson. Proc. Chem. Soc. 230 (1957).

146. M. Webster. Chem. Rev. 66, 87 (1966).

147. F. G. A. Stone. Chem. Rev. 58, 101 (1958).

148. F. N. Tebbe and E. L. Muetterties. Inorg. Chem. 6, 129 (1967).

149. L. Lunazzi and S. Brownstein. J. Magnetic Resonance. 1, 119 (1969).

150. E. E. Aynsley, R. D. Peacock and P. L. Robinson. Chem. and Ind. 117 (1951).

151. S. Brownstein, A. M. Eastham and G. A. Latremoille. J. Phys. Chem. 67, 1028 (1963).

152. H. S. Booth and D. R. Martin. J. Am. Chem. Soc. 64, 2198 (1942).

153. H. S. Booth and J. H. Walkup. J. Am. Chem. Soc. 65, 2334 (1943).

154. J. W. Moore, H. W. Baird and H. B. Miller. J. Am. Chem. Soc. 90, 1358 (1968).

155. F. J. Bockhoff, R. V. Petrella and E. L. Pace. J. Chem. Phys. 32, 799 (1960).

156. R. J. Gillespie and J. W. Quail. J. Chem. Phys. 39, 2555 (1963).

157. E. L. Muetterties and W. D. Phillips. J. Am. Chem. Soc. 81, 1084 (1959).

158. R. D. Peacock. J. Chem. Soc. 3617 (1953).

159. R. J. Gillespie and W. A. Whitla. Can. J. Chem. 47, 4153 (1969).

160. R. J. Gillespie and W. A. Whitla. Can. J. Chem. in press.

161. T. Birchall, R. J. Gillespie and S. L. Vekris. Can. J. Chem. 43, 1672 (1965).

162. T. Birchall, S. L. Crossley and R. J. Gillespie. J. Chem. Phys. 41, 2760 (1964).